

Chapter 9

The Physical Properties of Hair Fibers

Abstract This chapter describes tensile, bending and torsional testing including different parameters of each of these deformations and how these are affected by different types of hair including different types of hair damage. Expanded data sets are included for elastic moduli and other parameters of these deformations. A new section describing the historical development for assessing and measuring hair fiber curvature along with a new method for curvature has been developed and applied to more than 2,400 persons from more than 20 different countries. This method and data are featured in this section. Methods to determine the different dimensions of hair fibers including axial (length and curvature) and transverse dimensions (diameter, cross-sectional area and ellipticity) are described with much expanded data sets. Information on hair fiber friction (both high load and low load friction) and how friction varies with fiber diameter, comb composition and hair damage are included. Mechanical fatiguing, extension cycling and their effects on hair damage including scale lifting are described in the final section on the physical properties of hair fibers.

9.1 Introduction

Since the 4th edition, several important advances have been made in our understanding of the more important physical properties of hair fibers. A new method for hair fiber curvature Segmentation Tree Analysis Method (STAM) classifies this important property into eight different curl types. This method has been applied to more than 2,400 persons from several different countries over the three most important geo-racial groups (linking geography with race) across five continents. This quantization of hair fiber curvature is significant because of the importance of hair fiber curvature to all cosmetic hair assembly properties. As a result, I have attempted to assign hair curvature by STAM to as many parts of this text as feasible.

Additional data on hair diameters, ellipticity, elastic modulus, breaking stress and other important parameters are presented using larger data sets than in previous

editions. New data on the effects of age and sex on scalp hair diameter are presented. This discussion includes new findings on the effects of the menopause on the scalp hair diameter of females. Variation of fiber diameter and ellipticity along the hair shaft and age effects on cross sectional area, ellipticity, curvature and the scale index have also been added.

New and important findings on torsional and bending properties of damaged hair and the effects of different treatments on these properties have been included. Torsional properties have been under-utilized and are potentially just as important as tensile properties because torsion can reveal damage and prospective repair to the cuticle as well as the cortex, an inherent weakness of tensile testing. Torsional properties are also more sensitive to relative humidity changes or water content in the fibers than tensile properties. Additional evidence has been provided to confirm that tensile properties reside essentially in the cortex and not the cuticle for human hair fibers. Torsional measurements can also detect changes induced by hair spray films and conditioner binding in the cuticle that tensile measurements cannot discern. The relationship between structure and adhesion failure (fracture formation) in different parts of the hair is also presented.

Useful information on how hair is degraded with hot combs and by alkaline hair straighteners has been added in sections dealing with hair damaging treatments. New findings showing the importance of bending stiffness and friction on hair handle or feel is also described in Chap. 10 and a new approach to the assessment of tactile hair properties using a psycho-physiological technique has been offered in the literature.

For the main discussion in this chapter, the physical properties of human hair have been divided into two categories:

Elastic deformations

Other important physical properties

Another important classification that will be referred to routinely is single fiber and fiber assembly properties. Some of the more important single fiber properties described in this chapter are curvature, elastic deformations, friction, cross-sectional area (diameter), ellipticity and cohesive/adhesive forces.

Elastic deformations include stretching (tensile properties, cyclic extension and fatiguing), bending including stiffness or the resistance to bending, and torsion (twisting) and its resistance, rigidity. Hair damage/breakage properties have become of paramount importance to cosmetic science and hair breakage is described in Chap. 10. Tensile testing has been used for decades to assess damage to hair, but tensile testing does not closely simulate damaging/breakage effects from hair grooming.

The density of hair (mass/volume) is considered in this chapter followed by fiber dimensions including diameter, ellipticity, cross-sectional shape, and curvature followed by fiber friction as other important physical properties.

The last section of this chapter deals with fatigue testing, extension cycling and flex abrasion which are becoming more widely used because the former two methods simulate some of the damaging effects of grooming actions and can reveal

damage to the cuticle at a level that tensile testing cannot, while flex abrasion more closely simulates a few of the actions involved in hair breakage.

Several years ago, Robbins and Scott [1] hypothesized that most consumer assessments of hair (properties of fiber assemblies such as combing ease, style retention, flyaway, body, and manageability) may be approximated by algebraic expressions involving the single fiber properties of friction, stiffness, static charge, fiber curvature, weight, diameter, luster, and color. Hough et al. [2] described a somewhat similar analysis of hair body. Robbins and Reich [3] determined empirical relationships between combing ease and the fiber properties of friction, stiffness, fiber curvature, and diameter. This work demonstrated that hair assembly properties can indeed be defined by a few fundamental single fiber properties. Robbins has taken the conclusions from this study and proposed a general hypothesis for hair behavior. This general approach of relating fiber assembly behavior to single fiber properties has been expanded and is the basis for the discussion on consumer assessments in Chap. 10.

9.2 Tensile Extension and Deformations

9.2.1 Definitions and Conditions Important to Tensile Extension

For every “strain” (deformation) of an elastic substance, there is a corresponding “stress” (the tendency to recover its normal condition). The units of stress are force per unit area (F/A). The most common types of strain are stretching or elongation (the ratio of an increase in length to the original length), linear compression (the ratio of a decrease in length to the original length), shear (the ratio of the displacement of one plane relative to an adjacent plane), bending, and torsion [4]. These latter two strains are combinations of the former three. Only stretching, bending, and torsional strains are considered in this chapter. For a summary of stress strain models see the section entitled *Stretching Hair and Stress Strain Models* in Chap. 1.

Each type of stress and strain has a modulus (the ratio of stress to strain) that also has units of F/A. The elastic modulus for stretching is commonly called Young’s modulus. The bending modulus is called Young’s modulus of bending, and the torsional modulus is called the modulus of rigidity. But, keep in mind that these elastic moduli for stretching, bending and torsion apply to only limited amounts of deformation (small% strains) for hair fibers over the “elastic” region.

Human hair has been referred to as a substrate with only one dimension, “length,” suggesting why its tensile properties have been studied more than its other elastic properties. The usual procedure for evaluating the stretching properties of human hair involves stretching a fiber of known length (we usually used 5 cm fibers), at a fixed rate (a convenient rate is 0.25 cm/min) in water, in buffer, or at a fixed relative humidity (approximately 60% RH), near room temperature on an automated instrument such as an Instron Tensile Tester (Fig. 9.1) or a Dia-Stron

Fig. 9.1 A single hair fiber loaded in an Instron tensile tester for load–elongation study



Tensile Module. It is unfortunate that there is no standard test conditions in the cosmetic industry for this widely used procedure.

Tensile properties are whole fiber properties, as opposed to surface properties and evidence is strong that tensile properties are primarily cortical properties and not related to the cuticle. This experimental evidence is described next in this chapter with accepted models described in Chap. 1 that explain stretching and water absorption in terms of the cortex [5] with no cuticle involvement. Wolfram and Lindemann [6] suggested that the cuticle might contribute to the tensile properties, especially in fine hair. However, Scott (personal communication) provided support for the “no cuticle involvement” hypothesis, by evaluating the tensile properties of hair fibers that were abraded under controlled conditions. In no instance could he demonstrate a significant change in tensile properties where only cuticle had been abraded.

Robbins and Crawford [7] published the first experimental evidence that the cortex and not the cuticle is responsible for the tensile properties of human hair by

showing that severe damage to the cuticle only cannot be detected by tensile property evaluation. This work involved selective oxidation of the cuticle with m-diperisophthalic acid and is described in more detail with SEM's in Chap. 5. This oxidative treatment (m-diperisophthalic acid) produces extensive cuticle damage that is detectable microscopically. However, this damage could not be detected by either wet or dry tensile property evaluation. More recently, Persaud and Kamath [8] provided additional evidence that tensile properties are a property of the cortex. These scientists demonstrated that cetyl trimethyl ammonium bromide (CTAB) in the hair can be detected by torsional measurements but not by tensile measurements. Persaud and Kamath concluded that this quaternary surfactant absorbs in the cuticle and strengthens it. They suggested that CTAB does not produce changes in the cortex and therefore could not be detected using tensile measurements.

Additional supporting evidence for the non-cuticle involvement in tensile properties is the fact that wet extension of hair fibers to 30% damages the cuticle [9] yet on relaxation in water, tensile recovery occurs producing virtually identical elongation-recovery curves in a before and after evaluation. This basic elongation-recovery procedure (to 15%, 20%, 25% and 30% extension) is commonly used throughout the industry.

When keratin fibers are stretched, the load-elongation curve shows three distinct regions (Fig. 9.2). The lower curve in Fig. 9.2 represents stretching a hair fiber in water. The curve at the top of the chart represents stretching at 65% RH. In the Hookean region of the load-elongation curves, the stress (load) is approximately proportional to the strain (elongation). The ratio of stress to strain in this region is called the elastic modulus (E_s) or more commonly Young's modulus. Only a few

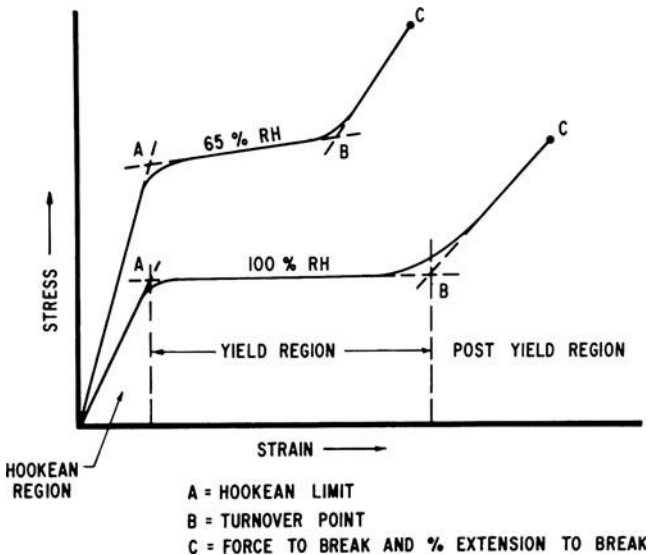


Fig. 9.2 Schematic diagram for load-elongation curves for human hair fibers

years ago, the elastic modulus was normally expressed in units of dynes/cm². Today it is usually expressed as GN/m² (Giga-Newtons per meter squared or (GPa) although Mega-Newtons per meter squared (MPa) is also acceptable) and may be calculated from this simple expression:

$$E_s = H g L / A \Delta L$$

where H = Hookean slope in g/mm elastic extension, g = gravitation constant (980.6 cm/s²), L = fiber length in cm, ΔL = fiber extension in cm, and A = fiber cross-sectional area in cm². This provides the elastic modulus in dynes/cm² which is converted to GN/m² by dividing by 10¹⁰.

The elastic modulus for stretching human hair, determined in our laboratories at 60% RH and room temperature, is 3.89×10^{10} dynes/cm² or 3.89 GPa which is 3,890 MPa. More data on the elastic modulus from other laboratories is described later in this chapter. Methods other than load–elongation have been used to determine the elastic modulus of hair fibers. These methods [10, 11] are also described later in this chapter.

Other important parameters of load–elongation curves are the Hookean limit (Fig. 9.2, Point A), the turnover point (Fig. 9.2, Point B), the percentage extension to break, the stress to break (in the fiber industry called “tensile strength” but more realistically called the extension to break), the post yield modulus (stress/strain) in the post yield region, and the work of elongation (the total area under the load–elongation curve).

An interesting study by Hamburger et al. [12] more than 60 years ago suggested that the pullout energy of cosmetically unaltered Caucasian hair at 65% RH is approximately equal to the Hookean limit which is considerably less than the stress to break. Berthiaume et al. [13] published results more than 40 years later showing that the pullout load for Caucasian hair is about 40–45 g (slightly higher than that of Hamburger et al. [12]), for African hair 30–35 g and for Asian hair 60–65 g. These data suggest that most undamaged hair fibers under stress will pull out before breaking. Scott found that more than one-half of the fibers collected from combing a few heads of female Caucasian hair in our beauty salon contained bulbs and therefore were pulled out; however 5 to about 35% of the hairs were broken. Hair fibers broken on heads actually exhibit different types of fracture patterns. In many cases evidence for cuticle fracturing before catastrophic failure can also be found on hairs growing on live heads, see Chap. 6.

These facts lead one to question the practical implications of tensile testing involving slow extension to break as a criterion for “strength”. Impact loading (by Robbins [14]), mechanical fatiguing (by Kamath et al. [15]) and extension cycling (by Gamez-Garcia [16]) seem to more closely simulate the damaging effects of combing and brushing than the slow strain rates and the extreme strains of ordinary tensile testing. See the discussion on these methods and the section entitled, *How Hair Fibers Break During Combing* described in Chap. 10.

Stretching hair fibers under ambient conditions can cause damage, well before catastrophic failure. For example, during stretching or extension at 45% R.H., signs

of cuticle separation and damage occur in regions of the cuticle (cell membrane complex or even the endocuticle) and it occurs sooner in the cuticle of tip ends (about 10% extension) of hair fibers than in the root ends (about 20% extension). Furthermore, this cuticle damage or fracturing [9] occurs sooner than fiber breakage which occurs at about 40–50% extension at moderate humidity and greater than 50% extension in the wet state.

Three important papers on the tensile fracturing of human hair were published by Henderson et al. [17] and by Kamath and Weigmann [18, 19]. These publications show that breaking or fracturing of hair fibers occurs differently in the cuticle versus the cortex and fracturing of hair fibers occurs in different patterns. Figure 9.3 describes the four most common fracture patterns for human hair. The fracture pattern found depends on the extent of hair damage, the relative humidity (whether the hair is wet or dry) and whether or not the fiber is twisted or contains flaws [9, 19].

For wet hair, if the hair and its cuticle are in good condition and near the root end, a smooth break tends to occur, see Fig. 9.4. As the fiber becomes dryer, below 90% RH, step fractures are more commonly observed (Fig. 9.3). Fibrillation and splitting (Fig. 9.3) are distinct cortical fracture patterns and these tend to occur more when the hair is in poor condition especially with oxidative damage and with twisted or kinky fibers [19] and when the relative humidity is low, rather than when the fiber is wet. One reason for that effect is that the cortex is less extensible than the cuticle when the fiber is dry, below 90% RH [17]. See Chap. 6 for electron micrographs illustrating these different fracture patterns for hair fibers.

If the cuticle is in poor condition, split ends can occur upon catastrophic failure. Split ends can also occur from oxidative damage (Chap. 10) and from step fractures and fibrillation, by way of mechanical action and the subsequent abrasive actions of combing and brushing. See the discussion on damage to hair from shampoos, grooming and weathering in Chap. 6.

Stretching in the wet state is very different than stretching in the dry state. This is because failure in the wet state generally involves hydrophilic layers, such as the

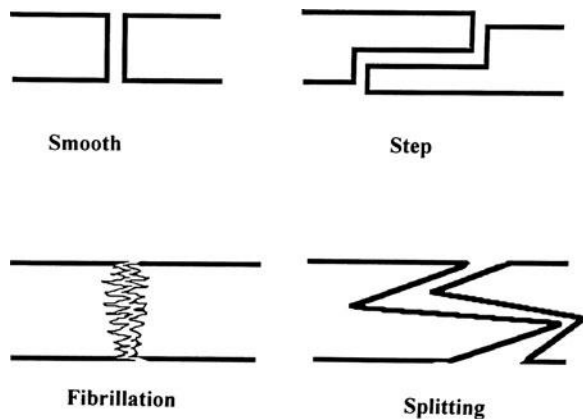
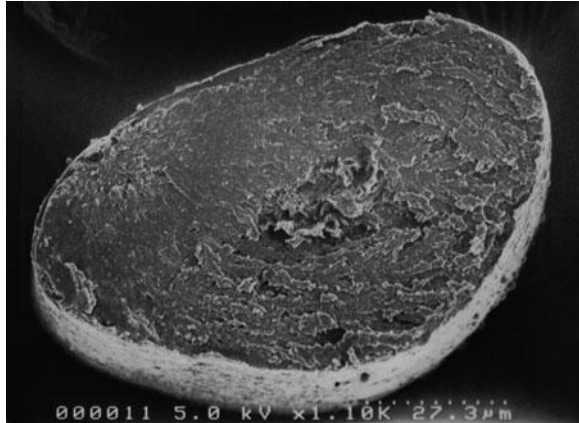


Fig. 9.3 Schematic depicting some of the more important fracture patterns for human hair

Fig. 9.4 A hair fiber broken by stretching in the wet state illustrating a smooth fracture (SEM kindly provided by Sigrid Ruetsch)



contact zone of the CMC or the endocuticle because it involves breaking bonds in hydrophilic layers. On the other hand, failure in the dry state generally involves breaking bonds in or between hydrophobic layers [20]. For example, failure at the junction of the Beta and Delta layers of the CMC occurs because of the weak hydrophobic bonding between branched hydrocarbons (18-MEA) and relatively short hydrocarbon amino acid side chains of the hydrophobic fibrous proteins in the Delta layer [20]. This site is conducive to failure when the cuticle layers are strained at low moisture levels. Such fractures at 65% RH or lower allow the flow of cuticle past cuticle during fiber extension [21], during extension cycling [20] or even bending.

Beta-Delta failure was originally cited by Negri et al. several years ago [22]. The lower the relative humidity (the moisture content of the hair), the lower the strain required to initiate failure between the upper Beta layer and the Delta layer as noted by Gamez-Garcia [16].

Stretching hair fibers to break in the wet state (approximately 50% extension) often produces what appears to be a clean break that macroscopically resembles a razor cut, see Fig. 9.4. However, on close examination of such breaks, we see that fracturing can occur in the cuticle (see Figs. 9.5 and 9.6) well before catastrophic failure. Extension of hair fibers at low RH and even low percentage extensions generally induces Beta-Delta failure [20–22], as illustrated in Chap. 6. Extension of hair fibers to only 10–20%, at 45% RH (or especially at higher humidities) and very slow strain rates, sometimes induces failure in the endocuticle [23, (Ruetsch, private communication) (see Chap. 6) very likely at or near the junction of the endocuticle and exocuticle. Such fractures result in the separation of the surface scales from the underlying layer producing an uplifting of scales, see Fig. 9.5 and Chap. 6. This type of endocuticular failure is not the norm under normal tensile-loading conditions or faster strain rates that are normally encountered in grooming. More recent evidence indicates that a very slow strain rate at higher humidity causes shear stresses within cuticle scales and leads to this type of failure [23].

Fig. 9.5 *Top*: Control hair from near the scalp with no lifted cuticle scales. *Bottom*: Hair fiber extended at low RH. Note the scale lifting from extension. Micrographs kindly provided by Sigrid Ruetsch

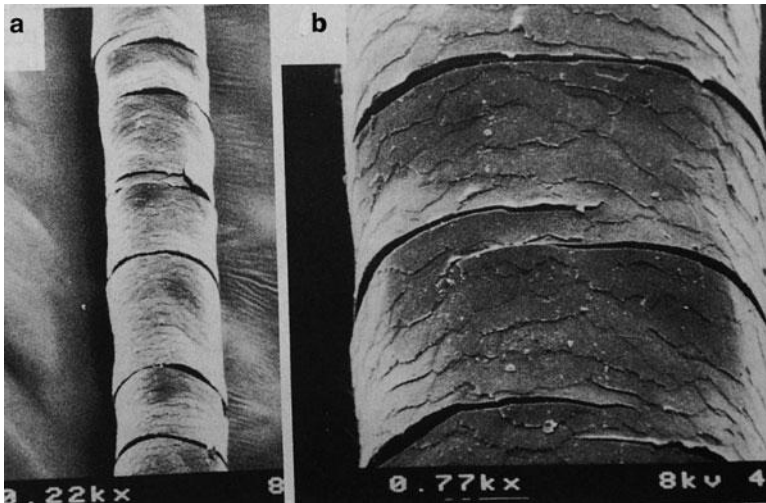
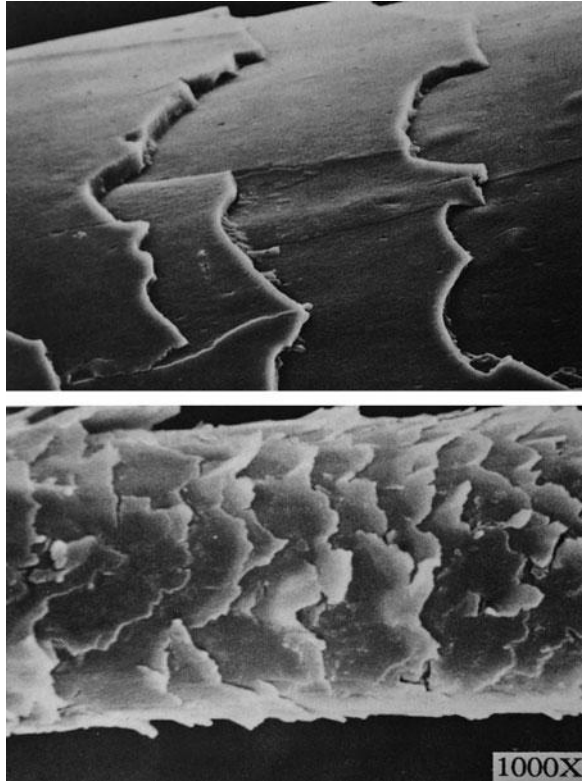


Fig. 9.6 Cracking of the cuticle caused by extension cycling to 200 strain cycles at 30% extension at 100% RH [16]. This cuticle damage is similar to that caused by stretching hair to break in water (reprinted with permission of the Journal of the Society of Cosmetic Chemist)

Extensions to about 30% or slightly higher, in the wet state, can produce multiple circumferential fracturing of the cuticle, with separation of entire cuticle sections from the cortex [18], see Fig. 9.6. Gamez-Garcia [16] demonstrated that this same type of effect can be produced by extension cycling at even lower extensions at high relative humidity or in water.

Stretching to break in the dry state, below 90% RH but not near 0% RH is more prone to induce uneven cortical fracturing. For example, a step fracture or fibrillated end or even split end is likely to result. Stretching or bending hair fibers as occurs during combing or grooming operations is capable of producing stress cracks in the non-keratin regions, the endocuticle and the intercellular regions. Subsequently, scale lifting can occur in the damaged regions of the hair fiber, see Chap. 6.

A hysteresis similar to that in Fig. 9.7 is obtained, when a keratin fiber is stretched up to 30% of its original length in water and then allowed to return to its original length (in water). Such a curve results in spite of potential cuticle damage (especially at high strains). The work of elongation is always greater than the work of recovery; thus, a hysteresis occurs, and the ratio of these two work values is called the resilience ratio (or hysteresis ratio) [24], another useful load-elongation parameter.

As indicated, we normally take fibers 5 cm long and stretch them to 20% of their length at a rate of extension and recovery of 0.25 cm/min. The rate of extension will influence the tensile results [25]. Sikorski and Woods [26] and Simpson [10] suggested an increase of approximately 5% in the elastic modulus for a tenfold

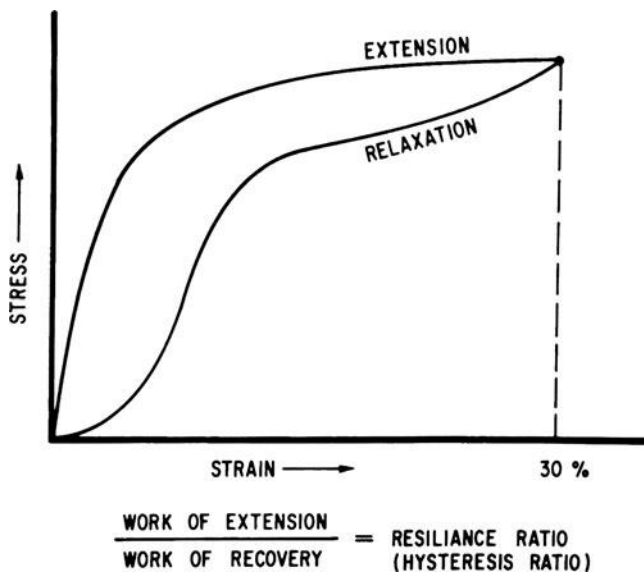


Fig. 9.7 Schematic diagram for load-elongation and recovery curves for human hair fibers

increase in extension rate. Stretching hair fibers to 20% and holding them for 4 h produces a temporary increase in length or a temporary set [27].

After stretching the fibers and relaxing them, as described above, we allow the fibers to relax overnight in water. The fibers can then be treated and re-stretched, thus making before-and-after treatment comparisons on the same fibers. Such a procedure, without treatment, provides reproducible load-elongation curves, confirming the validity of the before and after comparison. Speakman [28] and Sookne and Harris [29] first suggested this type of test procedure. Speakman referred to percentage changes in the work of extension. Harris coined the term “30% index” as the ratio of tensile values to 30% extension. An implicit assumption in this procedure is that calibration or stretching before treatment does not alter the reactivity of the fibers. Wolfram and Lennhoff [30] provided evidence that supports the validity of this assumption, however, at 30% extension cuticular damage occurs that should increase reaction rates for some reactions with stretched hair and may also affect the type of fracture produced. Work and force values to 15% and 25% elongation have also been used [31, 32]. Since calibration elongations, especially in the vicinity of 30% or higher, can produce cuticle damage that is not normally detected in load-elongation parameters stretching hair to lower percentage extensions (15–25%) is preferable.

9.2.2 The Effects of Relative Humidity on Tensile Extension of Hair

The moisture content of human hair varies with relative humidity (RH), increasing with increasing RH, (see the section entitled *Influence of Relative Humidity on*

Table 9.1 Elastic modulus (MPa) verses relative humidity of hair and wool fiber

	65% RH		100% RH ^a		Ratio E _S 65%RH/ E _S 100% RH
	Human Hair	Merino Wool	Human Hair	Merino Wool	
Elastic modulus [27]	5,394	3,040	2,059	1,177	Hair 2.62 Wool 2.58
	% RH		Wool E _S at given RH [@] / E _S at 100% RH		
	0 ^b		2.76		
	32		2.44		
	44		2.27		
	65		2.10		
	78		1.85		
	91		1.41		
	100		1.00		

@ [32]

^aIn pH 7 buffer

^bIn dry glycerine, this approximates 0% RH

Dimensions of Hair in this chapter). Thus changes in the moisture content of hair have a large effect on the tensile properties as shown by elastic modulus changes versus %RH in Table 9.1.

Speakman [33] and Menkart [34] conducted relatively extensive load–elongation studies at several relative humidities for wool fiber. These data show a regular increase in extensibility (percent extension to break) with increasing RH. Even though such extensive studies could not be found in the literature for human hair, undoubtedly a similar relationship exists, because:

1. Tensile properties of hair fibers at 55–65% RH compared with 100% RH (in water) show greater extensibility at the higher humidity (Fig. 9.2) and a lower elastic modulus (Table 9.1) and lower work and force values in general [34].
2. The dynamic elastic modulus of human hair has been reported to respond similarly to changes in RH [35].
3. There is virtually an identical quantitative binding of water to wool and hair as a function of RH [36, 37]. Therefore we conclude a similar stress/strain RH relationship (see Table 9.1).

9.2.3 Tensile Properties and Fiber Diameter

Both wet and dry tensile properties of chemically unaltered keratin fibers are directly proportional to fiber diameter. Figure 9.8 summarizes this relationship for the dry tensile properties via a plot of the Hookean slope versus fiber linear density at 62% RH. Since linear density is proportional to cross-sectional area and diameter, the tensile properties are also proportional to fiber diameter. Robbins and Scott [38] reported a procedure for determining both wet and dry tensile properties on

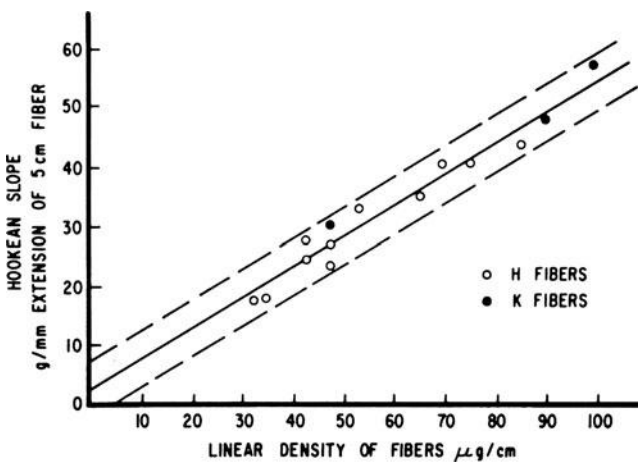


Fig. 9.8 Hair fiber elastic extension versus linear density (Reprinted with permission of the Journal of Cosmetic Science)

the same fibers from only one of these properties. This procedure depends on this fundamental relationship, that is wet and dry tensile properties are proportional to fiber diameter, and therefore, proportional to each other. An equation for predicting the dry Hookean limit at 60% RH from the Hookean limit in water (X) is: $Y \pm 3.75 = 2.18 X$ and for predicting the dry stress to break (B) at 60% RH from the wet force to 20% extension (F) is: $B \pm 10.3 = 3.92 F$.

9.2.4 Tensile Properties and Temperature

Rebenfeld [39] compared human hair with wool fiber by studying the effect of temperature on the load–elongation properties in neutral buffer solution,. Increasing temperature has an effect similar to increasing humidity on the shape of the load–extension curve [39, 40] (see Table 9.2). The elastic modulus for both human hair and wool fiber decrease with increasing temperature, but are lower for wool at any temperature, probably because of its lower cross-link density. The post-yield modulus and tensile stress at break decrease with increasing temperature, whereas extensibility increases.

The breaking stress = $M g/A$ where M = load in kg, g = standard gravity = 9.81 N/kg and A is the cross sectional area in meters squared.

$$\text{Elastic modulus} = \frac{Mg / A}{\Delta L/L}$$

where M = kg; g = standard gravity 9.81 N/kg; A is the cross sectional area in meters squared and $\Delta L/L$ is 2.0 and constant from 65% to 100% RH while it varies from 4.08 at 0% RH, to 3.21 at 17.7% RH and 2.58 at 44.2% RH as shown by Feughelman and Robinson [32].

The turnover point (extension to B in Fig. 9.2) undergoes a transition at 85.5°C for unaltered hair and at 66°C for partially reduced hair. Rebenfeld explained these

Table 9.2 The influence of temperature on the stress/strain properties of human hair^a

Temperature C°	pH 7		
	Elastic modulus MPa	Stress at break ^b MPa	% extension At break
21	2,080	168	48
35	1,770	129	
50	1,670	125	50
70	1,640	140	
90	1,360	99	72

^aCalculated from data by Rebenfeld et al. [39]

^bBy convention, the H term is in force/mm elongation for the elastic modulus, while it is in force units for the stress to break fibers and one divides by the quantity $\Delta L/L$ for the Elastic Modulus, see the equations above

results in terms of a disulfide–sulfhydryl interchange mechanism, whereby stressed disulfide bonds are relieved and transformed into stress-free positions at higher temperatures.

Crawford (private communication) examined the effect of temperature in a dry atmosphere on the wet tensile properties of hair. Crawford found significant changes in the force to 20% extension after heating to 100°C, 25 times for 15 min intervals. Permanent-waved hair appeared to be more susceptible to heat, undergoing a decrease of approximately 7%, as compared to 4% for unaltered hair. McMillen and Jachowicz [41] examined the effects of hot iron treatments on hair and identified a decrease in tryptophan level due to thermal induced decomposition, a small increase in the combing force and a yellowing effect on white hair. However, these scientists did not report tensile effects. A thermo-chemical technique for analysis of human hair has also been reported by Humphries et al. [42]. For discussion of stress strain models see the section entitled *Stretching Hair and Stress Strain Models* in Chap. 1.

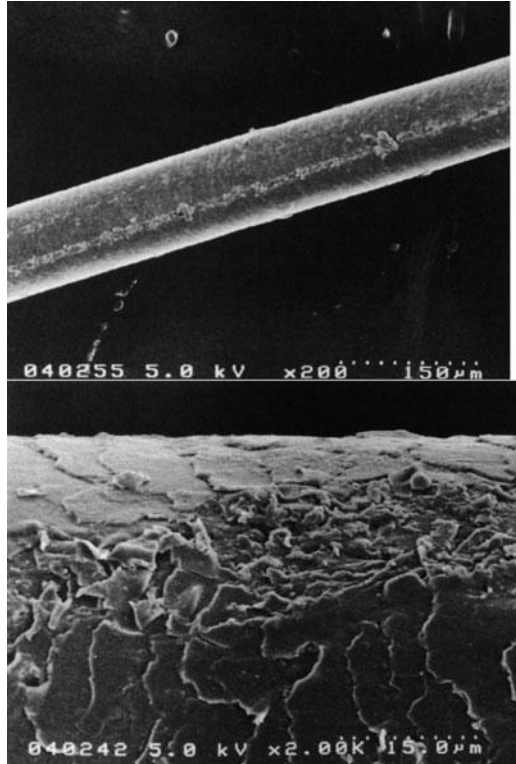
9.2.5 Twisting and Stretching Normal Hair and Hair with Natural Twists

Dankovich et al. [43] examined the effects of twisting hair fibers before and during stretching to determine the effects of twisting on tensile properties. They used two experimental procedures: One in which the hair was twisted at constant length, followed by extension to break while not allowing untwisting and the second procedure involved twisting and then untwisting at constant length followed by extension to break. Twisting an 80 micron hair fiber 45 turns/cm produced catastrophic failure. Therefore lower levels of twist were examined: 11, 23 and 38 turns/cm. Only small changes were produced in the stress and strain to break using 11 turns/cm. However, large changes were produced in the Hookean (decrease in Modulus) and yield regions (increase in Modulus). Extensive changes were produced in all stress strain parameters while simultaneously twisting at higher levels (23 and 38 turns/cm). These scientists concluded that the combination of tensile and torsion stresses (at these twist levels) weakens human hair fibers, but these levels of twist are far beyond what is normally encountered in actual practice on live heads.

The degree of recovery from twist deformation was examined after the fibers were relaxed for 5–10 min before stretching. Dankovich et al. [43] concluded that the tensile properties of human hair are recoverable from twist deformations at low and moderate twist levels as normally encountered in routine grooming operations. When the fibers were twisted and then allowed to untwist the tensile stress and strain did not change relative to controls, however, the initial modulus decreased with increasing levels of twist [43].

By examining scanning electron micrographs Dankovich et al. [43] found that twisting and untwisting hairs can produce cuticular damage which doesn't show up

Fig. 9.9 Results of twisting a highly elliptical hair fiber [43]. *Top*: Note damaged “line” where cuticle scales converge upon twisting. *Bottom*: Note the damage effect at higher magnification (reprinted with permission of the Journal of Cosmetic Science)



in tensile testing. This result supports the conclusion of Robbins and Crawford [7] that tensile properties are a property of the cortex with negligible contribution from the cuticle. When a highly elliptical hair is twisted (even at low twist) the cuticle cells are compressed into one another creating damage to the scales, see Fig. 9.9. This scale damage does not occur to the same degree in more circular hair fibers (because of less scale overlap). The effect of twisting hairs and hair damage is described in more detail later in this chapter. The above experiments involved the effects of twisting hairs on the tensile properties, and not effects of natural twists on the extension behavior as examined by Kamath et al. [19] and described later in this chapter.

9.2.6 Tensile Properties of Different Geo-Racial Groups

Data from six different laboratories was compiled comparing the breaking stress for both Caucasian and African type hair at 65% RH and room temperature [19, 44, 45]. The average breaking stress for Caucasian hair was 187 MPa. The average for

African hair was 151 MPa. These data as analyzed by the matched pairs *t*-test were significantly different showing that African type hair requires a lower stress to break than Caucasian hair. Unfortunately insufficient experimental details were described in some of these studies to determine the length of the fibers tested, the position on the scalp and age/weathering, and whether or not data for some hairs were rejected for breaking before entering the post yield region.

Relevant to these points is the fact that Duvel et al. [46] on Caucasian hair showed about an 8% loss in the tip ends of 41 cm hair fibers for the tensile breaking stress. This tensile loss could not be detected at 16 cm from the scalp end, but was detected between 16 and 24 cm from the scalp end (about 1 and 1/2 year's growth). These scientists also found a gradual loss of both covalently bound lipid and free lipid from the hair. Duvel et al. proposed that this ongoing loss of both free and covalently bound lipid by weathering actions leads to an increased susceptibility of the proteins of the cortex to degradation and eventually to a loss in the tensile breaking stress. Regrettably, data of this sort was not found for curly African type hair where weathering including grooming actions leads to small cracks in the hair [19] and appears to be more severe. However, long African hair is difficult to obtain for such a comparison because of its fragility.

Kamath et al. [19] demonstrated on African American hair (chemically untreated and not treated with hot irons) from one male that the breaking stress was very low at 123 MPa (ellipticity 1.89; indicative of a very high curvature probably Type VIII [47]). These scientists compared this hair to their earlier work on Caucasian hair [18] (also at 65% RH and room temperature) where the breaking stress was found to be approximately 200 MPa (pooled European dark brown hair, average ellipticity 1.17) to 220 MPa (highly elliptical, index = 1.6 Caucasian hair from one individual). Kamath, Hornby and Weigmann demonstrated that the African type hair had twists and at 65% RH, 22% of the fibers broke before 20% extension. When this "premature failure" occurred, Kamath, Hornby and Weigmann observed that the fibers often broke in a region of fiber twist. This effect was confirmed by examination of the broken ends of the hairs, see Fig. 9.10. Furthermore, Kamath, Hornby and Weigmann found that the cross-sectional area varied widely in the region of twist, see Fig. 9.11.

Kamath, Hornby and Weigmann found "premature failure" to be more prevalent in the dry state than the wet state (in fact it was virtually non-existent in the wet state) and concluded that premature failure was due to natural structural flaws in the twists of the fibers or flaws produced by mechanical damage associated with grooming actions. Of the seven hair types that Hardy [48] examined, he noted the highest frequency of kinks or twists in the most highly coiled hair with the most from African type hair.

Pili torti (Fig. 9.12, also see Chap. 3) is a congenital deformity resulting in highly twisted hair fibers and can be confused with highly twisted African hair, but it is even more twisted than kinky hair of Africans. In this disease, hair fibers often break in a twisted region only a short distance from the scalp because of defects created by natural twists in the fibers. The susceptibility of highly twisted Pili torti hair fibers to breakage supports the work and conclusions of Kamath et al. [19]

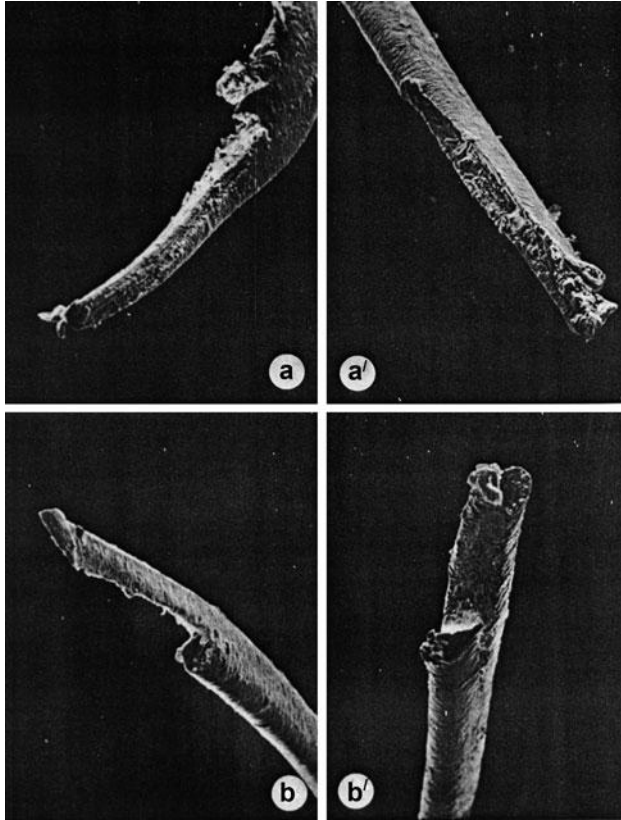


Fig. 9.10 An African American hair fiber broken in the region of twist [19] (reprinted with permission of the Journal of Cosmetic Science)

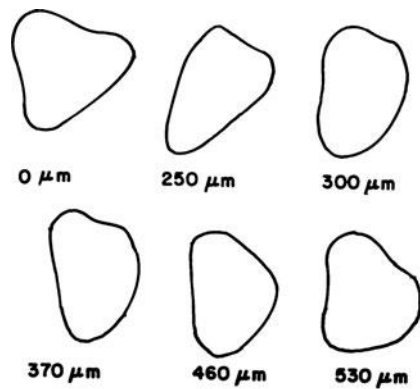
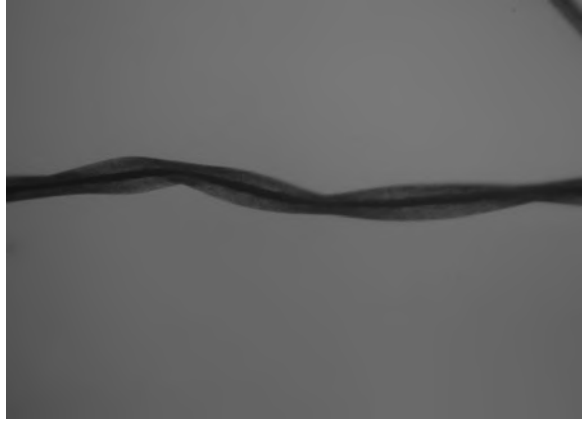


Fig. 9.11 Outlines of varying cross-sectional shapes of an African American hair fiber in the region of twist from Kamath et al. [19]. Note the large deviations from circularity (reprinted with permission of the Journal of Cosmetic Science)

Fig. 9.12 Pili Torti or twisted hair, an example of a congenital deformity in which an extremely twisted hair is produced and it tends to break easily in the regions of twists (also see Fig. 3.3). Light micrograph, kindly provided by John T. Wilson



showing that premature fractures and breakage of hair fibers of African type hair occur in the region of natural twists.

Porter et al. [47] found that the tensile properties of African hair (curl Type IV to VIII) for more than 12,000 hair fibers (65% RH) tends to decrease with increasing fiber curvature, $R^2 = 0.66$. Therefore, for African type hair 66% of the variation in breaking stress, a decrease from 206 to 173 MPa from curl Type IV to curl Type VIII can be accounted for by hair fiber curvature or effects associated with curvature such as twists or kinks, fiber composition and/or mechanical damage from grooming conditions. Porter et al. indicated that in their work, tensile properties were measured on the first 50 hairs that showed “normal failure profiles”. This suggests that data from those hair fibers that displayed “premature failure” were rejected providing higher values for the breaking stress in Porter’s work than in some of the other studies such as the study by Kamath et al. [19] or even for some comparisons with data for Caucasian or Asian hair.

The breaking stress for chemically untreated Caucasian hair fibers at 65% RH from 11 different laboratories/scientists [10, 18, 43–45, 49–51] averages 197 ± 15.8 MPa with an upper 95% mean of 207.6 and a lower 95% mean of 186.4 MPa. A similar distribution analysis of African hair for breaking stress from seven different laboratories [19, 44, 45, 47] over the curl range of IV to VIII shows a mean of 156.6 ± 31.7 with an upper 95% mean of 185.9 and a lower 95% mean of 127.4 MPa suggesting a lower mean and more variation for the African hair data.

Unfortunately we do not know with certainty the curl type range covered by the Caucasian hair in these studies, but it likely covers curl Types I to III and possibly I to IV. Therefore, these data suggest a larger effect of curvature on breaking stress over the curvature range of curl Type VI to VIII for African type hair than for Caucasian hair over the curvature range of curl Type I to III or IV which is most likely from weakening of the fibers from higher grooming forces for the higher curvature hair. In addition a correspondingly higher ellipticity range [47] should result in more and larger twists which would produce more natural flaws and weaker fibers.

The breaking stress from three different laboratories which directly compared Asian versus Caucasian hair averaged 191.1 MPa for Asian and 191.8 for Caucasian hair at 65% RH and room temperature, thus no significant difference. One of these studies compared 50 hairs from each geo-racial group (TRI-Princeton was the testing lab) while the number of hairs in the other two studies were not specified [45]. These data suggested no significant difference in the breaking stress of Asian versus Caucasian hair; however because of the larger diameter and lower ellipticity of Asian hair I would recommend additional study with many more hairs over all relevant curvatures for these two hair types before this conclusion is accepted.

Porter et al. [47] showed that for 12,050 African type hair fibers, Young's modulus decreases with increasing fiber curvature from 3,147 MPa for curl class IV to 2,670 MPa for curl class VIII. Young's modulus for Caucasian hair from seven different laboratories [10, 18, 43, 49–51] was compiled and a distribution analysis showed an average of 3,478 MPa with an upper 95% mean of 3,859 and a lower 95% mean of 3,098 MPa. Therefore, Young's modulus for stretching Caucasian hair (about 1–2% stretch) tends to be higher than for “average” African type hair. Whether or not Young's modulus for African hair of curl class IV is equivalent to that of Caucasian hair or other curl class IV hair will require direct testing.

Scott and Robbins [49] found no significant difference between Young's modulus for stretching Korean hair versus Caucasian hair, but this was on a limited number of fibers (25 from each group). In theory if the internal structures of Asian and Caucasian hairs are sufficiently similar we would expect the same Young's modulus for these two hair types.

9.2.7 Chemical Bleaching of Hair and Tensile Properties

Chapter 5 describes the chemistry of bleaching human hair. A major side reaction in the bleaching of hair involves the oxidation of cystine cross-links to cysteic acid residues. This disruption of disulfide cross-links in the cortex has a major influence on the wet tensile properties of hair. Alexander et al. [52] oxidized wool fibers to different extents with peracetic acid and determined the work required to stretch the fibers, both wet and dry, and the cystine contents of the fibers. They concluded that the disulfide bonds contribute largely to the wet breaking stress of the fibers. Furthermore, the wet breaking stress decreased almost linearly with the cystine content. In contrast, the dry breaking stress was virtually unaffected by disulfide bond rupture. In fact, Alexander et al. [53] found a weakening in the dry state only after more than 60% of the cystine cross-links were broken.

Harris and Brown [54] reduced wool fibers to different extents and methylated the newly formed thiol groups to prevent recombination to disulfide bonds. These scientists then determined changes in the 30% index of these fibers. Their conclusions were much the same as those of Alexander et al. [53], that is the wet breaking stress decreased with the cystine content but the dry breaking stress was virtually unaffected by cystine content except at high percentage rupture. Garson

Table 9.3 Tensile properties of frosted hair^a

Tensile parameter	Nonfrosted hair	Frosted hair	% loss in tensile property	% loss in cystine
<i>Wet tensile properties</i>				
Work to extend 20%	13.34	5.50	59	48
Hookean slope	13.25	5.79	56	48
Hookean limit	13.30	5.19	61	48
Force to extend 20%	16.67	7.01	58	48
Resilience ratio	0.587	0.585	0	48
<i>Dry (55% RH) tensile properties</i>				
Work to extend 20%	32.06	30.84	4	48
Force to extend 20%	36.71	33.80	8	48
Resilience ratio	0.173	0.115	44	48

Note: Work to 20% extension is g × cm, Hookean slope is in g force/mm elastic extension, Hookean limit is g, and force to 20% extension is g

^aData are normalized to a 70- μ m diameter basis at a length of 5 cm

et al. [55] measured the dynamic elastic properties of hair fibers. They found similar effects. These scientists found that the effects of oxidation are greater when measurements are made in water than at relative humidity ranging from 0% to 80%.

Oxidative bleaching of human hair on live heads provides similar results for the tensile properties. Robbins and Kelly [56] examined both the wet and dry tensile properties of frosted and non-frosted hair fibers from the same person (Table 9.3) that is hair that had been frosted on the head. Except for the resilience ratio, the loss in dry tensile properties was less than 10%, but the loss in wet tensile properties approached 60% at 48% disulfide cleavage. Therefore, these results are similar to the oxidation of wool fiber by Alexander et al. [53].

Alexander et al. [53] also suggested that both the dry and wet breaking stress of wool fibers are greatly influenced by peptide bond cleavage, but cleavage of the disulfide bond primarily affects the wet breaking stress. This effect likely occurs by breaking of crosslinks in the fiber and an increase in the water binding capacity of the fibers in critical regions of the cortex. The frosting treatment is an alkaline peroxide-persulfate system capable of some peptide bond cleavage, which likely accounts for the small losses in dry breaking stress. Peptide bond cleavage also likely accounts for the difference between the percentage decrease in cystine and the percentage loss in wet tensile properties.

Interestingly, the percentage change in the dry resilience ratio, an estimate of the ability of the fibers to recover from extension into the yield region, approximates the loss of cystine cross-links. Additional work is necessary to determine the significance of this observation. The above discussion suggests that the percentage loss in cystine, as estimated by cystine or cysteic acid analysis, is a good estimate of the loss in tensile properties of hair bleached by current “in use” treatments.

Since frosting of hair is an extreme bleaching treatment, an obvious question is to what extent milder bleaching treatments affect the tensile properties of hair. Several papers [56–58] describe bleach damage to hair either by cystine or cysteic

acid analyses [57] or by tensile properties [31, 58, 59]. In summary, these papers suggest that “in use” bleaching of hair commonly produces decreases in the wet tensile properties of up to 25%, with greater losses occurring when the fibers are frosted or stripped and in many cases of “in use” bleaching the changes in the dry tensile properties are very small and close to the limits of detection.

9.2.8 Permanent Waving Hair and Tensile Properties

Chapter 4 describes the chemistry of the reactions of permanent waves with human hair. Permanent waving involves reduction of disulfide cross-links accompanied by molecular shifting of proteins by bending the hair on rollers followed by mild re-oxidation. These reactions produce large changes to the tensile properties of the fibers during reduction but smaller changes after re-oxidation.

Data by Crawford (private communication) (see Table 9.4), using hair waved in the laboratory with a commercial home permanent at a 4:1 solution-to-hair ratio and then re-oxidized, showed a decrease in the tensile properties of approximately 5–20%. Beyak et al. [31] confirmed this finding for the wet tensile properties of permanent waved hair. This amount of tensile damage appears to be typical for a “normal” permanent-wave treatment, where approximately 20% of the disulfide bonds are ruptured during the reduction step [56]. Other reports in the literature, for example the paper by Tate et al. [60] show larger decreases in the wet tensile properties from permanent waving. Such effects are most likely from laboratory permanent waving as opposed to on head treatment and lab tests often involve a larger than “in use” solution to hair ratio.

Higher concentrations of mercaptan, higher pH [61], and higher solution-to-hair ratios all produce more extensive reduction [59, 62] and ultimately more tensile damage. The decrease in dry tensile properties is less than in the wet state. This is in agreement with the work of Harris and Brown [54], who showed that up to 60% elimination of disulfide bonds in keratin fibers, by reduction and methylation, produces only small effects on the dry tensile properties (65% RH). However, the wet tensile properties decrease almost linearly with the disulfide content.

Garson et al. [55] measured the dynamic elastic properties of hair and demonstrated that permanent-waving, similar to bleaching, provides greater changes to the elastic properties of hair in water than at relative humidity from 0% to 80%.

Table 9.4 Effect of permanent waving on the tensile properties of human hair (Crawford, private communication)

	Stress to break		Stress to extend 20%	
	Dry (65% RH)	Wet	Dry (65% RH)	Wet
Commercial home				
Permanent wave	–7%	–15%	–11%	–18%

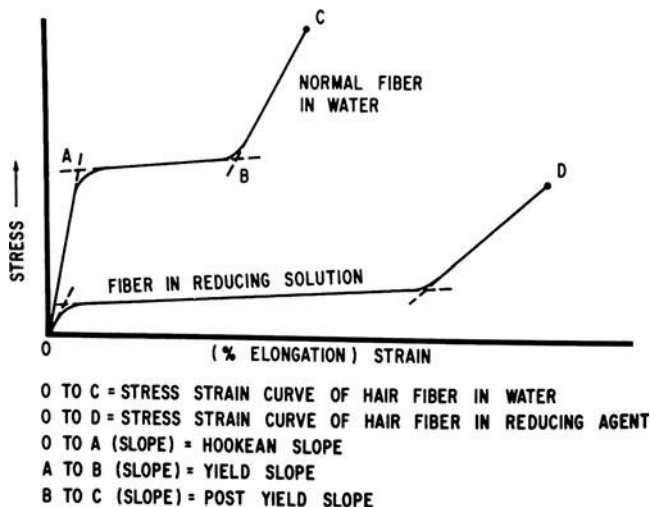


Fig. 9.13 Schematic diagram representing stress/strain curves for a hair fiber in reducing solution compared to a hair in water

Presumably, certain hydrogen bonds are inaccessible to water in “virgin” hair. However, elimination of specific disulfide bonds by oxidation and/or permanent-waving renders these additional hydrogen bonds accessible to liquid water or even at high regains (over 80% RH). Therefore, under these conditions those bonds are broken by water thus lowering the wet tensile properties more than the dry tensile properties.

Stretching hair fibers in aqueous solutions of reducing agents, compared to water, results in lower required stresses to achieve a given strain (see Fig. 9.13). This effect is due to the rupture of disulfide bonds, the breaking of hydrogen bonds, and molecular reorientation. Treatment of reduced hair with mild oxidizing agents (neutralization) increases the tensile properties, approaching the properties of the original untreated fibers. Such occurs if the fibers have not been reduced too drastically (beyond 30–50% disulfide rupture).

Load-elongation [63] and stress-relaxation [64] measurements may be used to follow the course of the reduction of keratin fibers by mercaptans. Extension into the post yield region is resisted primarily by the disulfide bonds [63], which is one reason that this region of the stress/strain curve holds special significance to the reduction reaction. However, Wortmann and Souren [65] pointed out that the main effect of reduction or the cleavage of disulfide bonds may be on the crystalline filaments. More specifically, the effect is likely on the interactions between the crystalline and surrounding structures rather than on the disulfide bonds themselves. Thus, the wet tensile properties serve as a valuable tool for studying the reduction of hair [61–66] its re-oxidation [63, 67], and the effects of the total cold-wave process [31, 58].

9.2.9 Alkaline Straightening and Tensile Properties

Alkaline straightening degrades both cystine and peptide bonds. Therefore, alkaline straightening must decrease both the wet and dry tensile properties of human hair. Nevertheless, I have not been able to find data in the literature to support this rather obvious conclusion. Data from Kamath et al. [15] demonstrated by fatiguing experiments that hair is weakened by alkaline straightening treatments. The hair used in this study was from a Black male age 31. This hair had never been treated with chemical or heat treatments. Both an alkaline and reduction type relaxer was shown to weaken the hair. With the alkaline straightener 8% of the fibers broke during treatment. In comparison, for the thioglycolate reduction treatment zero fibers broke during treatment. This effect shows more damage by the alkaline straightener in spite of the fact that a chemical neutralizer was not used after the reduction treatment by the thioglycolate system.

The fatiguing process involves attaching weights to the fibers and then dropping the weights repeatedly to stress the hair similar to the way it might be fatigued by continuous combing of the fibers. The data shows the largest distinction between untreated and treated fibers using the smaller rather than the larger weights. Therefore, the data (with smaller weights) are probably the most meaningful indicator of damage to the hair. These data clearly show that the hair is weakened or damaged by both treatments; however, more damage is indicated by the alkaline straightener than by the thiol type relaxer [15].

9.2.10 Dyes and Surfactants and Tensile Properties

Chapter 7 describes the chemistry of oxidation and ionic dyes in detail. Oxidation dyes are by far the most prevalent hair dyes, and consist of aromatic amines and phenols [68–70] that condense with each other and possibly with electron-rich side chain groups in hair. Oxidative dyeing is done in the presence of an oxidizing agent such as hydrogen peroxide at a pH of up to 10. The concentration of peroxide and alkali required depends on the difference between the starting hair color and the desired shade. Therefore, the primary tensile damage to hair by oxidation dyes depends on the extent of accompanying disulfide oxidation (bleaching) that occurs in the cortex of the hair. In theory, dyeing hair from a darker to a lighter shade should produce more wet tensile damage than dyeing hair from a lighter to a darker shade; however the more important factor is the extent of oxidation that occurs to the hair proteins in the cortex regardless of the shade difference.

Crawford (private communication) found small losses in tensile properties in hair dyed from a lighter to a darker shade with a commercial oxidation dye. Pande et al. [71] found 5–8% loss in the wet tensile properties (to 15% extension) for Permanent hair dyes and 2–6% loss for Demipermanent dyes. Pande et al. also

found that hair dyes provide protection from oxidative sun damage. In addition, the darker the dyes the more sun protection provided.

The tensile damage to hair by anionic and cationic surfactants or dyes in single treatments that is by short time intervals (hours) and moderate pH's is negligible. Zahn [72] examined the effect of anionic and cationic surfactants on the 25% index of wool and hair. Soaking wool fibers in sodium dodecyl sulfate for 7–41 days produced a decrease of only 6% in the 25% index. Shorter time intervals produced even less wet tensile damage. Zahn [72] indicated that for human hair the decrease is approximately one-half that of wool fiber, and these effects are reversible with water. Zahn indicated slightly larger effects from cationic surfactants. Scott (private communication) examined the stress/strain properties of hair after treatment with a cationic surfactant and found negligible changes. These results test the effects of surfactants on “chemically unaltered” hair, in single treatments, with no mechanical stresses applied. Interactions with other treatments were not considered.

Robbins and Reich, in unpublished work, conducted experiments showing that surfactants and mechanical stresses in combination (short-term treatments (min) attempting to simulate “in use” conditions) can damage the cuticle. But, damage to only the cuticle will not be demonstrable through changes in the tensile properties, a primary weakness of this type of test procedure.

Duvel et al. [46] cut long Caucasian hair into five sections from root to tip end and extracted and analyzed these sections by thin layer chromatography. These scientists showed three classes of major polar lipids including ceramides, glucosylceramides and cholesterol sulfate. In addition, they found as expected that the concentrations of all of these lipids as well as covalently bonded fatty acids decreased with increasing distance from the root end. The data on tensile properties also decreased as one moved from root to tip end. These scientists concluded that the progressive loss of structural hair lipids is a result of normal weathering of hair and grooming actions. Thus, weathering and grooming may help in some manner to contribute to the decrease in the tensile properties of the hair rather than to attribute the decrease in tensile properties to the loss of hair lipids alone.

9.2.11 pH and Tensile Properties

Speakman and Scott [73] found that the influence of pH on the tensile properties of human hair parallel the effects of swelling and pH on wool fiber. Valko and Barnett [74] showed that hair displays a minimum in swelling from pH 2 to 9 with a slight increase in swelling below pH 2 and a larger increase in swelling above pH 9, using extended soaking times (Fig. 9.14).

Breuer and Prichard [75] determined that when human hair is exposed overnight to solutions with pH values <2, it undergoes irreversible structural changes producing a decrease of up to 30% in the 20% index. Hydrolysis and structural rearrangements most likely occur from such a harsh acid treatment.

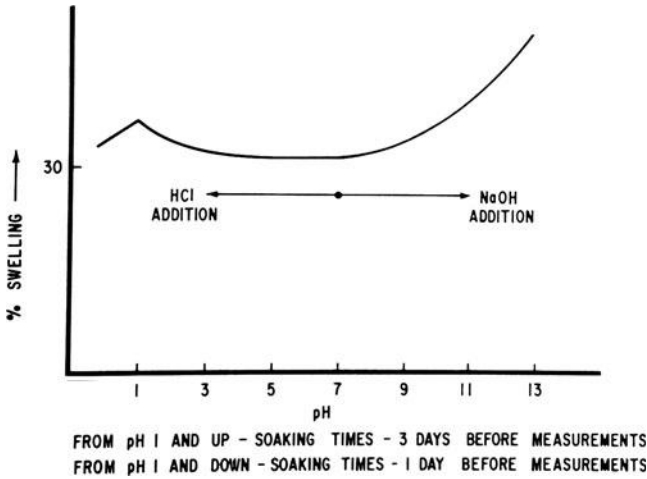


Fig. 9.14 Swelling of hair and changes with pH

9.2.12 Light Radiation and Tensile Properties

Sunlight and ultraviolet light have been shown to decrease the 15% index (in distilled water). Beyak [76] related this effect to the total radiation on the hair. These findings were interpreted as photochemical degradation of disulfide bonds and have been confirmed by Robbins and Kelly [77]. These scientists analyzed amino acids of both proximal and distal ends of human hair and found a significantly larger amount of cysteic acid and a significantly smaller amount of cystine in distal ends. Harris and Smith [78] provided evidence for ultraviolet disruption of cystine in wool fiber. Dubief [79] used the 15% index to follow changes induced in hair using different radiation sources and found about a 40% decrease in the 15% index after 3 months of summer sun exposure on a Paris rooftop. This effect calculates to about a 3 month Florida sun exposure of UV radiation for 24 h per day. See Chap. 5 for a discussion of the chemistry of these reactions and Chap. 10 on hair breakage.

Changes in the cuticle–cuticle CMC such as oxidation of the tertiary hydrogen atoms of 18-MEA has also been reported by Korner et al. [80] however such changes to the cuticle-cuticle CMC will not show up in tensile testing.

9.2.13 Hair Abnormalities and Tensile Properties

Korastoff [81] examined human hair from patients with hypothyroidism and acromegaly and showed a characteristic alteration in the yield region of the stress/strain curve (at low humidity) compared to hair from control groups. Swanbeck [82]

determined that patients suffering from congenital ectodermal dysplasia have hair of low tensile breaking force.

Monilethrix is a genetic anomaly in which hair fibers contain periodic constrictions along the fiber axis (see Chap. 3). Wilson [83] demonstrated that monilethrix hairs tend to fracture at these constrictions and therefore I conclude must exhibit abnormal stretching behavior. Trichorrhexis nodosa is another abnormal condition, wherein hair fibers contain nodes at irregular intervals along the fiber axis (see Chap. 3). These nodes actually contain tiny fractures and the fibers tend to form broom-like breaks [83] under stress. Therefore, nodosa hair fibers should also exhibit abnormal stretching behavior with premature failure at low strain levels. Pili torti is another congenital deformity in which severe twists occur in the fibers resulting in hair fibers that break easily. Therefore Pili torti hair must exhibit weak tensile behavior. Other hair shaft anomalies such as trichothiodystrophy and Menkes syndrome should also display abnormal stretching behavior consistent with the abnormal hair shaft condition associated with these diseases, see Chap. 3.

9.2.14 Reductive Polymerization in Hair and Metal Salts and Tensile Properties

Anzuino and Robbins [84] carried out in situ polymerizations of vinyl monomers in human hair. These scientists then studied the reactions of the polymer-containing hair with metal salts via wet load-extension testing. This reductive polymerization reaction decreased the wet tensile properties by approximately 15%. These scientists found that mercuric acetate treatment of hair containing polydimethylaminoethyl methacrylate, polyacrylonitrile, and polyethylene glycol monomethacrylate were the most effective systems for increasing wet load-extension properties. Although cross-linking through metallic bonding was proposed, an alternative mechanism involves reducing the water binding capacity of the fibers by the polymer and metal taking up space that could be occupied by water in critical water binding regions of the cortex.

9.3 Other Approaches to Evaluate Stretching Properties of Hair

Several other approaches have been used for studying the stretching properties of human hair. Among these approaches are vibration methods [10, 11], stress relaxation [64], stretch rotation [85], set and supercontraction [27], fatiguing [15] and extension cycling [16]. Several of these approaches will be described in some of the next sections of this chapter.

9.3.1 *Vibration Methods*

In this scheme, a fiber is attached to a beam with a known natural resonant frequency. Tension (within the Hookean region) is applied to the fiber. The beam is then deflected, and, from the change in the oscillation frequency of the beam with the fiber attached, and the natural resonant frequency of the freely vibrating beam, one can calculate the elastic modulus of the fiber. Huck and Baddiel [11] and Garson et al. [55] used this type of system to evaluate the elastic properties of human hair fibers. Huck and Baddiel attached both ends of hair fibers to an oscillating beam. This set up contained a third point of attachment in the middle of the fiber for applying tension. From the following expression, they calculated the elastic modulus:

$$E_s = \frac{8I^2L(B^2 - B_o^2)}{AZL^2}$$

B = the oscillation frequency with the fiber in position, B_o = the natural resonant frequency of the beam, L = the fiber length, I = the moment of inertia of the beam, A = the fiber cross-sectional area, and Z = the distance between the fiber ends.

The elastic modulus by this “dynamic” method is slightly higher than by load extension, a “quasi-static” method. Tests involving elastic deformations, where either stress or strain is held constant, are called static tests. In quasi-static tests, stress or strain is changed slowly with time, and in dynamic tests, stress and/or strain are varied rapidly with time.

9.3.2 *Stress Relaxation*

Stress relaxation is a technique in which the fiber is stretched to a given length, treated, and maintained at the stretched length while the decaying stresses are followed with time. Kubu and Montgomery [64] used this technique to follow the kinetics of the reduction of wool fiber. Robinson and Rigby [86] examined both wool and human hair fiber by stress relaxation. These scientists found differences along the axis of the fibers which they attributed to a decreasing free mercaptan level further from the root. This effect provides for less disulfide-mercaptan interchange and a slower rate of stress relaxation as the distance increases from the scalp.

9.3.3 *Stretch Rotation*

Hirsch [85] studied the elongation of hair under a steadily increasing load, together with a rotational movement. He attempted to explain this combination of stretching and torsion in terms of molecular structure. See the section on the torsional properties of hair in this chapter.

9.3.4 Set and Supercontraction

Brown et al. [87] defined set as a treatment that enables a keratin fiber to maintain a length greater than its original length. Chapter 4 describes setting as it relates to the cold-waving or permanent wave process. Supercontraction is not a stretching phenomenon. It is the condition in which a keratin fiber is fixed (by treatment) or held at a length less than its original length. Supercontraction is related mechanistically to setting and is also described in Chap. 4.

9.4 Bending and Fiber Stiffness

When a fiber is bent (see Fig. 9.15), the outer layers of the arc of the bent hair (A) are stretched, and the inner layers (C) are compressed. A region in the center, the neutral plane (B), is unchanged in length. Stiffness is simply the resistance to bending and is an important fundamental fiber property [88]. Recent evidence shows that bending stiffness of single hairs is very important to hair handle or

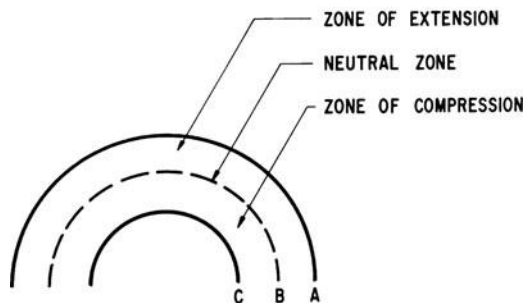
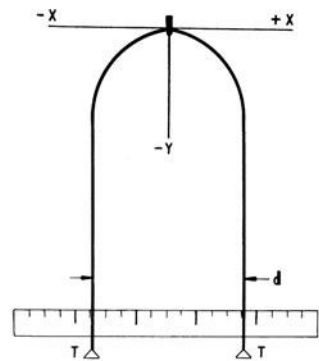


Fig. 9.15 Schematic diagram of the hanging fiber bending test [49, 89]. *Top:* Hair fiber photograph in the bending test. *Bottom:* Schematic of a bent hair fiber

feel, to combing forces and to hair breakage. See the section near the end of Chap. 10 for details.

9.4.1 Bending Methods

Several methods have been described for measuring the bending properties of hair fibers. For human hair, the balanced fiber method of Scott and Robbins [49, 89] appears to be the easiest to handle experimentally (except for very curly hair). This method provides less scatter (lower variances) than the other methods [49]. However, this method is only applicable to hair fibers of curvature Types I and II and possibly some of Type III, but not hairs with higher curvatures.

A newer method developed by Baltenneck et al. [90] involves a bending pendulum of parallel hair fibers. This method also appears to offer promise for determining the bending properties of hair fibers [90]. Baltenneck's method most likely could be used with hairs with higher degrees of curvature than the Scott and Robbins method.

The vibrating-reed method (oscillating fiber cantilever) has also been used with human hair [10]. The cantilever beam method [89], the loop deformation method [91], and the center load beam method [92] have also been described for textile fibers.

The method of Scott and Robbins involves attaching small equal weights to each end of the fiber. Each end of the fiber is individually threaded through a short length of plastic tubing. A tapered metal pin is inserted in the other end of the tube (the combined weight of pin and tube is known). The fiber is then hung over a fine wire hook and the distance d between the two vertical legs of the hanging fiber is measured (see Fig. 9.15).

The distance d is an index of stiffness of the fiber. The stiffness coefficient G (ratio of applied force to bending deflection) may be calculated from d using this expression:

$$G = T d^2 / 8$$

T is the force applied to each fiber leg in dynes ($g \times 980.6 \text{ cm/s}^2$).

The elastic modulus for bending E_B may also be calculated from d :

$$E_B = \frac{\Pi T d^2}{2A^2}$$

A is the fiber cross-sectional area, determined from diameter or linear density measurements.

Scott developed an equation that describes the hanging fiber shape by conventional X, Y coordinates and the d measurement. We have verified this equation by

showing that calculated fiber shapes are exactly superimposable on those of enlarged photographs of actual balanced hanging fibers (see Fig. 9.15).

The bending modulus E_B by this method at 62% RH and 75°F is approximately equal to Young's modulus for stretching (E_s) determined under similar experimental conditions by the load-extension method, $E_B = 3.79 \times 10^{10}$ dynes/cm² or 3,790 MPa. These values have not been corrected for fiber ellipticity. Such a correction may be considered academic, but it should make E_B slightly higher than E_s for human hair, because elliptical fibers orient to bend over their minor axis in this method.

Simpson's [10] values of E_B for human hair were higher 5.35×10^{10} dynes/cm² or 5,350 MPa. However, Simpson used the vibrating cantilever method. This procedure produces E_B values that vary with vibration frequency. Simpson also used a lower RH (50%).

The stiffness index of hair fibers by the method of Scott and Robbins provides falling curves when plotted against weight attached to the fibers. Routine measurements are made at 0.2 g total weight (0.1 g per fiber leg), and with a wire hook of 0.77 mm diameter (0.19–1.28 mm). For fine fibers, <50 μm in diameter, smaller weights (0.05 g per fiber leg) are recommended. (For additional details, see references 49, 89.)

9.4.2 Stiffness and Linear Density

The stiffness coefficient is directly proportional to fiber linear density. The data plotted in Fig. 9.16 provide an index of determination of 0.94 [49] demonstrating that 94% of the variation in stiffness (in this experiment) is accounted for by

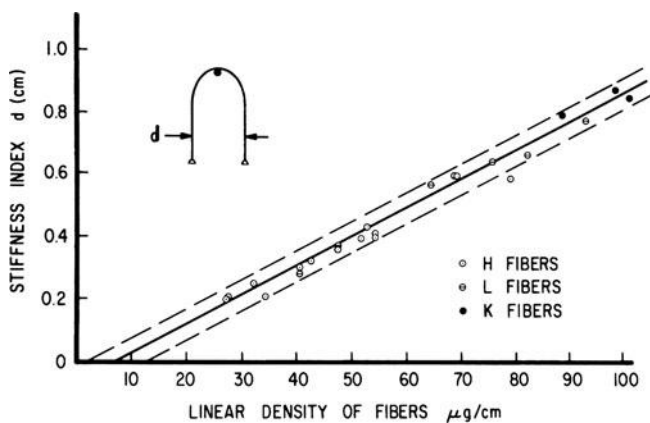


Fig. 9.16 Hair fiber stiffness index and linear density [49] (reprinted with permission of the Journal of the Society of Cosmetic Chemists)

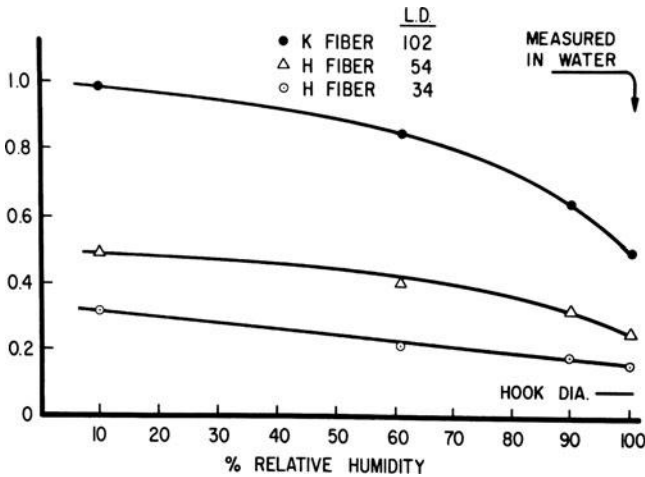


Fig. 9.17 Hair fiber stiffness versus relative humidity [49] (reprinted with permission of the Journal of the Society of Cosmetic Chemists)

variation in linear density. Therefore, consistent with theory, stiffness increases with fiber diameter. Theory predicts a fourth power dependence between fiber stiffness and diameter for a perfectly elastic system.

9.4.3 Stiffness and Relative Humidity

As one might anticipate, hair fiber stiffness also varies with RH. It decreases with increasing RH as shown by the Scott and Robbins method (see Fig. 9.17). We might conclude that hair fiber stiffness generally parallels fiber-stretching properties with respect to treatments. This conclusion is probably correct in most instances.

As indicated above, a novel approach to determining the bending properties of hair fibers was published by Baltenneck et al. [90] in which a bending pendulum composed of 39 parallel hair fibers, each 11 mm long and spaced 1 mm apart are fixed on a metallic support. The pendulum is then set into motion and the hair bending stiffness is assessed by the number of strokes observed until the pendulum stops. The data from this method on the effects of RH on bending stiffness agrees with that of Scott and Robbins [49], that is, the bending properties of hair decrease with increasing RH.

9.4.4 Bending Stiffness and Hair Damage

Baltenneck et al. [90] examined the bending properties of virgin and chemically damaged hair fibers. Their results show that virgin hair is less stiff than either

bleached (peroxide/persulfate bleach for 50 min) for most dry state conditions (20–80% RH). But, virgin hair is stiffer than permanent waved hair at 100% RH. Surprisingly, bleached hair did not show a difference in stiffness from virgin hair at 100% RH. This latter result is not consistent with results of Scott and Robbins.

9.4.5 Bending Stiffness and Hair Fiber Curvature

Elliptical fibers bend over their minor axis and most human hair fibers are elliptical rather than circular. Nagase et al. [93] found a statistically significant correlation of curl radius (Curl types I to IV) with ellipticity among hair from 132 Japanese women. However the index of determination was only 0.06 meaning that the ellipticity decreases only very slightly as the curl increases for relatively straight hair, that is only 6% of the variation in ellipticity could be explained by the curl radius. Therefore, from ellipticity effects alone, we would not expect a meaningful impact of hair fiber curvature on the bending properties of Asian type hair over the range of curvatures from Curl type I to IV. No large studies were found comparing curvature and ellipticity for Caucasian hair over Curl types I to IV.

However, African type hair is different. Porter et al. [47], from data on 12,050 hair fibers, found that African type hair becomes more elliptical with increasing hair fiber curvature ($R^2 = 0.947$). Therefore, 95% of the variation of ellipticity in African type hair can be explained by hair fiber curvature for curly hair. In addition, Porter et al. demonstrated that the cross-sectional area of African hair decreases with increasing fiber curvature. Elliptical ratios above 1.6 are common for African hair [47]. Therefore, other variables being equal we would expect the bending stiffness index to decrease with increasing hair fiber curvature for African type hair over the curvature range of curl types IV to VIII.

In contrast to the bending stiffness index, the bending modulus is a constant, calculated by dividing by the 4th power of the fiber diameter (diameter of minor axis). As indicated earlier, we know from work by Thibaut et al. [94] that the IF's and KAP's of the cortex of human hair become more asymmetrically distributed with increasing fiber curvature for African [94], Caucasian [94] and Asian hair [95]. This effect was demonstrated for Asian hair by Bryson et al. [95] resulting in different IF arrangements concentrated in the concave part of the curl versus the convex part of a curl, see Chap. 1 for details. Therefore the bending modulus should change with increasing hair fiber curvature because of the changing arrangements of these cortical structures with curvature.

9.4.6 Bending and Possible Cuticle Contributions

There is evidence that the cuticle also plays a role in the bending properties of keratin fibers as shown by Kawabata et al. [96] on wool fiber and by Masaaki [97],

Swift [98] and by Atushi et al. [99] on human hair fibers. Hadjur et al. [100] described a lack of symmetry in the number of cuticle cells near the minor axis versus the major axis of elliptical African hair fibers. A lack of symmetry in the cuticle of curly African type hair fibers versus greater symmetry for straighter hair of Asians and Caucasians should affect the bending and torsion properties. Nevertheless, I have not been able to find any studies relating hair fiber curvature to the bending properties of hair fibers.

9.5 Torsion and Fiber Rigidity

Hair fibers are routinely twisted during combing, brushing, and setting; however the extent of twist is relatively small compared to the twist required to break a fiber. The resistance to twisting is the torsional rigidity. By definition, rigidity is the torque required to produce a twist of one turn per centimeter [91]. Rigidity in twisting is analogous to stiffness in bending and is a fundamental property to hair fibers. Furthermore, torsion and fiber swelling methods measure stresses and therefore bonding perpendicular to the fiber axis better than any other method.

9.5.1 Torsion Methods

Several methods have been described for determining the torsional rigidity and the torsional modulus (modulus of rigidity) of hair and/or textile fibers [8, 37, 101–107]. Basically, these methods are related to the torsion pendulum method [8, 102, 105, 107]. The torsion pendulum method involves suspending a small pendulum from a fiber. The fiber is then set into free rotational oscillation. By determining the period (P) of oscillation (time of vibration, which generally averages 10–20 complete oscillations), the fiber length (L), the fiber diameter (D), and the moment of inertia of the pendulum (I), the torsional modulus E_T may be calculated.

$$E_T = \frac{128 \Pi \Pi L}{P^2 D^4}$$

The rigidity R (resistance to twisting) may be calculated from this expression:

$$R = 8 \Pi^3 I L / P^2$$

And the rigidity is related to its modulus by:

$$E_T = R / J A^2$$

A is the fiber cross-sectional area and J is a shape factor, usually assumed to be 1 for human hair and wool fiber.

Another useful torsion parameter is the logarithmic decrement (δ). This parameter describes the decay in amplitude of the untwisting pendulum with successive oscillations:

$$\delta = (1/n) \ln(a_1/a_n)$$

n = the number of oscillations and a_1 and a_n are the amplitude of the first and the nth oscillation. This logarithmic decrement is an indication of the torsional elasticity of the system. When $\delta = 0$, the fiber is perfectly elastic, and as δ increases the fiber becomes less elastic. The logarithmic decrement is related to the torsional loss modulus (E_T') in the following manner:

$$E_T' = E_T \delta / \Pi$$

A major drawback to the simple torsion pendulum method was that it could not be used while the fiber is immersed in liquids because of the damping effect of the liquid. However, Wolfram and Albrecht [107] devised a very clever scheme to overcome this obstacle by inserting the fiber into a small glass capillary tube, thus permitting the torsional properties of hair fibers (and other fibers) to be measured in both air and liquids. Other methods are available [103, 104, 108] for measurement of the rigidity of fibers immersed in liquids. For additional details, see the references indicated and the texts by Meredith and Hearle [108] and Morton and Hearle [92].

9.5.2 Rigidity and Moisture

The torsional modulus for human hair by the pendulum method is lower than either the stretching or the bending modulus at 60–65% RH. But more importantly, water has a greater effect on torsional properties than on either stretching or bending for both human hair and wool fiber (see data describing these three different elastic moduli: Tables 9.5 and 9.6).

For wool fiber the effect of water on the torsional properties is almost 3–4 times as great as on the bending or stretching properties, whereas for human hair the

Table 9.5 Comparison of the stretching, bending, and torsional moduli for human hair at 60–65% RH [106] (Scott, private communication)

E_S	E_B	E_T
3.89×10^{10a}	3.79×10^{10a}	0.89×10^{10a}
3890 ^b	3790 ^b	890 ^b

^aThese values are dynes/cm². E_B and E_S were determined at 62% RH and room temperature

^bThese values are in MPa

Table 9.6 Influence of moisture on stretching, bending, and torsional moduli

	E_s		E_B		E_T	
	0% RH/ 100% RH	65% RH/ 100% RH	0% RH/ 100% RH	65% RH/ 100% RH	0% RH/ 100% RH	65% RH/ 100% RH
Human hair	–	2.62 [30]	3.8 ^a	2.4 ^a	–	4.1 [103]
Wool fiber	2.76 [25]	2.58 [33]	–	–	16.1 [33]	9.2 [33]

^aCalculated from unpublished data by Dr. G.V. Scott

effect is nearly a factor of 2 between 65% and 100% RH (see Table 9.6) and it should be much greater from 0% to 100% RH.

Wolfram and Albrecht [107] found that the logarithmic decrement varies with fiber diameter. This parameter decreases with increasing fiber diameter in water, but it does not vary with diameter at 65% RH. This finding suggests that in water, the hair is less elastic or more plastic. These scientists implicate the cuticle as primarily responsible for this increase in torsional plastic behavior for human hair in water and as shown later in this section; cuticle effects on the torsional behavior of hair fibers are measurable in contrast to tensile effects.

9.5.3 Torsion and the Cuticle and Elliptical African Hair

Masaaki [97] examined the torsional modulus of rigidity on both intact hair and hair in which the cuticle was removed by rubbing. His results demonstrated that the cuticle is about 3.5 times as rigid as the cortex. Therefore, the cuticle plays a major role in the twisting properties of human hair fibers. These results are in agreement with a similar study on wool fiber by Kawabata et al. [96] who examined the bending and shear properties of wool fiber in which the scales were removed by chlorine treatment. Kawabata et al. found that the shear modulus of wool without scales decreased significantly, demonstrating that the cuticle does contribute to shearing effects in hair fibers.

Persaud and Kamath [8] demonstrated that the shear modulus decreased with increasing cross-sectional area for European dark brown hair. Since the ratio of cuticle to cortex increases as hair becomes finer, these scientists concluded that the cuticle is highly involved in the torsional properties of hair fibers. Since the cuticle to cortex ratio also decreases as hair diameter increases, these scientists conclude that the rigidity of the cuticle dominates this measurement. Their data also showed a large increase in energy dissipation for fine to medium hairs after saturation with water and they concluded that the cuticle to cortex ratio plays less of a role for a coarse fiber’s energy dissipation in the wet state. These authors interpreted this effect as a contribution of the high cuticle to cortex ratio in large log decrement values for the fine fibers versus the corresponding values at 65% RH.

As indicated, Dankovich et al. [43] demonstrated that twisting highly elliptical hairs even at low twist levels produces cuticular damage with scales compressing into one another from “tangential compression”. This cuticle damage was less in more circular hairs. Since Porter et al. [47] showed that ellipticity increases with increasing fiber curvature from Curl type VI to Curl type VIII ($R^2 = 0.95$), we would expect that this type of cuticle damage from twisting will increase with increasing fiber curvature for African type hair. African hair often contains natural twists; therefore, twisting hairs with natural twists should be even more complicated. Such an effect has not been reported in the literature.

9.5.4 Torsional Behavior of Damaged Hair

Bogaty [106] examined the torsional properties of permanent-waved and un-waved hair. His results, summarized in Table 9.7, suggested that waved hair is more rigid at low RH and less rigid above 90% RH than un-waved or virgin hair. Wolfram and Albrecht [107] examined the torsional behavior of permanent-waved, bleached, and dyed hair. These scientists confirmed the finding of Bogaty that permanent waved hair (reduced hair) is less rigid than chemically unaltered hair in the dry state. These same scientists also found that the rigidity ratio ($R_{\text{water}}/R_{65\% \text{ RH}}$) is lower for bleached hair than for dyed hair, consistent with the greater amount of disulfide bond cleavage by bleaching as compared to permanent dyeing.

If one takes ratios of the dry to wet torsional modulus in Table 9.7, it is apparent that there is a greater effect of moisture on the torsional properties of waved hair than on the torsional properties of chemically unaltered or virgin hair.

The torsional behavior of hair, more than the tensile behavior, is dependent on the cuticle or the external layers of the fiber because of greater shear forces in the periphery versus the center of the fiber during twisting. Torsional behavior is also more sensitive to water than tensile properties. Permanent waves and bleaches do change the torsional properties of hair, as demonstrated by Wolfram and Albrecht. Therefore, torsional methods should prove one day to be more sensitive to cuticle damage than current tensile methods.

Persaud and Kamath [8] used their torsional pendulum method to examine damaged hair and the performance of several hair care active ingredients including

Table 9.7 Torsional moduli of waved and un-waved hair from data of Bogaty [106]

% RH	Unwaved hair MPa	Waved hair MPa
41	1,190	1,250
58	1,060	1,130
65	890	990
81	730	760
93	420	400
100	220	140

a cationic surfactant, a conditioning polymer and hair spray films. These scientists also used the elliptical cross-section of hairs instead of assuming circularity to calculate torsional rigidity to refine their torsional data. Persaud and Kamath found that the torsional properties of hairs treated with hair spray dissipate more energy versus un-treated hairs. Persaud and Kamath suggested that the hair spray polymer is softer than the cuticle and deforms more than the cuticle thus energy dissipation is higher for hair spray treated fibers.

Persaud and Kamath [8] also examined the effects of a cationic polymer (Polyquaternium-10) and of a cationic surfactant (Cetyl trimethyl ammonium bromide) on bleached hair in this same study. Bleaching significantly reduces the shear modulus at 65% RH due to oxidation of disulfide bonds to cysteic acid and the subsequent additional water absorption in the hair (particularly in the rigid cuticle layers and in the matrix of the cortex). Treatment of the bleached hair with the cationic polymer produced a small increase in the shear modulus and in the average log decrement values confirming a detectable effect of ingredients on and in the surface layers of the fibers.

Treatment of bleached hair with 0.5% of the cationic surfactant produced a large increase in the shear modulus and a significant reduction in the average log decrement values relative to the bleached controls. This stronger effect is probably due to penetration of the surfactant into the cuticle layers and perhaps even into the cortex as opposed to the cationic polymer which is confined more to the surface of the fibers.

Thus Persaud and Kamath [8] demonstrated the sensitivity of the torsional method to all three of these hair treatments that act predominately on and in the cuticle; whereas tensile measurements did not show any significant changes with these same treatments confirming that tensile properties are a property of the cortex [7] and that torsional measurements are more sensitive to effects on and in the cuticle and to effects involving changes in water content of the total fiber.

9.5.5 Damage to Hair by Twisting

Twisting hair and twisting and stretching hair is described in the section entitled *Twisting and Stretching Normal Hair and Hair with Natural Twists* in this chapter.

9.6 Density of Hair (Mass/Volume)

The density of human hair in solutions of benzene-carbon tetrachloride was determined by the method of Abbott and Goodings [109]. The density of chemically unaltered hair at 60% RH varied from 1.320 to 1.327, depending on lot (dark brown European hair from DeMeo Bros., New York, and three samples taken from heads of volunteers). The density of our wool control was 1.320, identical with one lot of

Table 9.8 Variation in the density of wool fiber with RH [110]

% RH	Density
0	1.304
15	1.3135
25	1.3150
68	1.3125
85	1.304
94	1.2915
100	1.268

hair. Permanent waving did not change the density of hair. Bleaching (approximately 25% disulfide rupture) increased it, but only by 0.45%.

King [110] determined the density of wool fiber as a function of RH. Some of King's results are summarized in Table 9.8. King's data show that density changes are negligible for wool fiber from 15% to 85% RH or normal room humidity. One would expect the density versus RH relationship for wool and human hair to be similar, since their densities at 60% RH and their moisture binding versus RH relationships are virtually identical as demonstrated later in this chapter. Hearle and Peters [111] explained that the increase in fiber density with moisture regain from 0% to 15% RH is contrary to expectations and is not fully understood.

The objective of these density experiments was to determine the relative density of human hair and wool fiber and the influence of damaging cosmetic treatments on this important property. The results of these experiments confirm the conclusions of several others [91, 112]: the densities of human hair and wool fiber are similar, and there is no appreciable change in the density of human hair from permanent-waving or bleaching treatments.

9.7 Dimensions, Swelling and Effects of Fiber Shape on Reactivity

Two of the most commonly measured hair fiber dimensions are length and diameter. Assuming that a hair fiber approximates a cylinder, its volume, cross-sectional area, radius, and surface area may be obtained from formulae that describe the volume of a cylinder (V_{cylinder}), the area of a circle (A_{circle}), and the surface area of a right cylinder (S_{cylinder}), in terms of its diameter (D) and length (L).

$$V_{\text{cylinder}} = 0.7854 D^2 L$$

$$A_{\text{circle}} = 0.7854 D^2$$

$$S_{\text{cylinder}} = D \Pi L$$

Although human hair fibers vary in cross-sectional shape, from nearly circular to elliptical and even "triangular", normalizing for most elastic and other properties to

fiber coarseness can significantly reduce experimental scatter. A convenient equation for calculating the cross-sectional area of an ellipse is:

$$A_{\text{ellipse}} = \pi R_1 R_2$$

where R_1 is the radius of the maximum diameter and R_2 is the radius of the minimum diameter.

Whenever maximum and minimum diameters are given one may calculate the average diameter from the following equation:

$$D_{\text{average}} = \sqrt{D_{\text{maximum}} \times D_{\text{minimum}}}$$

Fiber thickness is usually characterized as fiber diameter or cross-sectional area. Corrections to diameter for ellipticity are often not employed and are usually not required except for highly elliptical hair fibers. Hair fiber dimensions are also necessary to calculate fundamental elastic properties, and dimensional changes are often employed to follow the course of chemical reactions with hair.

For measurement of short lengths of hair fibers (in the millimeter range or less) a microscope may be used, but for longer lengths (several centimeters or longer) a cathetometer is useful. Although fiber diameter may be measured directly with a microscope, or more crudely with micrometer calipers, other excellent methods are available for determining cross-sectional dimensions of human hair. More recently laser scanning equipment has been employed similar to the system described by Li and Tietz [113]. This approach should improve the precision of the measurements over microscopy especially when averaging over large sections and large numbers of fibers.

9.7.1 Methods to Determine Hair Fiber Dimensions

Both single-fiber and multiple-fiber methods are available for determining hair fiber cross-sectional dimensions or changes. Single-fiber methods include linear density, microscope (light or electron), vibrascope, micrometer caliper, and laser beam diffraction. For multiple-fiber determinations, a centrifuge and optical scanning devices may be used.

9.7.1.1 Linear Density Method

The linear density method is one of the methods of choice, for determining hair fiber coarseness (diameter). A fiber is cut to a given length (10 cm is convenient), conditioned at 55–65% RH, and weighed on a microbalance sensitive to 2 μg or

better. This gives the fiber weight in g/cm, which is divided by the fiber density, 1.32 g/cm^3 , to obtain the cross-sectional area in cm^2 (A).

$$A = \frac{\text{g/cm}}{1.32}$$

The area so calculated is independent of cross-sectional shape. The fiber diameter (D) may then be calculated, assuming circularity:

$$D = \sqrt{A/0.7854}$$

The volume (V) in cm^3 for a given weight (M) of hair may be calculated from the fiber density:

$$V = M/1.32$$

Finally, the length (L) of a fiber of volume V and radius r may be rechecked (since it is precut at a specified length and measured):

$$L = V/r^2\Pi$$

The length may then be used to estimate the surface area (Su).

$$Su = 2\Pi r L$$

This scheme assumes that the density of all hair fibers is the same. It requires a minimum of manipulations and is an excellent “averaging technique” for dry state dimensions of hair fibers. Cross-sectional area and volume estimates for circular and elliptical fibers should be relatively accurate, as well as diameter and radius for round fibers. This method does not provide an indication of ellipticity, but provides an average diameter with respect to length as well as to cross section (average diameter, not maximum or minimum diameter). The deviation of fiber diameter with increasing ellipticity is described in Table 9.9 which shows only about 1% difference in cross-sectional area by assuming circularity or a regular ellipse from 40 to 120 microns and from an elliptical ratio of 1.10–1.78.

9.7.1.2 Microscopic Method

Several excellent papers [114–116] describe experimental details for measuring the diameter of human hair fibers with a light microscope. Once the diameter is obtained, calculation of radius, cross-sectional area, volume, and surface area may be made as described in the previous section.

Table 9.9 Deviation of the diameter of a circle from the major and minor axes of an ellipse

Area assume	Average D assuming	Ratio D ₁ /D ₂ ^a							
		1.108		1.234		1.500		~1.78	
Circle μm ²	Circularity μm	D ₁	D ₂	D ₁	D ₂	D ₁	D ₂	D ₁	D ₂
1,257	40.0	42	38	44	36	49	32.7	53.3	30
Ellipse area		1,253		1,244		1,258		1,256	
11,310	120.0	126.3	114	133.3	108	147	98	156.5	92
Ellipse area		11,308		11,307		11,314		11,308	

D₁ = major axis of ellipse, D₂ = minor axis of ellipse and R₁ and R₂ = radius in μm

^aCalculations above assume that the cross-sectional shape is that of a regular ellipse and these equations were used for the average diameter and area of an ellipse:

$$D_{\text{average}} = \sqrt{D_{\text{maximum}} \times D_{\text{minimum}}} \text{ and } \text{Area} = R_1 \times R_2 \times \pi$$

The light microscope is an excellent instrument for determining dimensional changes in hair fibers while they react with either liquid or gaseous systems (including moisture in air). The light microscope can also be used to measure deviation from circularity; although, extensive manipulation and multiple measurements (10–20) along each fiber's axis are required for accurate measurement. A modern scanning electron microscope, with vernier, is also a useful instrument to measure dry state (approximately 0% RH because of evacuation) diameter of human hair fibers.

9.7.1.3 Vibrascopic Method

The vibrascope [117, 118] is a device that applies an oscillatory force of known frequency to a filament under tension. The fiber cross-sectional area (A) in cm² may be computed from the lowest (natural) frequency (f) in cycles per second that produces mechanical resonance. The tension (T) on the fiber is in dynes, the fiber length (L) is in cm, and its density is 1.32 g/cm³.

$$f_i = \frac{1}{2L} \sqrt{T/1.32 A}$$

The fiber diameter, radius, volume, and surface area may then be calculated as described.

This method assumes that the fiber is a homogeneous filament and provides an average diameter. Nonetheless, it has been shown by Montgomery and Milloway [117] to be in close agreement with microscopic measurements of the diameter of nylon fibers. The vibrascopic method, like the linear density method, is an excellent averaging technique and offers time advantages over microscopic methods.

9.7.1.4 Micrometer Caliper Method

This method works well for hard fibers like steel, tungsten, and glass, but not as well for softer fibers like human hair. It is a crude but fast way to approximate hair fiber diameter. Since hair fibers yield to low compression forces, and these forces are difficult to control, the micrometer caliper technique tends to provide low values for fiber diameter and a large variance.

9.7.1.5 Sieving Hair Fibers

Busch [119] used fine-mesh sieves to separate fine hair fibers from a bundle for further characterizations. It is conceivable that further separations of hair fibers may be achieved via sieving and average diameters approximated via this useful technique.

9.7.1.6 Laser Beam Diffraction Method

Brancik and Datyner [120] described the diffraction of monochromatic light from a laser to measure the diameter of single wool fibers in liquids. Busch [119] used a laser beam diffraction system with robotic control for characterizing hair fiber diameter and shape for a large number of hair fibers. Also, see the paper by Li and Tietz [113].

9.7.1.7 Centrifuge Method

The centrifuge method has been described by Valko and Barnett [74] and by Barnett [121]. This method involves treating a known weight of parallel fibers (400–800 mg and approximately 20 cm long) with a liquid, centrifuging to remove excess liquid between the fibers, and reweighing. This is a good averaging technique for multiple fibers and is well suited to follow reactions with hair fibers by measuring the percentage weight gain of liquid imbibed by the hair. This method may be used to approximate fiber volume changes in aqueous systems, since weight gains at different relative humidity correspond relatively well to volume increases (see Table 9.10). From volume changes, cross-sectional area, diameter, length, surface area, and other dimensional changes may be computed (see the section entitled Linear Density Method for details).

9.7.1.8 Optical Scanning Devices for Determining Fiber Diameter

OFDA (optical fiber diameter analyzer) laser scanning as described by Watt [123] was originally developed for the wool industry. However, this method has found

Table 9.10 Percentage weight and volume changes versus RH for wool fiber

% RH	Changes caused by absorption of water		
	% volume [122] increase	% weight [37] increase	% weight [74] increase
0	0	0	0
9	–	3.9	–
10	5.7	–	–
20	–	–	7.6
40	12.2	10.2	–
60	16.3	–	–
63	–	14.8	–
86	–	22.6	–
90	24.6	–	–
100	32.1	31.2	31.1

Table 9.11 Hair fine to coarse and fiber diameter by Courtois et al. [124]

Hair fineness	Fiber diameter (µm)
Very fine	<35
Fine	35–50
Medium	51–65
Thick (coarse)	66–80
Very thick (very coarse)	>80

application for most natural and synthetic fibers including human hair. This method essentially takes images of an array of fibers (several hundred in cross-section) and scans the field with a laser that measures the width or diameter of the exposed fibers that are free from other fibers. Temperature and relative humidity are also recorded at the time of measurement. This method offers time and cost advantages and averages a large number of hairs.

9.7.2 Fine Coarse Hair

Consumers usually evaluate fine or coarse hair by handle or feel; however scientists generally evaluate these parameters by measuring fiber diameter or cross-sectional area. Fine and coarse distinctions are used for qualitative comparisons in the cosmetic industry, but there are no accepted quantitative definitions of these terms analogous to wool fiber. One reference that defined fineness of human hair quantitatively by fiber diameter is by Courtois et al. [124] in a study of ageing and hair cycles. This reference defined hair fineness by the diameters summarized in Table 9.11.

Although such a classification of hair fineness by diameter as in Table 9.11 might be useful in some cases, it describes the average hair of Caucasians and Africans as coarse and the hair of Asians (described below) as very coarse. However, this is not the way we normally classify Caucasian hair. To date, I have

Table 9.12 Fine-coarse wool fibers defined by fiber diameter [111]

Type of wool fiber	Diameter in μm
Ultrafine merino	<17.5
Superfine merino	17.7–18.5
Fine merino	<19.5
Fine medium merino	19.6–20.5
Medium merino	20.6–22.5
Fine	<24.5
Medium	24.5–31.4
Fine crossbred	31.5–35.4
Coarse crossbred	35.5

not been able to find any other reference that used this quantitative classification by Courtois et al. [124].

On the other hand, coarse and fine are more clearly defined quantitatively for the wool industry because the diameter of wool fibers is related to both the end use and to the breed of sheep/animal. Table 9.12 shows definitions for wool fiber diameters expressed as fine or coarse with additional distinctions. In general, wool fibers <25 μm in diameter are used for garments whereas coarser grades are used for outerwear or rugs. Such distinctions for wool fiber are clearly more useful than for human hair; however, some quantitative distinctions for coarse and fine human hair could be useful to the cosmetic industry.

9.7.3 *Variation in Fiber Cross-Sectional Shape with Emphasis on Diameter and Ellipticity*

9.7.3.1 **Fiber Diameter by Geo-Racial Group**

The term race applies to sub-populations or groups of people similar in several biological characteristics. In the past, races developed and persisted because travel over large distances was limited, thus, similar peoples interacted and procreated. The geographic or racial differences that are found today in hair and skin type are most likely remnants of prior adaptations to temperature, sun exposure and other environmental influences.

The words ethnic and ethnicity have been misused in the cosmetic industry. Ethnicity relates more to similarities in or shared social customs. Race relates more to similarities in physical characteristics. In the following pages I refer to geo-racial groups linking geographic origin to race. I will try to refrain from using the phrase ethnic hair, but I will sometimes inadvertently use the term geo-ethnic. The cosmetic industry frequently refers to these three primary geo-racial hair types: African type hair originates primarily from south, west, or central Africa and the donors with a few exceptions tend to have heavily pigmented skin. Asian type hair originates from mid-eastern and south East Asia and the donors tend to have light to

medium skin pigmentation. Caucasian hair originates from northern Europe or North Africa and the donors tend to have lightly pigmented skin, but some may have heavily pigmented skin.

These geo-racial groups will be referred to frequently in the sections involving hair fiber shape focusing on fiber diameter, ellipticity and hair fiber curvature. These three geo-racial groups correspond to the Ethiopian, Mongolian and Caucasian groups used in a prior edition of this book. Fiber curvature and cross-sectional shape as well as pigmentation variations of human scalp hair are controlled genetically (Chap. 3) and these fiber shape characteristics control much of the cosmetic and physical behavior of human hair. Therefore, geo-racial information on hair characteristics can and has been useful to the cosmetic scientist, although a century from now it will likely be less useful.

Other classifications such as by curvature type will ultimately become more important to cosmetic science than the three geo-racial groups because curvature is so important to all cosmetic hair assembly properties as discussed in the last part of Chap. 10. Consider the fact that the cosmetic behavior of scalp hair of a Caucasian of Curl type IV hair by the STAM procedure [47] (see the section entitled, *Measuring Hair Fiber Curvature in this Chapter*) has more in common with Curl types IV of the African and Asian groups than with a curl Type I or II of their own geo-racial group. The commonality is in the way their hair behaves with regard to the more important cosmetic hair assembly properties described later in Chap. 10.

During the latter days of this century and the next, populations of Curl types III, IV and V will likely increase and Curl types I and VIII will decrease. So, in the near future we must learn to type hair even better by its physical characteristics and become more quantitative with regard to its relationships to its important cosmetic hair assembly properties. Table 9.13 summarizes the general qualitative characteristics of the scalp hair of the three major geo-racial groups.

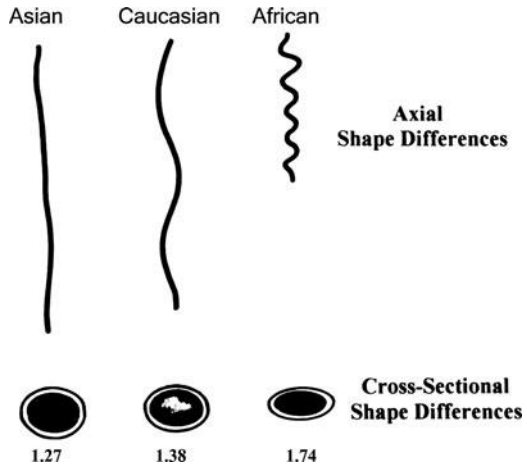
It is generally accepted that on average the hair of Africans and Asians is coarser than that of Caucasians [125, 126]. Randebrock [126] suggested that human hair from the scalp varies from 40 to 120 μm in diameter. Kaswell [127] indicated that the diameter of human scalp hair varies from 15 to 110 μm . The lower end of this estimate likely includes infants and children's hair. Yin et al. [112] suggested that Caucasian hair of adults (the finest of the three major races) varies from 50 to 90 μm . Yin is talking about the variation in diameter means of the hair of individuals rather than the total variation among individual hairs among different

Table 9.13 Hair fiber characteristics by geo-racial group

Geo-race	Fiber characteristics [125, 126]			
	Coarseness	Curvature	Cross-sectional shape	Color
Caucasian	Fine	Straight to curly	Nearly round to oval	Blond to dark brown
African	Coarse	Wavy to wooly	Slightly oval to elliptical	Brown-black to black
Asian	Coarse	Straight to wavy	Nearly round to slightly oval	Dark brown to brown-black

See Fig. 9.18

Fig. 9.18 General shapes of human hair of different geo-racial origins



Caucasians. We found slightly greater variation for the means of Caucasian individuals' hair than suggested by Yin et al.

Other sources cite even larger variation for example, Elert [128] cites from 17 to 181 μm . Elert most likely is referring to variation among individual hairs and not mean fiber diameters for individuals, and Elert likely includes minimum to maximum fiber diameter for adult, children's and infants' hair rather than means. For example, Nagase et al. [93] measured maximum and minimum hair fiber diameters on hair from 132 Japanese females ranging from 10 to 70 years of age. The maximum diameters, of 8,926 hairs, varied from 30 to 170 μm averaging $95.3 \pm 16.5 \mu\text{m}$ and the minimum diameters varied from 30 to 130 μm averaging $74.4 \pm 10.5 \mu\text{m}$.

Table 9.14 summarizes means for human scalp hair diameter by geo-racial group from several references showing that hair from Caucasians is finest and hair from Africans is coarser while hair from Asians is coarsest. For this table, I attempted to use averages from hair of 10 or more persons per group. In a few cases I could not do so. The pooled hair was averages of 10 hairs from each group with hairs from more than one person. The Steggarda and Siebert [129] data used in previous editions was deleted because these scientists used hairs from only five females.

The actual diametric variation of individual hairs must be greater than shown in the distributions of Table 9.14 which are obtained from averaging means of several hair fibers for several subjects. The three largest studies of the data listed in Table 9.14 are the study by Nagase et al. [93] on scalp hair of Japanese females ages 10–70 and the study of Trotter and Dawson [133] on hair of "American whites" and French Canadians [131]. Data was extracted from these two latter studies for females of ages 10–89. Nagase et al. measured and listed maximum and minimum diameters while Trotter and Dawson measured linear densities on the hair of American whites and French Canadians. For French Canadian hair, these scientists also measured maximum and minimum diameters and linear densities from which the calculated diameters compared favorably.

Table 9.14 Mean fiber diameter (MFD) and cross-sectional area of scalp hair of three geo-racial groups (females)

Reference	Asian scalp hair		African scalp hair		Caucasian scalp hair	
	MFD (N)	Area	MFD (N)	Area	MFD (N)	Area
Wolfram [130]	77 (20)	4,657	66 (20)	3,421	72 (20)	4,072
Syed [44]	–	–	77 (10%)	4,657	74 (10%)	4,301
Trotter [131]	–	–	–	–	66.8 (154)	3,504
Trotter et al. [133]	–	–	–	–	70.5 (120)	3,902
Franbourg [132]	78 (18)	4,804 ± 159	77 (16)	4,274 ± 215	69 (20)	3,857 ± 132
Nagase [93] J	84.2 (132)	5,568	–	–	–	–
Tajima [135] J	83.3 (113)	5,450	–	–	–	–
Otsuka et al. [134] J	81.2 (7,585)	5,178	–	–	–	–
Otsuka et al. [134] C	80.23 (957)	5,056	–	–	–	–
Galliano [136] C	87.2 (19)	5,974	–	–	–	–
Porter [47]	–	–	71.2° (274)	3,979°	72.5 (16)	4,124
Mean	81.6 ± 3.6 (n = 8,854)	5,241 ± 173	72.8 ± 5.3 (n = 320)	4,083 ± 521	70.8 ± 2.6 (n = 340)	3,960 ± 275
Total persons	–	–	–	–	–	–
Vermall [137] MENE	85.1 (n = 20) C	5,688	75.8 (n = 19)	4,513	68.2 (n = 21)	3,653
Trotter [133] MENE	–	–	–	–	69.0 (131)	3,739

MFD in μm ; N = No. persons; Area in μm^2

Most of these studies used a microscopic method except for Franbourg [132] and Nagase et al. [93] who used a laser method. The studies by Trotter [131, 133] are calculated from linear densities for females and males ages 10–49. Otsuka and Nemoto [134] did not describe methods. When maximum and minimum diameters were cited this equation was used to calculate the mean fiber diameter $D = \sqrt{d_{\text{max}} \times d_{\text{min}}}$. ¥ pooled hair, J Japanese hair, C Chinese hair, €MEN ages 20–30 by Vermall [137] and 10 to 49 for Trotter, F represents area calculated by the following formulae: $A = r_1 \times r_2 \times \Pi$ for an ellipse or by $A = \text{MFD}^2 \times 0.7854$ for a circle giving essentially equivalent areas otherwise areas are quoted from the paper. ° Calculated from relationship by Porter et al. [47] for Curl Class and Area and the average Curl Class for African hair

Table 9.15 Approximate scalp hair diameters by race/country for females (ages 10–89) [134]

	Asian		Caucasian	
	Japan (J) + China (C)	Japan + China + Thai	USA Eur. + Am	W. Germany
Approx. D (μ)	~81	~79	~53	~58
N	8,537	16,380	574	595

^aActual, averages were not given in this paper. The above diameters are estimates of diameters rounded off from midpoints of bar-graphs [134]. It is unfortunate that the actual data with statistics, sampling details and measuring methods were not published in this very large and useful study

The percentage standard deviations of the data of the two studies by Trotter and the one by Nagase were similar and close to 17% which was used to estimate the likely range of means from individual persons for each of the three geo-racial groups. These estimates for Asian hair, 54–110 μm , for African hair 48–96 μm and 46–94 μm for Caucasian hair. This is a much more conservative and very different estimate than the 95% confidence intervals for the actual data of Table 9.14 which is for Asian hair 84.9–78.3 μm and 78.99–64.51 μm for African hair and 72.99–68.6 μm for Caucasian hair. The 95% confidence interval is actually the range within which the actual mean of that data is likely to reside at the 95% level.

The study by Otsuka and Nemoto [134] was the largest study found in the literature for human hair diameters (Table 9.15). This paper did not describe details of how the hair was obtained or measured. The data of Table 9.15 shows that the Asian hair sampled was coarser than the Caucasian hair examined. These data also show that sampling or the actual populations chosen to represent either the Asian or Caucasian hair groups can have an influence on the dimensions found. For example hair from females in Japan and China provided a slightly larger diameter than hair from females from Japan, China and Thailand combined.

The diameter estimates for the Asian hair in this study by Otsuka and Nemoto are close to those of the averages of the studies of Table 9.14; however the estimates for the Caucasian hair are considerably lower than those found for Table 9.14. Otsuka and Nemoto suggest about a 30 μm difference between Caucasian hair and Japanese hair, but the data of Table 9.14 suggest about half that difference. I conclude that part of this difference (between Otsuka and Nemoto data and the data of Table 9.14) is from real diametric differences and part to sampling, scalp site and to un-described methodology [134]. For example, Trotter and Dawson [131, 133] found that hair of French Canadians (N = 136) was 4 micrometers coarser than hair of European “white Americans” (N = 183). In the data of Table 9.15 we see a similar difference for the two Caucasian groups, but part of this difference may also be due to experimental variation.

Trotter and Dawson found that the hair of the French Canadians was darker in color than that of the Americans which could be due to differences in physical characteristics resulting from genetics and in this case related to geographical distribution of the different Caucasian populations. For example, the Trotter and Dawson data may include hair of northern Europeans (American whites) versus southern Europeans (French Canadians), a difference which is frequently

Table 9.16 Calculated maximum D and minimum D and cross-sectional areas for Asian, African and Caucasian hair

Hair type	Ave D	Max D	Min D	Elliptical ratio ^a	Cross-sectional area	Ave. curl type
Asian	82	93.4	72.7	1.28 ^a	5,333	II
Caucasian	70	82.8	60	1.38 ^a	3,902	II, III
African	72	93.6	55.8	1.68 ^a	4,104	IV to VIII

Diameter values in μm and area in μm^2 (average D is from Table 9.14)

All other values calculated from these equations via iteration

$$\text{Elliptical Ratio} = \text{Max D/Min D}$$

$$\text{Ave D} = \sqrt{\text{Dmax} \times \text{D min}}$$

$$\text{Cross - sectional area} = \pi \text{Rmax} \times \text{Rmin} (\text{R} = \text{radius})$$

^aSee Table 9.17 for references on elliptical ratios

speculated and described for a limited number of individuals hair, but for which I could not find a large supporting study.

Frequency graphs for each group of women in the study by Otsuka and Nemoto [134] approximate a Gaussian distribution. Random sampling of large groups of women in most populations likely are similar provided ages are limited from about 10 to 60. When a large percentage of older persons are included, especially older men, the distributions will tend to deviate from Gaussian; see the section in this Chapter entitled, *Hair Diameter of Males versus Females*. Table 9.16 was constructed primarily from calculations to approximate the average maximum and minimum diameters and cross-sectional areas from the three major geo-racial groups. Whether one calculates cross-sectional areas assuming circularity or a regular ellipse the results are within 1% of each other (see Tables 9.9 and 9.16).

A discussion of how hair fiber diameter varies with age is described in this chapter in the section entitled, *Fiber Diameter, Cross-sectional Area, Fine Coarse Hair and Hair Growth*.

9.7.3.2 Hair Fiber Diameter and Ellipticity Variation Along the Fiber Axis or Length

In 1942, Seibert and Steggerda [138] examined long hairs cut from the scalps of 7 Caucasian and 9 Mayan females. They selected the longest 80–100 hairs averaging 40–50 cm long and measured maximum and minimum diameters on these fibers sectioned at 2, 10, 20, 30, and 40 cm from the original cut near the scalp. In all but 3 of 16 cases the hairs were larger in area and maximum diameter at their terminal or distal end than at the basal cut. This effect is significantly different by the non-parametric sign test. In addition, the ellipticity (major to minor axis of the diameter) tended to decrease in the direction toward the scalp.

About 50 years later, Hutchinson and Thompson [139] reported changes in the major-axis diameter of human scalp hairs that they associated with changes occurring inside the follicle, during the growth of human hairs. Hutchinson and Thompson concluded that hair fibers do not grow as uniform cylinders. But, they

hypothesized that from the distal end of each hair fiber for a distance toward the scalp of about 6–8 cm an increase in diameter occurs that they associated with the start up of anagen (approximately 5–7 months growth). After that distance of 6–8 cm, their data showed a gradual decrease in the major-axis, but not the minor axis of the fiber. The overall effect from that point is a gradual decrease in fiber ellipticity, cross-sectional area and diameter of each hair shaft.

When reading this paper, I was skeptical because the authors miscalculated cross-sectional areas by a large factor and they hypothesized in some instances without data. But after reading the previous paper by Steggarda and Siebert [138] and the following paper by Nissimov and Elchalal [140] I came to accept the gradual decrease in the major axis from the distal end of the fiber.

Nissimov and Elchalal [140] confirmed this effect and they observed the opposite effect during pregnancy. That is during pregnancy the major axis of the fibers increased from distal to proximal end by 4.5% through 35 weeks of pregnancy. This study was conducted on 15–20 hair fibers each from 13 non-pregnant women (average age 36 years) and 12 post-term pregnant women (average age 29 years). The major axis of the hair fibers in the control group of non-pregnant women during this same 35 week period decreased from distal to proximal end by 5.2%. The decrease in the major axis of hair fibers from only 4 Caucasian non-pregnant women observed by Hutchinson and Thompson was 16.4%. Only a small (likely non-significant) increase of 2.5% was observed in the minor axis on these same hair fibers.

Such variation within each hair fiber helps to explain the wide variation that we observe in maximum and average fiber diameters and ellipticity and when considered with variation among individual hairs on a head and between heads why large sample sizes are necessary to provide meaningful data when measuring hair fiber diameter parameters.

9.7.3.3 Ellipticity of Human Scalp Hair by Geo-Racial Group

Table 9.17 shows that hair from Africans has a greater deviation from circularity (average major axis to minor axis D_1/D_2 of 1.74) than hair from the other two geo-racial groups and compares favorably with the calculated value of Table 9.16.

The hair from Asians is the most circular with an average elliptical ratio of 1.27 and for Caucasians, this ratio is 1.38 and is very close to be calculated values of Table 9.16. These data suggest that the calculated circular diameter for Asian and Caucasian hair averages about 13% and 16%, respectively, from the major and minor axes of noncircular fibers. Therefore, in most circumstances, the assumption of circularity is an acceptable approximation. However, this deviation averages about 26% or greater for most African hair. So, the assumption of circularity for African hair should be carefully considered.

The confidence intervals above in Table 9.17 suggest that there is a 95% probability that the true mean is within this interval. The distributions of the individual geo-racial groups are normal and the Asian, African and Caucasian means are all significantly different by parametric and non-parametric statistics.

Table 9.17 Ellipticity of hair fibers from three geo-racial groups

Source	Asian		African		Caucasian	
	Mean (N)	Range	Mean (N)	Range	Mean (N)	Range
Steggarda [129]	1.25 (10)		1.65 (9)	1.25–2.05	1.35 (10)	
Wolfram [130]	1.29 (20)	1.21–1.36	1.84 (20)	1.67–2.01	1.49 (20)	1.43–1.56
Syed [44]	–		1.83 ^a	1.69–2.09	1.29 ^a	1.06–1.52
Vernall [137]	1.23 (20) J		1.69 (19)		1.44 (21)	
Franbourg [132]	1.23 (5)	1.16–1.28	1.78 (14)	1.67–1.85	1.32 (11)	1.25–1.39
Nagase [93] J	1.28 (132)	1.02–2.19	–		–	
Porter et al. [47]	–		1.67 (241)			
Mamada et al. [141] J	1.28 (38)				1.40 (35)	
Galliano et al. [136] C	1.31 (19)				1.40 (16)	
Trotter [131]					1.36 (340)	1.09–2.13
Trotter et al. [133]					1.36 (300)	
MEAN	1.27		1.74		1.38	
†Confidence Interval	1.239–1.296		1.655–1.831		1.332–1.426	
‡Estimated Ranges	1.02–2.19		1.25–2.09		1.06–2.13	

Ellipticity is D_{max}/D_{Min} ; No. persons = (N)

^aPooled hair, C Hair from Chinese, J Hair from Japanese

† Confidence intervals suggest a 95% probability that the true mean is within this interval

‡ Estimated ranges suggest the variation in ellipticity found among individual hairs

The estimated distributions suggest variation in ellipticity found among individual hairs from the data by Nagase [93] and by Trotter [131, 133].

The study by Nagase et al. [93] contained 132 Japanese females ages 10–70 and a total of 8,926 hairs were measured for maximum and minimum diameter. Therefore, this study is the most reliable with respect to the range of ellipticity for individual hairs (not means) for this geo-racial group, which varied from 1.02 to 2.19 with a mean of 1.28 comparing favorably with the average of all the studies of 1.27. This study by Nagase et al. also shows that individual hairs from Asians can vary in ellipticity from nearly circular to highly elliptical.

Trotter and Dawson [133] and Trotter [131] measured ellipticity on 6,400 Caucasian hair fibers from 242 males and 398 females. This study is described in more detail in the next section of this Chapter. Statistical analysis indicated no difference in ellipticity between males and females. Ellipticity for these 6,400 hairs varied from 1.09 to 2.13 similar to the range found by Nagase et al. on the hair of Japanese females. Note that the ranges for these two studies are similar, but the means are different 1.36 for Caucasians versus 1.28 for the Japanese. Also, the ranges are larger than for the Africans because of the much larger number of hairs used in the Caucasian and Japanese studies. These distributions are obviously not Gaussian, but when 25 or more hairs are averaged the means are quite reliable. Also note that, the size and shape of hair fibers vary along the fiber length as described earlier. Some of these variations have been attributed by Orwin [142] to growth patterns and environmental effects.

9.7.3.4 Hair Fiber Ellipticity and Age Among Caucasians and Asians

Hair Fiber Ellipticity and Age Among Caucasians

To date, I have been able to find several studies of hair fiber ellipticity versus age [131, 133, 143]. Three of these papers are from the anthropological literature by Trotter and cited in the previous section. In Trotter's earliest paper [131], she took hair from 340 Caucasians (American whites) ages 0–79 and measured the major and minor axis diameters of hairs taken from the vertex and calculated both cross-sectional sizes and ellipticity. Ten hairs were used per subject.

Trotter and Dawson [133] also measured the major and minor axis of 10 hairs per subject from the vertex of 300 Caucasians (French Canadians), 122 males and 178 females age 1–89. If we combine the results of these two studies we have ellipticity measurements of 6,400 hairs from Caucasians. The results are summarized in Table 9.18 showing an average ellipticity of 1.36 for Caucasians with a range of 1.09–2.13 in the study on Americans. Trotter separated the data for the French Canadians into seven different age groups for males and females and eight different age groups for the American Caucasians allowing matched pairs statistical analysis testing for seven groups of the data showing no significant difference for the ellipticity between Caucasian males and females in both studies and an average ellipticity of 1.36 for Caucasians.

Hair Fiber Ellipticity for Caucasians from Infancy Through Childhood

Trotter and Duggins [143] ran another study among Caucasian children by having hair sent to them periodically at 1 year intervals starting with infants through puberty. This study was discontinued after 17 years because of drop-outs. These scientists started with 15 infants each at 1 month (50 hairs) and 7 months (50 hairs) and summed these two data points to represent 100 hairs at age 1 (closer to ½ year). Then they measured 100 hairs from each of these same 15 subjects at 2 years of age, with one additional child at age 2 and continued with these 16 children until age 7. At age 8 one dropped out, but at age 11 four other children dropped out until age 13

Table 9.18 Hair ellipticity for two groups of Caucasians [131, 133]

Group	No. subjects		Mean ellipticity		Ellipticity range	
	Males	Females	Males	Females	Males	Females
French Canadians	122	178	1.37	1.38		
American Caucasians	120	220	1.35	1.34	1.09–1.75	1.11–2.13
Total Caucasians	242	378	1.36	1.36	1.09–1.75	1.11–2.13
Matched pairs test ^a	Prob < t = 0.28		Prob < t = 0.69		1.31–1.43	1.27 ^b –1.48

^aNote, the mean ellipticities for males and females are exactly the same. The matched pairs groups (seven pairs or groups of the same ages) were not matched in terms of numbers of subjects

^bOnly eight subjects in this group

Table 9.19 Means for the effects of age on the hair index from approximately 1 month through age 10 for the same 14 Caucasian children

Age	Average index ^a	Maximum/minimum diameter (ellipticity)
1 month	79.42 ^b	1.26
2 years	69.36	1.44
3 years	69.64	1.44
4 years	70.93	1.41
5 years	70.71	1.41
6 years	72.07	1.39
7 years	72.07	1.37
8 years	73.07	1.37
9 years	73.14	1.37
10 years	72.29	1.38
7 months	73.57	1.36

^aThe hair index is the ratio of the minimum diameter to the maximum diameter times 100. The ellipticity is the reciprocal of the index times 100
 Data were evaluated by the Wilcoxon signed rank test for paired observations, and ^bindicates the values that are significantly different from all others. The lines indicate the values that are not significantly different from each other

when four more dropped out rendering the study suspect beyond 10 years of age. Their data up to 10 years of age are summarized in Table 9.19.

Not counting the 1 month and 7 month sampling, Trotter and Duggins had collected yearly data points measuring 100 hairs from each of 14 subjects from age “1” through age 10. Trotter and Duggins [143] commented on the small difference found between the males versus females. However, since only six males and eight females were in this study I concluded that the sample size is too small for a meaningful comparison.

I analyzed these data of Trotter and Duggins by not combining the 1 month and 7 month data and by not examining data beyond age 10. I used the Wilcoxon signed rank test for paired observations. The results are summarized in Table 9.19 and demonstrated that the largest change occurs after 1 month where the hair is more round in the earliest stage of infancy. The 1 month data is significantly different from all other ages including the 7 month measurement ($P < 0.0001$). It would also appear from diameters that another change occurs a few years later.

Hair Fiber Ellipticity Versus Age Among Asians

Another useful study on ellipticity versus age is at higher ages and is from a paper by Nagase et al. on Japanese hair [144]. The authors of this paper [144] measured ellipticity among 132 Japanese females. These scientists found no statistically significant effect for the variation of ellipticity with age from 10 to 70 years.

Regression analysis provided an average ellipticity of 1.28 with a significant p value, but an index of determination (r^2) of 0.0001 showing that the variation in ellipticity by age among Japanese females was very small (0.01%) or not meaningful.

This study on the hair of Japanese women shows no effect of age on hair fiber ellipticity between the ages of 10–70 while two studies on Caucasian males and females over a similar age range also showed no effects of age on scalp hair fiber ellipticity. I would speculate a similar effect for African hair, but not with a high level of confidence because of the very large hair fiber ellipticity among that geothnic group.

9.7.3.5 Fiber Diameter, Cross-Sectional Area, Fine Coarse Hair and Age and Hair Growth

Infants' is Finest and Children's' Hair is Fine; for Females it is Coarsest (Largest Diameter) Near the Mid-Forties but Males' Hair is Coarsest in the Late Teens to Early Twenties

As described in Chap. 1, the mechanism for hair growth involves three stages: a growing period called anagen; a transition period, catagen and a resting period, telogen. At telogen, the “old” hair falls out and is replaced by a “new” hair fiber. The time-span of the growth period (anagen) determines how coarse and how long scalp hair fibers will become. The time-span of anagen is shortest for infants, longer for children and longest from puberty to young adulthood, see Table 9.20.

Trotter and Duggins [143] studied hair fiber cross-sectional areas from infancy through childhood on the same 14 Caucasian subjects that they studied ellipticity from 1 month through 10 years of age. Their cross-sectional area data along with fiber diameters (calculated assuming circularity) are summarized in Table 9.21.

The data of Table 9.21 were analyzed by the Wilcoxon signed-rank test for paired observations showing highly significant differences between the cross-sectional areas at 1 month, 7 months and 2 and 3 years from all other ages. Several of the other pairs were not significantly different as indicated by the connecting lines

Table 9.20 Hair growth period, fine coarse hair and hair length of Caucasians females

Hair type	Approximate Max. length (cm)	Approximate Diameter (μm)	Est. anagen (Yr)
Infant	~15	30 (N = 26) ^a	~0.5
Children (0–9)	~60	62 (N = 82) ^b	~4 yr
Adult (15–29)	~100	74 (N = 98) ^b	~6 yr
Adult (30–89)	–	70 (N = 75) ^b	~5 yr
Vellus	~0.1	~4	–

^aPecoraro V et al. [146], 26 full-term infants; hairs taken within 76 h of birth (13 males and 13 females)

^bCalculated from Bogaty [145] and from Trotter and Dawson [131, 133]

Table 9.21 Cross-sectional area and calculated average diameters versus age for hair from Caucasian children from Trotter and Duggins [143]

Age	Cross-sectional area (μm^2)	Calculated average diameter (μm)
1 month	529 ^b	31
7 months	957 ^b	35
2 years	1,929 ^b	50
3	2,357 ^b	55
4	2,721	59
5	2,787	60
6	3,064	63
7	3,193	64
8	3,271	65
9	3,407	66
10	3,457	66

^aDiameters calculated assuming circularity

^bSignificantly different from all other values. Lines indicate those values that are not significantly different from each other by the matched pairs test

in this table. Clearly, the cross-sectional areas are smallest at 1 month. The cross-sectional areas and therefore average diameters are also smaller at 7 months, 2 years and 3 years compared with all other values except 1 month. Three to four times the percentage change in cross-sectional area occurs between 1 and 7 months and 7 months and 2 years compared to the total change that occurs between 4 and 7 years of age. These dimensional changes in the hair fiber correspond reasonably well with the generalized description by Furdon and Clark [147] that the fine hair of infants tends to be lost by about the sixth or seventh month and is replaced by a coarser hair that grows longer. This hair then is replaced by an even coarser hair at about 2–3 years of age that grows even longer.

Hair Fiber Diameter Versus Age for Males and Females

The study by Otsuka and Nemoto [134] on the hair of Japanese males (1,177) and females (7,580) between the ages of 10 and 60 shows a larger and earlier decrease in hair fiber diameter for men than for women; see Tables 9.22 and 9.23.

For Japanese males, the study by Otsuka and Nemoto shows that scalp hair fiber diameter increases to a maximum to the late teenage years and then it decreases relatively rapidly with increasing age, see Fig. 1.10. These data suggest that for Japanese women, scalp hair diameter increases to a maximum near the age of 40 and decreases thereafter.

Similar effects (a peak in diameter during the teenage years for males followed by a gradual decline after that and an increase in diameter for women during the teens to the 40s when a decline begins) can be seen in a study by Trotter and Dawson [133] for hair of French Canadians (see Table 9.23). Trotter and Dawson noted this effect was not statistically significant by comparing subgroups of males

Table 9.22 Hair fiber diameters versus age for Japanese men and women [134]^a

Age	Predicted diameter(μm)	
	Men	Women
15	84	79
20	84	81
25	83	82
30	81	82
35	79	82
40	76	82
45	72	80
50	68	78
55	63	75

^aData points were estimated from a graph in this paper [134] and prediction equations calculated. Data points for diameters of the table are from the prediction equations and all were within $\pm 1\%$ of the graph data points rounded off to the nearest micrometer. Prediction equations were, for men $Y = 95.58 - 0.484 X - 0.01279(X - 32.75)^2$; for women $Y = 84.11 - 0.0483 X - 0.01387 (X - 33.7)^2$ where Y = predicted diameter and X = age

Table 9.23 Scalp hair fiber diameter (in μm) and age for males and females

Approximate ages	Instantaneous rates of change of diameter in μm/year				
	10–14	15–19	20–29	30–49	50 plus
^a Males Japanese	84	86	83	78	63
^b Males French Canadians	68	74	73	71	64

Instantaneous rates of change of scalp hair diameter (OFD) for Caucasian females by age £

Age	Instantaneous rates of change of diameter in μm/year	
	Average instantaneous rate ^a	Mean diameter (μm) ^b
25	0.45	63.94
30	0.33	65.90
35	0.22	67.27
40	0.097	68.06
45	-0.021	68.25
50	-0.14	67.86
55	-0.26	66.86
60	-0.38	65.27

^aAverage of instantaneous rates from regression models

^bCalculated mean diameter values from model for OFD

£ Robbins and Dawson et al. [148]; maximum for female Caucasians between ages 43 and 46

versus females. However, the study of Trotter and Dawson involved only 136 females and 82 males compared to 18,262 females and 1,177 males in the Japanese study.

The work of Courtois et al. [124] comparing hair fiber diameters on the same male subjects over a period of several years provides support for a decrease in hair diameter of male Caucasians with age between the ages of 25 and 49. Courtois et al. [124] studied 10 Caucasian adult male subjects (starting at ages 25 up to 49 years of age) by making observations periodically over 14 years. These scientists demonstrated a reduction in the duration of the growth period (anagen) coupled with a decrease in the diameter of hair shafts with increasing age. In addition, the time interval separating the loss of a hair in telogen and the appearance of a replacement hair in anagen also increased.

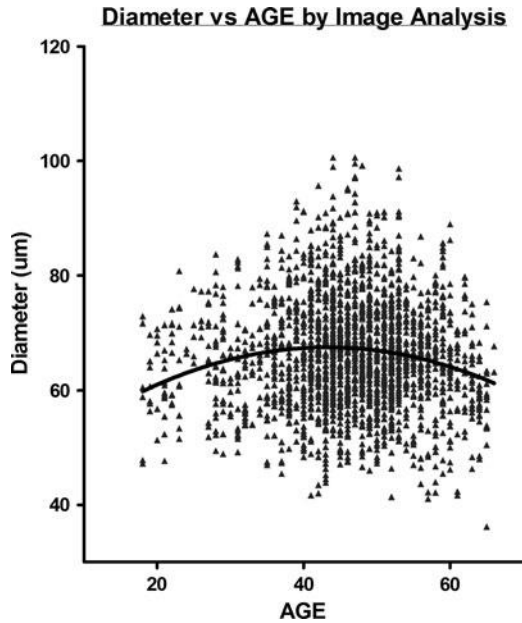
Therefore, this study by Courtois et al. [124] on Caucasian adult males demonstrated that hairs on the same male Caucasians after puberty become finer over the years confirming the conclusions of Otsuka and Nemoto [134] on age and fiber diameter on different Japanese males. This study by Courtois et al. on adult Caucasian males also confirms the conclusions on the effects of age on the diameter of scalp hair of male Caucasians from the French Canadian data of Trotter and Dawson.

A very large study by Robbins and Dawson et al. [148] measured mean hair fiber diameters from 250 to 400 hair fibers from each of two sites one on the left and one on the right parietal region on more than 1,000 female Caucasians from age 18 to 66. In this study both an Optical Fiber Diameter (OFD) system and an Image Analysis system were used for diameter measurement; therefore, these data were not included in Table 9.14. However, data comparing the OFD method with laser, microscopic and linear density methods on the same 39 hair samples demonstrated 77.31 μm for the OFD and 75.57 μm for the laser (no significant difference), 71.34 μm for the linear density and 66.7 μm for the microscopic method with both of the latter methods providing significantly different diameters from the OFD method.

The OFD and the IA data from this large study of female Caucasians were regressed against age providing a curvilinear relationship, see Fig. 9.19. The maximum mean fiber diameter occurred between 43 and 46 years of age (by both diameter measurements) and is likely linked to the peri-menopause. The quadratic equation for the OFD method provided a $p < 0.0001$, $r^2 = 0.0257$ and a root mean square error of 9.380 with a maximum diameter at age 43. A cubic equation provided a $p < 0.0001$, $r^2 = 0.0282$ and the root mean square error was 9.370 and a maximum diameter at age 46, see Fig. 9.19. Data from the quadratic model along with instantaneous rates of diameter change with age are summarized in Table 9.23.

The data from Table 9.23 shows that hair fiber diameter in the parietal region of female Caucasians increased from about age 18 until about 43–46 whereupon it peaked and then decreased with increasing age. This effect contrasts with data for males [131, 133, 134] where the maximum for mean fiber diameter peaks in the late teens to early twenties, see Tables 9.22 and 9.23.

Fig. 9.19 Hair fiber diameter for Caucasian females by an image analysis method from Robbins and Dawson et al. [148]



Data for scalp hair diameter of Japanese females has been shown to occur somewhere around the age of 40 [134] and the median menopausal age occurs at about 50–51 for women of most industrialized countries including Japan. Therefore, it is likely that menopausal status has a similar effect on scalp hair diameter of women of most industrialized countries and that estrogens are somehow involved in hair fiber diameter. Therefore the mean fiber diameter for hair from Japanese women may actually be a little higher than found in the study by Otsuka and Nemoto and closer to the age of 43–46 as shown for Caucasian women by Robbins and Dawson et al.

The quadratic model for the subjects in the Robbins and Dawson et al. study suggests that the instantaneous rates of change of diameter (Table 9.23) or the speed of hair diameter change actually decreased at a constant rate of $-0.0236 \mu\text{M}/\text{year}$ (2nd derivative of the quadratic model). Even though the actual diameter increased from age 20 to about 45 the rate and amount of diameter increase actually decreased and it continued to decrease at this constant rate to about age 45 whereupon the diameter began to decrease and this process continued with advancing age.

The Effect of Scalp Site on Hair Fiber Diameter

Mirmirani and Dawson et al. [149] demonstrated that mean fiber diameters for female Caucasians are significantly higher in pre- versus post-menopausal women for the frontal but not the occipital site. The larger study by Robbins and Dawson et al. [148] shows that the parietal region follows a similar pattern to the frontal site. The

maximum mean fiber diameter in the parietal region occurred in the vicinity of the peri-menopause which is characterized by irregular periods or cessation of periods for less than 12 months. These studies collectively suggested that menopausal status has a major impact on scalp hair fiber diameter for the frontal and parietal regions but not the occipital site. This study also suggests that more studies on different scalp sites are necessary to fully understand the properties of human scalp hair.

The follicle is the sac that each mammalian hair fiber grows in. In sheep, fine-wool breeds tend to have follicles of narrower diameters whereas longer follicles correlate with longer wool fibers as shown by Orwin [152]. We would expect similar trends to exist in human hair. Furthermore, Lindelof et al. [150] provided evidence that the size and shape of the human hair follicle tends to correlate with the hair fiber shape. However, there is strong evidence that hair fiber composition and the distribution and orientation of different proteins in the cortex provide the major contribution to the hair fiber shape (see Chap. 1 for a more complete discussion of this subject).

Why Hair Fiber Diameter of Males Versus Females Provides Inconsistent Results

Steggarda and Seibert [129] examined scalp hair fibers from six different racial groups and claimed significant differences by sex. However, these scientists examined hair fibers from only five males and five females for each group measuring 70–100 hairs from each person.

The confusion in the scientific literature about the diameter of hair of males versus females can be explained by examining the studies of Otsuka and Nemoto [134], Robbins and Dawson [148] and the work of Trotter and H.L. Dawson as summarized in the preceding section. These studies all show that hair fiber diameter for females increases until about 40–46 years of age, however the work of Otsuka and Nemoto and Trotter and Dawson and Courtois all show that the diameter of scalp hair of males peaks much earlier, somewhere near the age of 20. Therefore, diameter comparison of the scalp hair of males versus females is most likely very dependent on the sampling ages. If additional differences exist between the scalp hair of males and females due to geo-racial effects (between Asians and Caucasians) these will only be evident after larger scale comparative studies are conducted.

The largest difference in the diameter between hair of males and females most likely occurs at middle age (near ages 35–46), where the diameter of the hair of females is near a maximum and the diameter of the hair of males had been decreasing for about two decades. This difference most likely will become smaller as we move to younger ages from middle age to the teenage years and should either become equal or cross over near ages 15–20.

Fine Hairs do not Grow as Long in Length as Coarse Hairs

Infants' hair generally does not exceed 15 cm length and it is very fine. Pecoraro et al. [146] examined the hair of 26 new born infants within 76 h of birth. These scientists found that the average diameter was 30 μm and estimated the anagen period to be only a few weeks. Children's' hair prior to puberty usually does not exceed 60 cm long and it is coarser than infant's hair as shown by Bogaty [145]. But, adult hair has the capacity to grow even longer and is even coarser. With advancing age, hair fibers become finer [131, 133, 134, 148] and will not grow as coarse [124, 134] or as long as in prior adulthood. Courtois et al. [124] demonstrated for male Caucasians that with increasing age beyond puberty, anagen becomes shorter. Saitoh et al. [151] examined the hair of one Japanese male at 60 years of age. Saitoh et al. found the average anagen for hair fibers growing on the vertex of the scalp was 23 weeks and the range was 17–94 weeks for “coarse” hair. These same scientists [151] found longer anagen time spans for two other subjects 21 and 30 years of age, but the time spans for anagen exceeded the time allocated for writing the paper so additional data was not available.

Because of the relationship of the time-span of anagen to hair fullness on the scalp and to longer and coarser hairs, anagen to telogen ratios have been used to measure either hair growth or hair loss. The evidence shows that coarse hairs on the same person become finer with advancing age [124] confirming the conclusions of Otsuka and Nemoto [134] on age and fiber diameter on different persons. Furthermore, the growth period and hair length (if never cut) also become shorter. These facts suggest that neighboring hairs on the same scalp that are finer should also not grow to as long a length as coarser hairs (never cut). Furthermore, fine versus coarse hairs among different persons will likely not grow as long in length and they will have a shorter anagen time span.

Hair Fiber Diameter Varies by a Factor of About 2 on Each Scalp

Most of the work in the scientific literature is on scalp hair from the vertex or the crown area of the scalp, although hair from other areas of the scalp is sometimes used [149]. Garn in his PhD thesis at Harvard University in 1948 was one of the first to claim that scalp hair is finest at the temples and most coarse at the lower sideburns on “normal” scalps. “Normal” scalp usually means pre-alopecia or before the phenomenon of balding begins. The lower sideburns are actually beard hair which is coarser than scalp hair of the vertex. Tolgyesi et al. [152] demonstrated that beard hair also contains a higher amount or higher percentage of hairs with medulla. Beard hair is also more elliptical and has more irregular cross-sectional shapes than scalp hair. Beard hair also has lower disulfide content (cross-link density) than human scalp hair [152].

For adult Caucasian individuals, the average diameter (from the vertex or crown areas) usually ranges from about 46 to about 94 micrometers. Scalp hair diameter shows large differences among neighboring hairs on the same head, ranging from a

factor of less than 1.4 to more than 2.0 on adult Caucasian women [112]. Garn is essentially in agreement with Yin et al. [112] on these ranges on an individual scalp, claiming as early as 1948 that the average diameter of neighboring hairs on the same scalp may vary by more than a factor of 2. Hair on different regions of the scalp grows at different rates as described in Chap. 1. DeBerker et al. [153] have shown that on “normal” scalps, hair grows slowest on the temples (0.39 mm/day for males ~14 cm/yr) and faster on the vertex (0.44 mm/day for males ~16 cm/yr) where it grows coarser.

Fine Hair Tends to be Lighter in Color than Coarse Hair

The extreme case supporting this conclusion is that vellus hair, the finest of all hairs does not contain pigment, whereas most permanent hairs the coarsest of scalp hairs generally contain pigment. Caucasian hair on average is finer than Asian or African hair and on average it is lighter in color. Schwan-Jonczyk [154] demonstrated that the size of the pigment granules in scalp hair is larger in Asian and African hair than in Caucasian hair. Fitzpatrick et al. [155] described that the hair of Africans tends to be black and that the pigment granules of the hair of those of African descent tend to be larger than those of dark European hair. Schwan-Jonczyk [154] also determined that the pigment granules from dark European hair are on average larger than those of blonde and red hair.

In addition to pigment size, the main pigment of darker hair is eumelanin, whereas pheomelanin is the primary pigment of most red and some blonde hairs. There are undoubtedly exceptions to this conclusion that fine hair tends to be lighter in color than coarse hair, because hair color is determined by several variables including the type of melanin pigment, the size of the pigment granules and the density (frequency) of the pigment granules that are dispersed throughout the cortex of human scalp hairs, however there are several other references supporting this conclusion and some of these are described below, also see Chap. 5 for additional details.

Pecoraro et al. [146] examined hair from 26 infants within 76 h of birth considering hairs from 13 males and 13 females. These scientists found that the mean coarseness of dark hairs from dark complexioned newborns was 37 μm while the average diameter for light colored hairs from light complexioned newborns was 22 μm .

Trotter and Dawson [131, 133] examined hair of children and adult Caucasians (French Canadians and Americans). They concluded that coarse hair tends to be darker than fine hair [131, 133]. In addition, Bogaty [145] concluded from his review of the anthropological literature that Caucasian children’s hair is on average finer, rounder, less frequently medullated and lighter in color than adult’s hair, see Table 9.24.

Table 9.24 Caucasian children's hair is finer and lighter than adult's (N = 310)^a

Ages	Diameter (μ)	% brown-black	% blond-dark blond	% light blond
0–4	58	35	50	15
5–9	66	75	22	3
10–14	69	96	4	0
15–19	74	98	2	0
20–29	73	98	2	0
30+	70	97	3	0

^aData from anthropological study of French Canadian hair by Trotter and Dawson [133]

Is Gray Hair Coarser than Highly Pigmented Hairs on the Same Scalp?

Whether gray hair is coarser than highly pigmented hairs on the same head is still in question because of mixed results. This subject is covered in detail in Chap. 5 in the section entitled, *Hair Pigment Structure and Chemical Oxidation*. See these [156, 157] and other relevant references in Chap. 5.

Cross-Sectional Size and Hair Fiber Curvature

Porter et al. [47] found a significant negative correlation between hair fiber curvature and cross-sectional area ($R^2 = 0.98$) from 12,050 African type hair fibers that varied from curl class IV to VIII, see Table 9.25. Therefore, 98% of the variation in cross-sectional area of this type of hair over this curvature range can be explained by hair fiber curvature and the cross-sectional area decreased with increasing fiber curvature over this curvature range.

Even though we were unable to find direct data on curl type versus cross-sectional area for Asian or Caucasian hair, the data of Table 9.25 shows this same directional trend on averages for cross sectional area and curvature for these three hair types. For example, the average cross-sectional area for Asian hair is highest and that for African hair is lowest with Caucasian hair in the middle. While the inverse holds for Curl Type. It will be interesting to see if this same trend exists within these populations (Asians and Caucasians), because if it does then hair fiber

Table 9.25 Cross-sectional areas and curvature for average Asian, African and Caucasian hair

Hair type	Ave D	Max D/Min D	Cross-sectional area	Ave. curl type
Asian	82	93.4/72.7	5,333	II [158, 159]
Caucasian	70	82.8/60	3,902	II, III [158, 159]
African	72	93.6/55.8	4,104	IV to VIII [158, 159]

Diameter values in μm and area in μm^2 (average D is from Table 9.14)

All other values calculated from these equations via iteration

Elliptical Ratio = Max D/Min D

Ave D = $\sqrt{D_{\text{max}} \times D_{\text{min}}}$

Cross-sectional area = $\pi R_{\text{max}} \times R_{\text{min}}$ (R = radius)

curvature could be calculated from cross-sectional area data provided a suitable model equation could be developed.

Hair fiber diameter correlates positively with cross-sectional area. Otsuka and Nemoto [134] have shown that hair fiber diameter of Japanese females from ages 40 and up decreases with age. Furthermore, Nagase [93] determined that hair fiber curvature of the hair of Japanese females ages 10–70 increases with age. Therefore, we can conclude for Japanese females ages 40 and higher hair fiber curvature correlates negatively with diameter and cross-sectional area of hair.

9.7.4 *Effects of Fiber Cross-Sectional Shape on Properties and Reactivity*

The previous section shows how the fiber cross-sectional shape can vary between and within different geo-racial groups and Figs. 9.20–9.25 illustrates some of the shape variation of human hair. As indicated, hair fiber cross-sectional shape varies

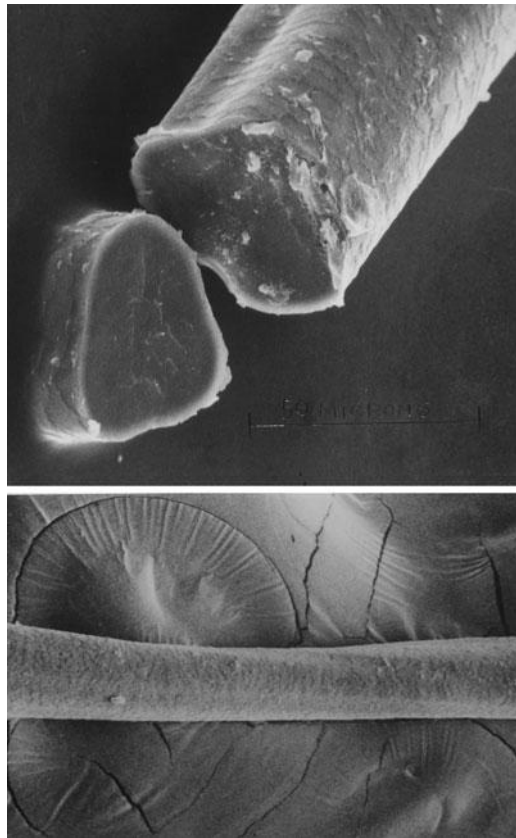


Fig. 9.20 Caucasian hair fiber with a slight twist (*bottom*) and flattened areas on the surface (*top*). Another common non-circular shape of Caucasian hair

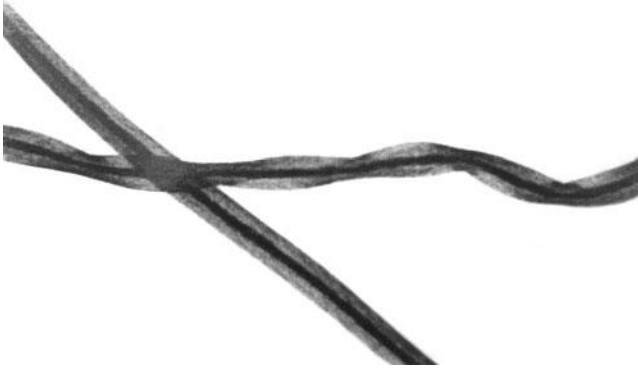


Fig. 9.21 African American hair fiber with multiple twists. Light micrograph kindly provided by John T. Wilson

Fig. 9.22 An African American hair fiber illustrating a fiber twist at higher magnification than for Fig. 9.21. Light micrograph kindly provided by John T. Wilson



within each geo-racial group and even on a single person's head. Even though we talk about the hair of Caucasians as representing relatively circular hair fibers, Figs. 9.20 and 9.23–9.25 show the “normal” variation that encompasses non-circular cross-sectional shapes that can be found on Caucasian scalp hair.

Indented areas are frequently observed (Fig. 9.20). Twists in human hair fibers are not un-common especially in African type hair (Figs. 9.21 and 9.22).

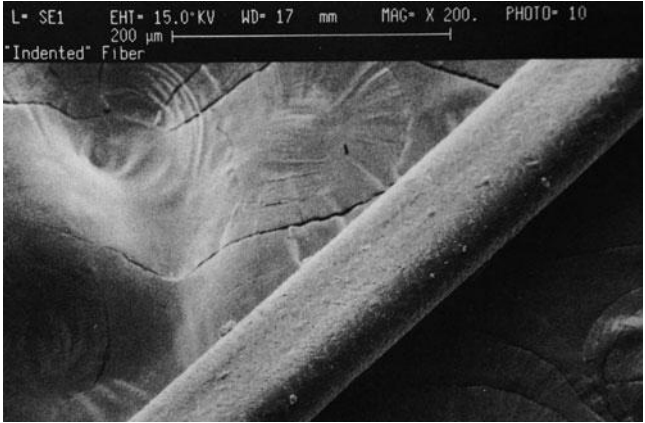


Fig. 9.23 A Caucasian hair fiber with a large indented area on its surface. Note the irregular shape on the rest of the hair created by this indent

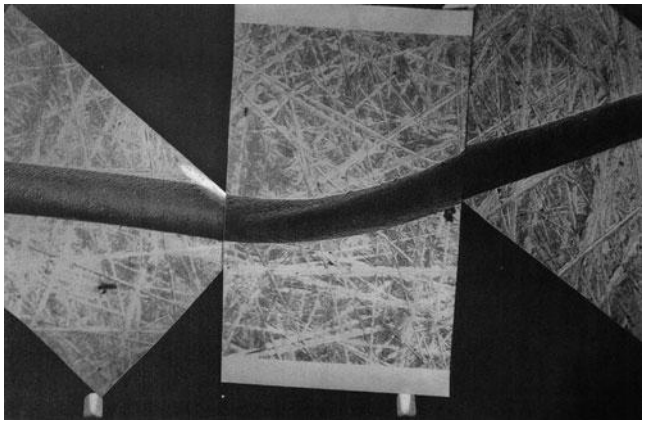


Fig. 9.24 An electron micrograph illustrating a common twist in a curl of a Caucasian hair fiber

Figures 9.20 and 9.24 illustrate twists in Caucasian hair and Figs. 9.21 and 9.22 showing more extensive twists in African American hair. Flat spots and high spots are also common (Figs. 9.23–9.25) in hair of all origins. Widely varying diameters occur in fibers from the same scalp and even on the same hair fiber. As indicated, a rule of thumb is that hair fiber diameter on the same scalp varies by about a factor of two [112].

These different fiber shapes affect not only the physical properties of the fiber such as fiber breakage and abrasion resistance, but, fiber shape also affects the physico-chemical reactivity of the fiber. Figure 9.25 shows an electron micrograph of an irregularly shaped hair fiber from the scalp of a Caucasian female. This fiber contains flat and high spots that form ridges along the axis of the

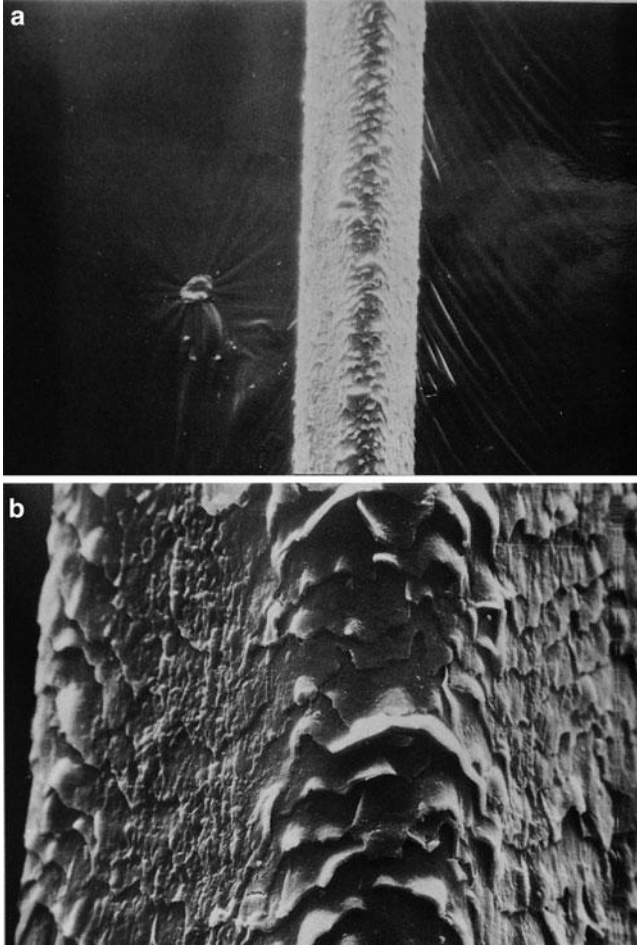


Fig. 9.25 Scale lifting on a highly irregular shaped hair fiber surface. Note the greater lifting on the fiber "high spot" where the scales are most severely bent

fiber. This hair fiber had previously been permanent waved and dyed on the scalp and then treated in the laboratory with alternating treatments of triethanolammonium lauryl sulfate and stearylalkonium chloride. This type of treatment raises scales on fibers that are damaged in the cuticle cell membrane complex or the endocuticle.

The scale lifting that resulted occurred more on the high spots along the ridges of the fiber than on the flat areas. This effect in scale lifting not only represents a difference in reactivity along the fiber cross-section, it makes the scales on the ridges more susceptible to fragmentation and removal and subsequently makes these high spots more susceptible to further penetration and damage by chemical treatments and rubbing actions.

This fiber shape induced reactivity difference is only one example of the variation in reactivity on hair fibers caused by fiber shape variation. Undoubtedly many of the experimental variations that we observe in hair science that are difficult to explain may be caused by fiber shape variations and oftentimes they go unexplained.

9.7.5 Scale Type of Mammalian Hair is Related to Hair Fiber Diameter

A series of papers were written in the 1920s by Hausman [160] on structural features of the hair of mammals. Hausman classified cuticle scales of different mammals on the basis of their size and shape into two general kinds that he called imbricate and coronal, see Fig. 9.26. Hausman then divided the imbricate type scales into five different kinds and the coronal scales into three different kinds, see Fig. 9.26. Human scalp hairs fit into the flattened imbricate classification of Hausman. Hausman [160] defined the scale index as the scale interval (free proximo-distal diameter) of a cuticle scale (F) in Fig. 9.26 divided by the shaft diameter or $F/D = \text{scale index}$. After examining 190 samples of dorsal under-hair of many species of mammals, Hausman concluded that the scale index is related more to the diameter of the scales than to the scale type classes that the species have been assigned to, thus the scale index is inversely related to the diameter of the hair shaft.

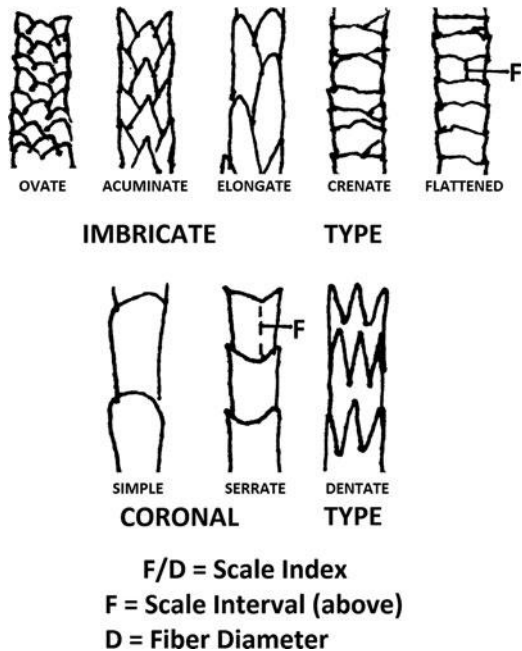


Fig. 9.26 The scale index and different scale shapes of mammalian hair fibers (adapted from Hausman [160])

Hausman did not provide a statistical model for this relationship. Therefore, I examined his graph of Scale Index versus fiber diameter for different mammalian species. From that graph, I estimated the Scale Index versus fiber diameter from 24 data points for different mammals over the range of 7–99 μm and using JMP statistical software calculated a quadratic model as the best fit with an R^2 of 0.916 and a p value of < 0.0001 .

This equation $\{Y = 0.0382 - 0.01333 X + 0.000209 (X - 48.0385)^2\}$ where $Y =$ the predicted value of the scale index and $X =$ fiber diameter provided predicted values for the scale index versus diameter as summarized in Table 9.26 The predicted data of this table show that the scale index is inversely related to the fiber diameter and this relationship is strong. An interesting observation is that Hausman did this work nearly 90 years ago and it is still very useful.

Wynkoop [161] examined the form of cuticle scales and the extent of medulla (described in Chap. 1) with respect to age. However, Wynkoop used too few subjects' times hairs. For example, other than age group 0–9 and 20–29, she used 3 hairs from only 1 to 9 persons per group. However, Wynkoop did show a better fit of scale index and extent of medulla with fiber diameter than with age. From what we currently know about fiber diameter, scale interval and extent of medulla, large variations are inherent in data of these variables. Therefore,

Table 9.26 Scale index versus hair fiber diameter for mammalian hair fibers [160]

Estimated scale index	Diameter	Predicted scale indices
1.48	7	1.31
1.3	9	1.22
1.02	11	1.13
1.1	12	1.08
0.7	15	0.96
0.88	18	0.86
0.68	20	0.79
0.7	24	0.96
0.52	26	0.62
0.78	27	0.60
0.4	34	0.45
0.5	36	0.42
0.48	38	0.39
0.38	42	0.34
0.26	50	0.27
0.22	60	0.22
0.16	70	0.20
0.14	74	0.19
0.16	76	0.18
0.20	78	0.18
0.18	83	0.16
0.07	93	0.09
0.06	96	0.06
0.06	99	0.03

I conclude that if Wynkoop would have used more hairs and more subjects for each age group, she would likely have shown a relationship of both scale index and age and the extent of medulla with age. For example since children's hair is finer than adults hair there should be more medulla in adult's hair than children's hair, see Chap. 1 in the section entitled *Medulla* for details on the medulla and fiber diameter.

Takahashi et al. [162] examined the scale interval for a large number of Asian and Caucasian scalp hair fibers. The total number of subjects was 89 Japanese and 214 Chinese for Asian hair and 160 Germans and 50 Americans for Caucasian hair. Two hundred and eighty two hairs from these Caucasian females and 200 hairs from the Asians were measured at more than 300 points on each hair fiber for the scale interval which was found to be $6.61 \pm 0.52 \mu\text{m}$ for the Asian hair and $6.98 \pm 0.60 \mu\text{m}$ for the Caucasian hair. This difference is significant beyond the 0.001 level. Using the average diameters for Asians and Caucasians from Table 9.14, I calculated the scale indices for these two groups to be 0.103 for the Caucasians and 0.0796 for the Asians hair. These values are reasonably close to the predicted values of 0.115 and 0.087 from the quadratic prediction equation for the data extracted from Hausman's graph on different mammalian species. See the section in Chap. 1 entitled *The Cuticle*.

The question now is what is the effect of the scale interval (F in Fig. 9.26) on hair properties? My conclusion is that since the scale index (F/D) is strongly correlated with hair fiber diameter then the scale interval F is also. So, if we normalize the data to fiber diameter the effects will largely be compensated for in our calculations. Furthermore, cuticle scale thickness (thickness of each cuticle cell times the number of cuticle layers) both of which Takahashi et al. [162] demonstrated to be larger in Asian versus Caucasian hair will play a stronger role than the scale interval or scale index in fiber reactivity. Takahashi et al. in this same paper determined that wet cuticle fragmentation is different in Japanese versus Caucasian hair. Therefore, the cuticle composition including the ratio of exocuticle (A-layer plus exocuticle) to endocuticle will play a larger role in cuticle damage than the scale interval or the scale index. I also conclude that the primary changes versus age of these parameters will occur in infants, versus children's versus adults' hair with possibly the elderly being different from younger adults. However, none of these effects have been examined to date.

9.8 Hair Fiber Curvature

9.8.1 Factors Related to the Origin of Fiber Shape

Not considering permanent waving or straightening, the longitudinal fiber shape (curvature) is genetically determined (see Figs. 9.27 and 9.28). Curvature is related to the degree of coiling including natural crimps and bends of hair fibers and is the



Fig. 9.27 Hair of different fiber curvatures illustrating how hair assembly volume increases with curvature by the Robbins–Reich method



Fig. 9.28 Hair of different fiber curvatures by the Segmentation Tree Analysis Method (STAM) illustrating curvatures from level I to VII. I could not find hair of level VIII for this illustration

most important fiber characteristic involved in styling, combing, and other aspects of hair assembly behavior. Permanent waves and hair relaxers function primarily by changing fiber curvature to produce either a curlier or a straighter hair. Figure 9.27 depicts hair fiber curvature by the Robbins–Reich system and Fig. 9.28 by the STAM. When curvature is low, the hair is relatively straight as in tresses with ratings of 0, 2 and 4 in Fig. 9.27 and STAM I and II in Fig. 9.28. When hair is relatively straight, friction and stiffness play a very important role in hair assembly behavior. However, when the hair is very curly as in tress 16 by Robbins–Reich or IV by STAM or even curlier, then fiber curvature has the ability to dominate other fiber properties and control hair effects.

The Robbins–Reich method for determining hair fiber curvature works well for curl classes I through IV (Fig. 9.28), but does not distinguish as well as STAM for higher curvatures. Furthermore, since the STAM curvature method has been applied to so many subjects (more than 2,400) in so many different countries and it can be applied to curl types I to VI from curl radius or curl diameter data or even calculated from hair fiber ellipticity; for these reasons this author recommends the STAM method for hair fiber curvature over his own method.

The dominant feature relevant to the origin of hair fiber shape is the distribution of different types of cortical cells in the fiber. In general, hairs that are straight contain a distribution of cortical cells that may be pictured as concentric circles. That is they are symmetrically arranged about a common axis in the center of the fiber. On the other hand, curly hairs contain different types of cortical cells on the inside of the curl relative to the outside of a curl. Therefore, the cortical cells of curly hairs tend to be distributed more in a bilateral type arrangement. For a more complete discussion of hair fiber shape including a review of the current status of the origin of hair fiber shape see the section in Chap. 1 entitled *The Origin of Hair Fiber Curvature*.

9.8.2 A Historical View of Approaches to Measure Hair Curvature

Many attempts have been made to classify the longitudinal shape or the curvature of human hair fibers both in the anthropological and cosmetic fields of hair science. In a review paper, Trotter [163] described the history of curvature classification wherein she indicated that in the early nineteenth century, there were two qualitative distinctions for human hair, straight-wavy hair and woolly or tufted hair. The next meaningful step in the classification of hair curvature occurred in the mid to late nineteenth century and involved combinations of curvature and cross-sectional shape characteristics. Then in 1900, Deniker [164] provided four semi-quantitative classes for curvature for physical anthropology:

Straight and smooth hair

Wavy hair: a long curve from one end to the other

Frizzy hair: hair rolled spirally with rings 1 cm or more in diameter

Woolly hair: spiral curves from 1 to 9 mm in diameter

Martin in 1928 [165] published his 3 major curvature classes with sub-groups:

Smooth: straight, smooth, shallow wave subgroups

Wavy: wide waves, narrow waves, curly subgroups

Kinky: frizzy, loose kinks, tight kinks, tight spirals subgroups

Another important step was to provide more quantitative classifications or definitions for the longitudinal shape of hairs. Hardy [48] defined several longitudinal shape characteristics and measured these for seven different populations including the following:

Kink: “a sudden constriction and twisting of the hair shaft producing an obvious discontinuity in curvature”.

Curl radius or radius of Curvature: compare each curve of a hair to curves of a transparent template consisting of circles of known radius.

Average Curvature: is “the inverse of the average radius of curvature”.

Ratio of maximum to minimum curvature: Ratio of the “highest to lowest” radius of curvature of a hair fiber.

Crimp: (Hardy adopted the definition of the wool industry) “number of times the direction of curvature changes per unit length”.

“Ratio of natural to straight length”: the effect of curling on the hair fiber length.

Others have used some of Hardy’s definitions or minor modifications to approximate or assess hair fiber curvature. For example, Nagase et al. [93] and Kajiura et al. [166] used the curl radius. Robbins and Crawford [167] used the inverse of the ratio of maximum to minimum length. Porter et al. [47] used curl diameter and De La Mettrie et al. [158] and Loussouarn [159] combined three parameters used separately by others including curl diameter, the ratio of maximum to minimum length [3, 48, 167] and the number of wave crests for a given length [3]. Robbins and Reich [3] described another approach based on the number of wave crests divided by the ratio of the minimum to maximum length, see Fig. 9.27. But, to date none of these methods have received wide acceptance outside of their own laboratories.

The STAM described first by De La Mettrie et al. [158] classified the curvature of hair from 1,442 subjects, see Fig. 9.28. Subsequently, Loussouarn et al. [159] published data with measurements and curvature classification on hair from an additional 1,007 subjects. A third paper from this same laboratory by Porter et al. [47] used the STAM to examine the behavior of African type hair as a function of curvature and provided minor adjustments to the original parameters for classification.

Using data from several different researchers and technical papers [48, 129, 166, 168] where either curl radius or curl diameter are provided, one can show that this measurement permits meaningful classifications, over the first five curl groups. Furthermore, ellipticity [47] may be used to calculate Curl type classes between IV and VIII when STAM curl typing has not been done. Such a method for the entire curl range is described in the next section of this Chapter, entitled *Curvature by the STAM method can be approximated by Calculation from Ellipticity*.

The STAM method consists of measuring three parameters after the 6 cm hair fibers are washed in dilute detergent rinsed with water and allowed to dry to their natural curvature for at least 5 min:

The smallest curl diameter is then measured for each fiber = CD

The ratio of the straight length 6 cm to the curled length is then taken = L_6/L_C

The number of wave crests are counted on a 5 cm fiber when it is held at 4 cm = W

Curvature is then classified by the following criteria:

$$\text{Curl Type I} = \text{CD} > 10.8 \text{ cm}$$

$$\text{Curl Type II} = \text{CD between } 5.7 \text{ and } 10.8 \text{ cm}$$

$$\text{Curl Type III} = \text{CD between } 3.1 \text{ and } 5.7 \text{ cm}$$

$$\text{Curl Type IV} = \text{CD between } 1.2 \text{ and } 3.1 \text{ cm}$$

$$\text{Curl Type V} = \text{CD} < 1.2 \text{ cm and } L_6/L_C < 5.9 \text{ and } W < \text{ or } = 3 \text{ waves}$$

$$\text{Curl Type VI} = \text{CD} < 1.2 \text{ cm and } L_6/L_C < 5.9 \text{ and } W = \text{ or } > 4 \text{ waves}$$

$$\text{Curl Type VII} = \text{CD} < 1.2 \text{ cm and } L_6/L_C > 5.9 \text{ and } W = \text{ or } > 5 \text{ waves}$$

$$\text{Curl Type VIII} = \text{CD} < 1.2 \text{ cm and } L_6/L_C > 5.9 \text{ and } W = \text{ or } > 6 \text{ waves}$$

Curl types I through IV are classified by curl diameter alone. The other measurements are used to distinguish between Curl types V through VIII.

9.8.3 Curvature by the STAM Method can be Approximated from Ellipticity

Ellipticity has been shown to increase with fiber curvature in separate studies with large numbers of hair fibers on hair of widely differing curvatures, one study on Japanese hair by Nagase et al. [93] on more than 8,900 hair fibers (small effect) and another study on African type hair by Porter et al. [47] on more than 12,000 hair fibers (larger effect). Since these two ranges of ellipticity and curvature cover the entire scale of curvatures and ellipticity for human scalp hair, this relationship should exist for all geo-racial hair including Caucasian. A regression equation was calculated by taking a total of 9 data points, 3 directly from the graph of Nagase et al. [93] and 5 from the prediction equation from Porter et al. [47]. One further assumption was that an ideal ellipticity of 1 occurs at an ideal Curl type of 1 for STAM Curvature [47]. The relationship is best described by this cubic equation of the natural logarithm of Curvature versus Ellipticity (E):

$$\begin{aligned} \ln \text{ Curl type} = & - 1.8087 + 1.9765 E + 4.0319(E - 1.474)^2 \\ & + 10.039(E - 1.474)^3 \end{aligned}$$

The $R^2 = 0.9993$; $p < 0.0001$ and Root Mean Square Error = 0.02351

Table 9.27 Calculation of STAM curl type from ellipticity

Type of hair	Ave. curl type ^a	Calc. curl type ^b	Ave. ellipticity
£	1.0	1.0	1.0
€	2.3	2.43	1.34
€	2.6	2.9	1.45
€	4	4.15	1.596
¥	5	4.7	1.63
¥	6	5.54	1.668
¥	7	6.5	1.7
¥	8	8.2	1.74
China	1.62 [158]	2.04	1.23 [136, 137]
Asian	1.92 [159]	2.16	1.26 [Table 9.17]
Japan	2.03 [93]	2.22	1.28 [93]
India	2.41 [158]	2.58	1.38 [137]
Caucasian	2.57 [159]	2.50	1.36 [Table 9.17]
Brazil	3.19 [159]	3.05	–
African	5.93 ^c	8.2	1.74 [Table 9.17]
W. Africa	6.33 ^d [47]	–	–

£ assumed for model equation, € Japanese hair from Nagase et al. [93], ¥ from Porter et al. [47]

^aFrom curl type DATA of Loussouarn et al. [159], de la Mettrie et al. [158] and Nagase et al. [93]

^bCalculated from regression models by CRR from data of Porter et al. [47] and Nagase et al. [93]

^cSubjects from: South Africa 141, Ghana 98, Kenya 47, Jamaica 50, US 85, N. Africa 133, from references [47, 158]

^dSubjects from Ghana 35, Liberia 34 and Kenya 47 with highly coiled hair [47]

The reliability of this model is supported by the data of Table 9.27 showing a reasonable fit for the calculated Curl types which are generally within plus or minus 0.5 from the referenced STAM values; however for the one African sample the calculated value is off by 2.2 which may be due to a poor ellipticity value. More data is required to provide a better feeling for the real reliability of this model, however it should serve as a reasonable approximation. This model will likely work best for mean ellipticity values from more than 20 hairs for a hair sample rather than for individual hairs. The hair of the people of India by ellipticity and Curl type is more Caucasian-like than East Asian-like and the model confirms this observation which is consistent with genetic studies.

9.8.4 Variation of Curvature Across Populations and Countries

Table 9.28 summarizes data from the Loussouarn et al. [159] study by STAM for hair fiber curvature for three major geo-racial groups. The American Anthropological Association (AAA) issued a statement on race on May 17, 1998 stating that, “human populations are not unambiguous, clearly demarcated, biologically distinct groups” [169]. Furthermore the statement said, “Genetics indicates that most physical variation about 94% lies within so-called racial groups.” The AAA

provided this relevant example [169], “Dark skin may be associated with frizzy or kinky hair or curly or wavy or straight hair”.

It is true; linkage of hair fiber curvature to skin color alone just does not work. For example dark skinned people of African descent will most likely have very curly to kinky hair while similarly dark skinned people from northern India will most likely have very straight hair and many dark skinned people from southern India (sometimes called Dravidians) will have curly to wavy hair. But, if we link geographic origin, with racial origin and the tendency for skin color of the geo-racial group then the association with hair type increases markedly as shown by the data of Tables 9.24–9.29.

The following discussion considers curvature classification of hair fibers from more than 2,800 persons from the following references [47, 48, 129, 158, 159]. From these data sets we considered that Native Americans fit into the Asian group and that most other Americans can fit into one of the other three major geo-ethnic groups while most of the peoples of Europe, Asia and Australia also fit into these three groups.

The data of Table 9.28 shows that more than 90% of the African type hair examined is distributed primarily in Curl types V through VIII. Nevertheless, the hair of small percentages of panelists of African origin who are currently located in the United States and Northern African countries were classified in curl groups III and IV. Asian hair is most frequently found in curvature classes I through IV with a maximum percentage in group II. Caucasian hair is also found in groups I through IV, although the data shows it to be more of a Gaussian type distribution over these 4 curl types than for Asian hair.

From the data of Table 9.28 there appears to be a clean break for Asian and Caucasian hair between curl groups IV and V with virtually no persons above group IV from these two populations. Now if we consider geography alone, for the United States or Europe all eight curvature classes will be found. And if we consider skin color alone, all eight curl types will also be found. Therefore this summary of the data of Table 9.28 shows more meaningful distinction among hair curvature types can be made by considering geographic origin that I call

Table 9.28 Hair curvature by STAM for three major geo-ethnic groups from de la Mettrie et al. [158], Loussouarn et al. [159] and Porter et al. [47]

Hair type (No. subjects) ^a	Percentage of subjects with hair in STAM curvature grouping							
	I	II	III	IV	V	VI	VII	VIII
Asian hair N = 456	29	52	17	2	0	0	0	0
Caucasian hair N = 389 ^b	12	35	37	16	0	0	0	0
African hair N = 554 ^c	0	0.3	1.5	7	25.1	37	19.6	9.5

^aPrimarily from China, Japan, South Korea and Thailand [158, 159]. The percentages were estimated from graphs in the paper [159] since actual percentages were not provided

^bPrimarily from Denmark, France, Germany, Poland, Spain, UK and Russia [159]. The percentages were estimated from graphs in the paper since actual percentages were not provided

^cSubjects from: South Africa 141, Ghana 98, Kenya 47, Jamaica 50, US 85, N. Africa 133, from references [47, 158]

Table 9.29 Curvature of Asian hair by country from study by De La Mettrie et al. [158] and Nagase et al. [93]

Country	Percentage of subjects with hair in STAM curvature grouping							
	I	II	III	IV	V	VI	VII	VIII
Korea N = 28	22	57	21	0	0	0	0	0
Japan ^a N = 40	13	67	20	0	0	0	0	0
Japan ^b N = 230	29	43	24	4	0	0	0	0
Thailand N = 65	19	46	32	3	0	0	0	0
China N = 213	45	48	7	0	0	0	0	0

^aData from de la Mettrie et al. [158]

^bCalculated from curl radius data by Nagase et al. [93]

geo-ethnic or geo-racial groups than by considering either skin color or geographical regions alone.

The data of Table 9.29, constructed from the data of De La Mettrie et al. [158] and Nagase [93] shows hair curvature distributions from 4 different Asian countries. A concern is in the small sample numbers for the Korean and Japanese hair classifications by de la Mettrie, that is the number of subjects is so small that the total distribution is most likely not representative of the hair for those countries. This conclusion is reinforced by the data of Table 9.29. The De La Mettrie et al. data [158] of Table 9.29 from only 40 Japanese subjects shows hair classified in curl Types I, II and III only, while the data by Nagase et al. [93] measuring curl radius of hair from 230 Japanese subjects provides an average curl diameter of 8.8 cm and a distribution from 1.2 to 32 cm corresponding to a STAM curl classification over all four curl Types I to IV. The Nagase data also provides 43% in Curl type II while the de la Mettrie provides 67%. The average curl diameter (peak in the distribution curve) by Nagase et al. corresponds to curl type II which is the largest percentage Curl type found by de la Mettrie for Japanese hair also, see Table 9.29.

The data by Nagase [93], Hardy [48] and Kajiura et al. [166] are different studies where the curl radius was measured, while the study by Porter et al. [47] measured curl diameter, but STAM was not used for classification of hair curvature in the manuscripts of these later four studies. Therefore, I converted curl radius to curl diameter for Table 9.30 and classified the data by the STAM procedure showing good agreement with expectations. For the data by Syed et al. [44] I calculated the cross-sectional area and ellipticity and used the equations above to approximate the Curl type between curl classes IV to VIII.

This type of hair fiber curvature classification can be done conveniently from curl radius or curl diameter data for curl types I through V and from ellipticity data for Curl types I through VIII.

The conversion of curl radius or diameter or ellipticity from different laboratories to the STAM hair curvature types of Table 9.30 provides good agreement with the classifications found by De La Mettrie et al. [158] and Loussouarn et al. [159] and illustrate the robustness of the STAM method. Because it is robust enough to permit comparisons across different laboratories

as shown by these curl assignments in Table 9.30, it allows useful curvature distinctions. Furthermore, because of the large database provided by de la Mettrie et al. and Loussouarn et al., I recommend that our industry adopt this method (or a minor modification of it) for future hair fiber curvature comparisons. Wherever possible in this book I have tried to refer to hair curvature comparisons by the STAM hair curvature types.

9.9 Water (RH), pH and Solvents and the Dimensions of Hair

9.9.1 Hair and Wool Have Similar Water Binding Amounts and Groups

Stam et al. [122] used a microscopic method to measure changes in the length and diameter of human hair fibers at different RH's and calculated changes in cross-sectional area and volume (see Table 9.31). These data show a small increase in fiber length and a large increase in diameter with increasing RH. This swelling behavior of hair is related to its fundamental structure as described in Chap. 1 in the section entitled, *Swelling Behavior of Hair*.

Although the swelling behavior of keratin fibers is usually explained in terms of its intermediate filament-matrix components, Swift [170] and others have provided evidence that the non-keratin portions of hair may also be important to fiber swelling. For example, Swift demonstrated by microscopic studies involving the penetration of fluorescent labeled proteins into hair in an aqueous medium that a large order swelling occurs in the non-keratin regions of hair. The diameter swelling of hair by water from the dry state is usually given as about 14–16%. On the other hand, X-ray diffraction measurement of intermediate filament separation distances by Spei and Zahn [171] indicates that swelling of only 5.5% occurs in these regions.

Swift [169] therefore proposed that the difference may be explained by the large order swelling that occurs in the non-keratin regions of hair, primarily the endocuticle and the cell membrane complex of hair. However, greater swelling is

Table 9.31 Dimensional changes of human hair versus RH [122]

% RH	Moisture absorption			
	% increase in diameter	% increase in length	% increase cross-sectional area	% increase in volume
0	0	0	0	0
10	2.3	0.56	4.7	5.7
40	5.1	1.29	10.5	12.2
60	6.9	1.53	14.3	16.3
90	10.6	1.72	22.3	24.6
100	13.9	1.86	29.7	32.1

expected in the keratin associated proteins than the intermediate filaments. For additional details on hair swelling, see Chap. 1.

The hysteresis in the moisture absorption-desorption curves of keratin fibers is an interesting phenomenon. At any given RH between 0% and 100%, human hair contains less water when absorbed from the dry state compared to when it undergoes desorption, that is when it loses water from the wet state (see Table 9.32). Chamberlain and Speakman [36] observed this phenomenon earlier for human hair and Speakman [37] observed it for wool fiber (see Table 9.33). Additional water binding when the hair is wet occurs because certain groups in hair that are capable of binding water are not accessible to water vapor from the shrunken dry state. On the other hand, when the hair is highly swollen with liquid water these groups are accessible and water binds to them.

Stam et al. [122] found that tension on hair fibers influences their dimensions (moisture content) at different RH's. For example, stretching hair fibers below 60% RH provides less swelling than for un-stretched hair, while stretching hair at RH above 60% provides more swelling than un-stretched hair.

Table 9.33 shows that moisture loss (desorption) and regains (absorption) for human hair and wool fiber are virtually identical. It has been suggested [30] that the moisture regains of human hair and wool fiber are virtually identical up to about 90% RH, where they diverge wool to a regain of 33%, and hair to about 31%, the difference most likely due to the higher cross-link density in human hair. However, even if divergence does occur, the actual difference in moisture regain by these two fibers is relatively small which suggests that to a large extent the same functional groups are responsible for water binding in hair and wool fiber.

Table 9.32 Absorption versus desorption of moisture [122]

% RH	Absorption % increase in volume	Desorption % increase in volume
0	0	0
10	5.7	6.8
40	12.2	13.0
60	16.3	17.3
90	24.6	25.1
100	32.1	32.1

Table 9.33 Water content of human hair and wool fiber versus RH

% RH	Human hair (weight gain) [36]		Wool (weight gain) [36]	
	% absorption	% desorption	% absorption	% desorption
0	0	0	0	0
8	3.9	5.1	–	–
35	–	–	8.4	9.7
40	10.2	12.0	–	–
63	14.8	16.7	14.3	–
86	22.6	23.3	–	–
100	31.2	31.2	31.9	31.9

The rate of moisture regain is considerably slower from water vapor than from liquid water (diffusion-controlled reaction). Liquid water at room temperature will penetrate the hair in less than 15 min and in <5 min at 92°F (~33°C) [122], whereas 18–24 h is required for single fibers to equilibrate in a humid atmosphere, with even longer times for a fiber assembly as shown by Steinhardt and Harris [172].

9.9.2 Variation of Fiber Surface Area with Diameter

For a given weight of hair, the fiber surface area is inversely proportional to the fiber diameter. Table 9.34 shows how the calculated fiber surface area varies with diameter for 1 g of hair (assuming it is a right cylinder).

9.9.3 The Swelling of Human Hair Changes with pH

The swelling of human hair in aqueous solutions after 24 h or longer at different pH values exhibits four distinct parts [109–111] (Fig. 9.14):

1. A minimum in swelling from pH 4–9
2. Above pH 10, a large increase in swelling
3. pH 3–1, a slight increase in swelling
4. Below pH 1, a slight decrease in swelling

The minimum in swelling from pH 4–9 is consistent with the observation of Steinhardt and Harris [172]. In the absence of added electrolyte, there is no combination of wool fiber with mineral acid or alkali from pH 5 to 10. This is in the vicinity of the isoionic point of hair (the neutral point for the total fiber, which is when the number of positively charged and negatively charged groups is equal). The large increase in swelling above pH 10 is largely due to ionization of diacidic amino acid residues in the hair and partly due to keratin hydrolysis. The increase in swelling from pH 3 to 1 is due to the combination of acid with the dibasic amino acids. Breuer [75] attributed the decrease in swelling below pH 1 to an irreversible structural change.

Ehrhardt (private communication) observed alkaline swelling in 0.1 N NaOH after only 5 min of reaction with hair at 95°F (~35°C). Under these conditions, a

Table 9.34 Fiber diameter and surface area

Fiber diameter (μm)	Calculated ^a surface area (cm ² for 1 g hair)	Calculated relative surface area
40	758	3.0
80	379	1.5
120	253	1.0

^aFor 1 g of hair, assuming it is a right cylinder

similar effect was not observed using 0.1 N hydrochloric acid. The swelling of human hair in acid below pH 3 is slightly less than that of wool fiber [114], and has been attributed to the higher cross-link density of human hair [34, 114].

9.9.4 Solvents and Swelling of Human Hair

Valko and Barnett [74] and Barnett [121] showed that acetonitrile, triethylphosphate, and glycerol swell hair to a lesser extent than water. In fact, glycerol is sometimes used in tensile or torsional testing to approximate 0% RH [25] because of the lack of hair swelling when hair fibers are immersed in this solvent. Dimethyl formamide, ethylene glycol monomethylether, and diethylene glycol monomethylether swell hair similar to water, although the rate of swelling by these solvents is slower than the rate of swelling by water [74, 121]. Glacial acetic acid and formic acid swell hair to a greater extent than water [74, 121]. Formamide and urea (aqueous solutions of urea) also produce swelling beyond that of water, probably by promoting greater cleavage of hydrogen bonds than produced by water [66, 121].

Amines such as ethyl amine, at 25% in water or higher concentrations, swell hair to a greater extent than water. These solutions rupture peptide and amide linkages and ultimately disintegrate (dissolve) the hair (after several days) [74, 121]. Concentrated solutions of alkali halides (25–60%), after several days, produce extensive dimensional changes to hair [74, 121]. Barnard and White [114] found extensive swelling by potassium iodide, sodium bromide, lithium bromide, and lithium chloride solutions, but not for sodium chloride. Those halide salts that produce extensive swelling of human hair are believed to be capable of breaking hydrogen bonds that water alone is incapable of breaking. For additional details on this subject, see the section on supercontraction in Chap. 4.

9.9.5 Hair Swelling by Permanent Wave Agents

Shansky [173] developed a special cell to follow hair swelling under the light microscope. He used this system to study permanent-wave reactions with human hair and found that the reduction step produces an increase in diametral swelling which increases with increasing disulfide bond rupture [173, 174]. Shansky also found that rinsing with water, after reduction, produces additional swelling. He attributed this effect to osmotic forces, since there is a lower salt concentration outside the fibers after rinsing. Neutralization then reverses swelling. This de-swelling effect is caused by the reformation of disulfide cross-links [173, 175].

Ekstrom [116] described a moving boundary between swollen and un-swollen fiber as the reducing front penetrates the hair during permanent waving and

depilation. Keil [176] using the polarizing microscope noted a similar moving boundary in his studies on permanent waving. Wickett [177] studied the reduction of hair with sodium thioglycolate above pH 10 when diffusion of the mercaptan into the hair is rate-controlling and demonstrated moving boundary kinetics. However, for reaction at lower pH values (below pH 9), the nature of this reaction depends on the reactivity of the particular individual's hair. For one individual whose hair was highly reactive, the reaction followed pseudo-first-order kinetics. In this situation, the permanent wave was reaction-controlled. However, for another individual's hair (difficult-to-wave hair) the reaction exhibited moving boundary kinetics.

Powers and Barnett [174] found that a large excess of reducing solution at pH 10 (for reduction times of 15 min or longer) produced swelling in excess of 200% and effectively destroyed the hair. They also found that the amount of swelling increased with increasing pH from 8 to 10. This effect is related to the increasing rate of disulfide rupture with increasing pH. Finally, these scientists indicated that the effectiveness of the neutralization step in permanent waving could be assessed by relating it to the swelling action of hair in water. In general, hair swelling methods have been valuable for providing information about chemical alterations to human hair, relevant to permanent wave reactions. For additional details see Chap. 4.

9.9.6 Swelling Test for Hair Damage

Klemm et al. [178] described a swelling test to assess hair damage by permanent waves and bleaches. This test consists of measuring hair fiber diameter swelling in a series of three solutions: the first treatment is water for 10 min; the second, 60% lithium bromide for 60 min; and the third, water for 10 min. From an empirical equation, numerical values of swelling behavior may be calculated. This method distinguishes between single and multiple permanent waves and between single and multiple bleaches on hair. It essentially compares swelling in water versus lithium bromide, one of the most effective hydrogen bond breaking agents known. The results rely on the fact that the more damaged a hair fiber the more hydrogen bonds are capable of being broken by this powerful hydrogen bond breaking agent.

9.10 Hair Fiber Friction

Friction is the force that resists motion when one body slides over another. The classical laws of friction were formulated by Leonardo da Vinci and later by Amontons, with whom they are generally associated. Amontons Law states that

the frictional force necessary to slide one surface over another is proportional to the normal load pressing the two surfaces together (W).

$$\text{Frictional force} = \mu W$$

The proportionality constant (μ) is called the coefficient of friction. The frictional coefficient is generally independent of the area of contact. At low loads, when the fiber undergoes a large amount of deformation the true area of contact changes significantly. Thus, at low loads, the area of contact affects the coefficient of friction. The force necessary to initiate movement determines the coefficient of static friction ($\underline{\mu}_s$). The force necessary to maintain movement when the body is in motion determines the coefficient of kinetic friction ($\underline{\mu}_k$). $\underline{\mu}_k$ is almost always less than $\underline{\mu}_s$.

These laws of friction apply to dry, un-lubricated surfaces and to boundary lubricants (very thin solid or nonfluid films separating the surfaces). But, these laws do not apply to hydrodynamic lubricants [179], such as fluid layers that separate the moving surfaces (for example, engine-lubricating oils). Generally, lipid on the surface of the hair provides a reduction in friction. This is an experimental variable of concern to control. For example, by careful cleansing of the test surfaces of the fibers or by testing in surfactant solutions this variable may be controlled. There are several theories attempting to explain friction. For discussion of these theories, see the book by Howell et al. [180], *Friction in Textiles*.

Two important variables relevant to friction on hair are relative humidity (or moisture content of the hair) and the normal load (W) pressing the two surfaces together. It is helpful to consider friction on hair in terms of two conditions for relative humidity and two conditions of load, thus forming the 2×2 matrix below.

		Low RH (60% RH or lower)	High RH (in water)
↑ Load	High (g)	Dry high load	Wet high load
	Low (mg)	Dry low load	Wet low load
		Relative humidity →	

The dry high-load condition is the state that simulates hair friction conditions relevant to dry combing or brushing of hair. The wet high-load condition is relevant to wet combing. On the other hand, the dry low-load condition is relevant to those critical hair-on-hair interactions involved in style retention and hair body. Robbins [181] described three different experimental conditions to characterize hair fiber friction by these three relevant humidity-load conditions. These three approaches are summarized in the next section.

9.10.1 *Methods for Measuring Friction on Hair Fibers*

Two different capstan methods (a fiber over a rod) have been used to measure frictional coefficients of single hair fibers [182, 183] at high load both in air (low RH) and in aqueous media. The apparatus used by Schwartz and Knowles [182] involves draping a fiber with equal weights on each end over a cylinder. One weight is placed on a torsion balance to measure the frictional forces developed as the cylinder is moved against the fiber.

The method of Scott and Robbins [183] involves attaching the root end of a hair fiber to the load cell of a device such as an Instron tensile tester. The fiber is weighted at the tip end and partially wrapped around two mandrels (these may be rotated) but more relevant results are obtained when the mandrels are not rotated. The mandrels are attached to the crosshead. As the crosshead moves downward the mandrels are rubbed against the fiber and the frictional load is recorded. In a capstan system (such as this), the coefficient of kinetic friction (μ_k) may be calculated from the following expression:

$$\mu_k = \frac{1}{\phi} \ln \frac{T_2}{T_1}$$

where ϕ is the angle of wrap in radians, T_2 is the tension after passing over the rod, and T_1 is the tension before passing over the rod. This equation assumes that friction is independent of load, a condition valid for the load ranges used in these two studies of frictional effects on human hair. Scott and Robbins used a 1 g load (high load, on the tip end of the hair) small enough so that the total load (weight plus frictional load) did not exceed the fiber yield point.

Different rubbing speeds (in the vicinity of 10 in. per minute or higher) do not appreciably change the friction coefficient [183]. However, Robbins [181] demonstrated that friction increases with decreasing rubbing speed in the vicinity of 0.5 in. per minute and it appears to level near 0.05–0.02 in. per minute, probably approaching static friction. At these lower rubbing speeds, greater differences can be demonstrated between treatments, especially on dry hair. Therefore, the preferred laboratory conditions for simulating the actions involved in wet combing of hair involve a load of approximately 1 g/fiber, with the fiber immersed in water, at a low rubbing speed in the vicinity of 0.02 in. per minute. To simulate dry combing, the preferred conditions are also a load of approximately 1 g per fiber, near 60% RH, and a low rubbing speed of approximately 0.02 in. per minute.

Wrap angle changes produce significant differences in friction, as indicated by the capstan equation above. Thus, the friction coefficient increases with increasing wrap angle. The above two friction methods measure coefficients of kinetic friction and the low rubbing speed system approaches static friction. Since Amontons law states that static friction is generally higher than kinetic friction, there is probably a directional similarity between static and kinetic friction.

Robbins [181] also developed a procedure for determining dry static friction at low load (in the milligram range) by modification of the incline plane fiber loop method of Howell and Mazur [184]. This procedure attempts to measure those intimate fiber-fiber interactions associated with hair body and style retention. The procedure involves determining the angle of slip for a small hair fiber loop sitting on two parallel hair fibers. Above 1 mg load, the friction coefficient decreases very slowly with increasing load. However, below 1 mg load, the friction coefficient increases abruptly with decreasing load (see Fig. 9.29). The diameter of the fiber loop (in the vicinity of less than 2 cm) affects the friction coefficient. Presumably this effect is due to scale distortion as the loop becomes progressively smaller resulting in an increase in the true area of contact (A) as described by this equation:

$$F = AS$$

A = true area of contact

S = shear strength of materials in contact

Larger hair fiber loops are recommended (in the vicinity of 5 cm diameter) providing a load of 1–2 mg, depending on fiber thickness. At low load (mg range), the fiber system is sensitive to cohesive/viscosity forces from thick layers of product deposits, because the fiber system at such low loads has difficulty ploughing through thick viscous deposits. For example, a pomade-type combing aid (consisting of petrolatum and mineral oil) was evaluated and shown to dramatically increase the apparent friction coefficient at low load due to the cohesive nature of the viscous pomade. However, when this same pomade was tested by a high-load dry friction method, the friction coefficient decreased relative to the untreated control fibers. These effects show that this pomade will hold fibers of an assembly

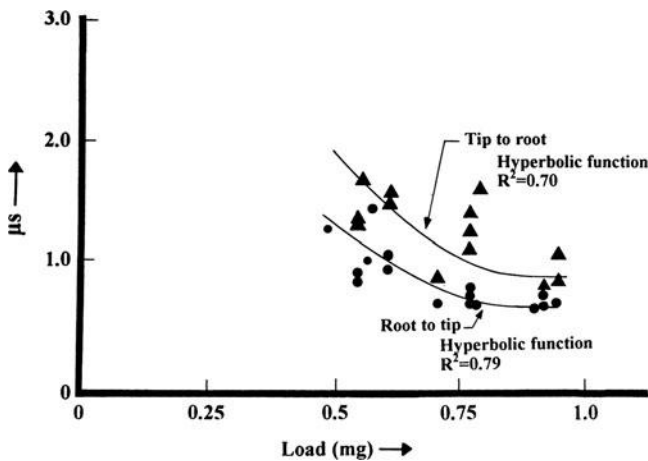


Fig. 9.29 The directional nature of the frictional coefficient of human hair and its variation with load (at 60% RH)

in place better, because fiber movement at low-load forces (mg range) will be resisted by the cohesive forces of the viscous pomade ingredients. However, when high-load forces are applied as in combing, a viscous product can act as a lubricant and thereby facilitate comb on hair and hair on hair movement. This experiment verifies the need for both low- and high-load friction methods to develop a more complete understanding of hair product behavior. Other approaches to measure fiber friction are described in the books by Howell et al. [180] and Meredith and Hearle [185].

9.10.2 *Relative Humidity and Friction*

As indicated above, wet friction for human hair is higher than dry friction (see Table 9.35). In addition, both static and kinetic friction and the differential friction effect increase with increasing RH, that is with increasing water binding by the hair. These same phenomena have been observed for wool fiber [186, 187].

9.10.3 *Friction and Fiber Diameter*

Scott and Robbins [183] found that high-load friction is independent of hair fiber diameter. This effect agrees with theory and with the results of Fishman et al. [188]. However, Martin and Mittleman [189] reported a slight increase in friction with wool fiber diameter. For low-load hair on hair friction, the fiber diameter effect is difficult to test, because as fiber diameter increases, the load also changes and thus the friction coefficient changes.

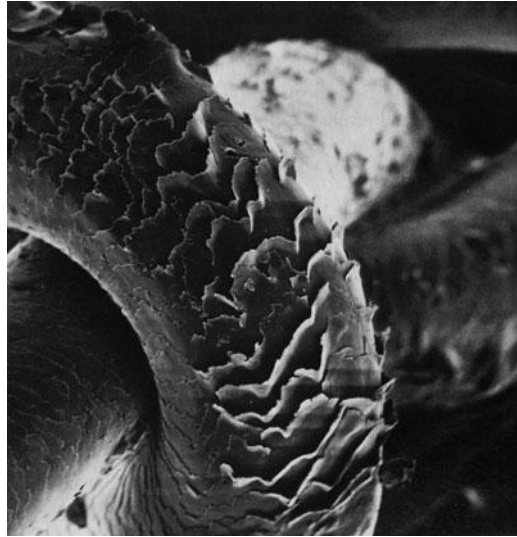
9.10.4 *The Directional Friction Effect*

As with most animal fibers, human hair shows a directional friction effect, that is, it is easier to slide a surface over hair in a root-to-tip direction than in a tip-to root-direction (see Figs. 9.29 and 9.30). This directional friction effect is useful for orienting hair fibers for experimentation. For example, take a hair fiber between the thumb and forefinger, and gently rub back and forth along the fiber axis. If rubbing

Table 9.35 Friction coefficients for hair on comb substrates (high-load condition) [182]

	Coefficient of kinetic friction		
	Hard rubber	Nylon	Aluminum
Dry	0.19	0.14	0.12
Wet	0.38	0.22	0.18

Fig. 9.30 SEM of a knotted hair fiber, illustrating the cuticle cell surface structure. Note the raised scales caused by the severe bending stress of the knotted fiber



is done correctly, the fiber will move in the direction of the root end or one will note that it is easier to rub over the hair in the root to tip direction. Moistening the fingers makes this effect even more apparent, because the differential friction effect increases with increasing moisture in the fiber surface layers.

Table 9.36 illustrates this effect when rubbing hair fibers against a hard rubber surface in dilute shampoo and creme rinse solutions. Note that the differential friction effect is greater in the creme rinse solution than in the test shampoo. This is because the test creme rinse lowered the root-to-tip friction coefficient more than it lowered the tip to root coefficient.

Scott and Robbins [183] and Schwartz and Knowles [182] examined root to tip rubbing in more detail, because the friction coefficient for root to tip rubbing is lower than tip to root rubbing and it produces less abrasive damage to the hair.

Swift and Bews [190] suggested that totally or absolutely dry wool fiber (0% RH) does not display a differential friction effect (absolutely dry wool against a glass surface). However, Swift pointed out that absolutely dry wool is a hypothetical condition. King [186] demonstrated a differential friction effect (DFE) from dry wool against horn, and Robbins [181] for human hair against hard rubber. The DFE does become smaller with decreasing RH, but whether or not the DFE disappears

Table 9.36 Directional friction effect for human hair at high load (Scott, private communication)

	High cleaning shampoo (μ_k)	Creme rinse (μ_k)
Rubbing root to tip (μ_1)	0.425	0.293
Rubbing tip to root (μ_2)	0.546	0.475
Directional friction effect (DFE)	0.285	0.621
DFE = $\frac{\mu_2 - \mu_1}{\mu_1}$		

completely at absolute zero RH is academic. Swift and Bews [190] proposed the following explanation to account for the decreasing DFE with decreasing water content in animal hairs.

The two major layers of cuticle cells, the exocuticle and endocuticle, may be expected to behave differently with respect to moisture regain. The exocuticle, because of its high cross-link density, should not swell so readily as the endocuticle, with its paucity of cross-links and high density of ionic groups. Swelling of the endocuticle on regain could convert it to a gel-like structure which could contribute to the DFE in animal hairs [180, 185, 187, 191].

9.10.5 Mandrel and Comb Composition and Fiber Friction

Both Scott and Robbins [183] and Schwartz and Knowles [182] found wide variation in the coefficient of kinetic friction for rubbing human hair fibers against different mandrel compositions. Some of Schwartz's results are summarized in Table 9.35. Most interesting are the relatively low values on aluminum, suggesting a benefit for aluminum combs. However, Wolfram and Hambidge [192] determined that the frictional characteristics of combing materials are not a very important factor in hair combing. This result suggests that hair on hair friction the cause of tangles and snags is more important to combing forces than hair on comb friction.

Experimentally, it is generally easier to test friction of hair against another substrate than to test hair-on-hair friction. It is likely that the relative frictional effects of hair against rubber or another substrate will correlate well (but not perfectly) with hair-on-hair friction, as evidenced by the results of Table 9.35 showing lower dry than wet frictional coefficients for all substrates.

9.10.6 Normal Room Temperatures do not Affect Hair Friction

Scott and Robbins [183] found that temperature changes from 75 to 110°F (~24–43°C) produced virtually no changes in the high-load friction coefficient. Other temperature ranges have not been reported.

9.10.7 Bleaching (Oxidation of Hair) Increases Hair Friction

Scott and Robbins [183] demonstrated that bleaching hair increases hair fiber friction. Furthermore, friction increases with increasing bleach damage. This same effect has been observed both at high load and at low load. The results of Table 9.37, in "shampoo" illustrate this effect, while those in conditioner illustrate the effect of conditioners on bleached hair. These results suggest that the stronger

Table 9.37 Effect of bleaching on hair fiber friction [183] (high load)

	μ_k in shampoo	μ_k in conditioner rinse
Unmodified hair	0.249	0.220
1 \times mild bleach	0.342	0.190
3 \times mild bleach	0.427	0.193

interaction of bleached hair with cationic conditioner ingredients is consistent with the higher concentration of ionized cysteic acid groups at or near the surface in bleached hair [53]. The influence of bleaching and its frictional effects on the cosmetic properties of hair are discussed in Chap. 10.

9.10.8 Permanent Waving Increases Hair Friction

Permanent waving not only changes hair fiber curvature, but it also increases hair fiber friction [182]. The influence of permanent waves on cosmetic hair assembly properties is discussed in Chap. 10.

9.10.9 Shampoos and Hair Friction

Table 9.38 summarizes some of the data of Scott and Robbins [183] for the wet friction coefficients of shampoos at high load. The coefficient of friction for hair fibers treated with the high conditioning shampoo is lower than for hair treated with the high cleaning shampoo. This effect suggests easier wet combing by the conditioning shampoo and has been verified.

9.10.10 Conditioners and Hair Friction

From friction behavior versus concentration of different cationic types, Scott and Robbins [183] suggested three types of cationic conditioner ingredients. Table 9.39 illustrates this behavior in which the cationics were tested by determining the friction coefficient of hair fibers against hard rubber first in the higher concentration solutions (0.1% and 0.01%) and then simply by changing solution to deionized

Table 9.38 Friction coefficients by shampoos [183] (high load)

	Hair on hard rubber (μ_k)
High cleaning shampoo	0.342
Experimental high conditioning shampoo	0.155

Table 9.39 Influence of cationic concentration and rinsing effects on hair friction [183]

	Concentration		
	0.1% μ_k	0.01% μ_k	0% ^a μ_k
Cetrimonium bromide (CTAB)	0.390	0.298	0.537
Stearalkonium chloride (SBDAC)	0.450	0.394	0.298
Distearyldimonium chloride (DDAC)	0.171	–	0.298
Imidazolinium quaternary (IQ)	0.188	0.169	0.166

^aThis point was determined after the higher concentration (0.1%) simply by changing solution to deionized water, to simulate rinsing

water, to simulate rinsing. For CTAB, the friction coefficient decreased with concentration from 0.1% to 0.01%. For a “simulated rinse” (0%), it increased, indicating that CTAB is not bound tightly to the hair fiber surface.

SBDAC illustrates another type of behavior, where friction decreases with concentration; however, on rinsing to 0% it remains low. Both IQ and DDAC illustrate the third type of behavior, where the friction coefficient is low under all test conditions. These data suggest a point of superiority for DDAC and IQ over CTAB. The decrease in the friction coefficient with concentration and with rinsing for SBDAC is unexpected. These results indicate the necessity for thorough rinsing with this ingredient for optimum conditioner performance.

Scott and Robbins [183] tested CTAB above and below its critical micelle concentration, using salt to promote micelle formation. No significant difference was found in the friction coefficient, suggesting that molecular sorption rather than micellar sorption occurs to affect the friction coefficient in systems of this type. For additional discussion of conditioners and the effects of reduced fiber friction on hair properties, see Chap. 10.

9.11 Mechanical Fatiguing, Extension Cycling and Scale Lifting

Kamath et al. [193] of Textile Research Institute in Princeton tested mechanical fatiguing of human hairs by employing loads of 20–40 grams (generally 30 g) for a fixed number of cycles up to 100,000. Controlled humidity and temperature is a requirement for this type of testing as for most hair fiber testing. At 30 grams load, the strain is generally just beyond the Hookean region and is similar to “some” of the strains encountered in combing and brushing of hair [194] where repetitive or cyclic stresses occur at very rapid strain rates. Mechanical fatiguing is essentially impact loading hundreds to thousands of times [193–196]. A hair fiber with an attached weight can be impacted either by fatiguing (many times) or against another object such as another hair fiber or a comb tooth (once or a few times) and is described in Chap. 10 and in two publications by Robbins [14, 195].

Extension cycling on the other hand has been used by Gamez-Garcia [16] where he employed strains of 10–30% under conditions of controlled humidity and

temperature, generally for 50–200 cycles. Gamez-Garcia found the most damaging effects to the cuticle at low relative humidity produced microscopic damage with strains as low as 10% stretch.

These methods (fatiguing, extension cycling and impact loading) are relatively new (compared to tensile testing) and they simulate “some” of the damaging actions and effects from combing and brushing. Tensile testing is useful for investigating changes to the cortex of the fiber from treatments or physical actions. But, tensile testing is not so meaningful in terms of simulating the stresses normally encountered by hair fibers on consumers’ heads because hair fibers are not normally stretched 25–50% of their length or at exceedingly low strain rates as employed in most tensile tests. Furthermore, the fact that cuticle damage cannot be detected by tensile testing is another important negative. However, torsional testing can reveal cuticle damage. The following discussion illustrates some of the results from these newer test methods.

Cyclic stretching and fatiguing of hair fibers occurs in everyday grooming actions and these actions ultimately lead to cuticle deformation and cuticle fragmentation (Figs. 9.31–9.35).

Gamez-Garcia [16] demonstrated that cuticle cracks in the non-keratin regions can be induced by only 10% extension at low humidity (Fig. 9.31) creating cracked and lifted scales. He also showed that the extent of crack formation depends on the number of cycles. Kamath et al. [193] observed similar findings for mechanical fatiguing of hair fibers. Figure 9.32 illustrates the effects of fatiguing on the cuticle and Figs. 9.33 and 9.34 shows the effects on the cuticle and the cortex of hair by fatiguing followed by stretching the fibers to break.

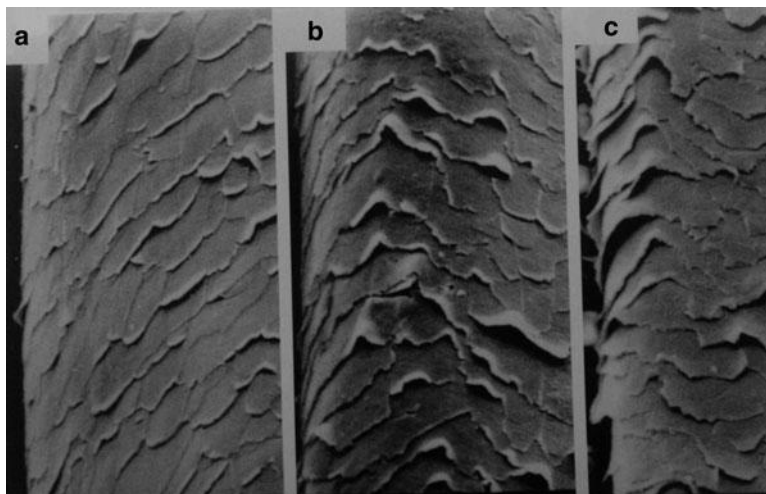


Fig. 9.31 Scale lifting caused by extension cycling to 10% at 10% RH [16]: (a) to 50 cycles, (b) to 100 cycles and (c) to 200 cycles from Gamez-Garcia [16] (reprinted with permission of the Journal of the Society of Cosmetic Chemists)

Fig. 9.32 Scale lifting caused by fatiguing chemically undamaged hair to 100,000 cycles with a 30 g load in 31 h and then extended just below the failure load. Electron micrographs at two different magnifications kindly provided by Sigrid Ruetsch

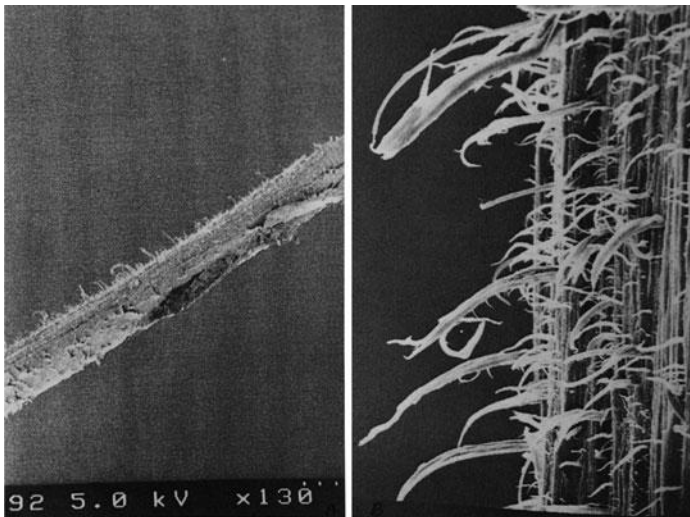
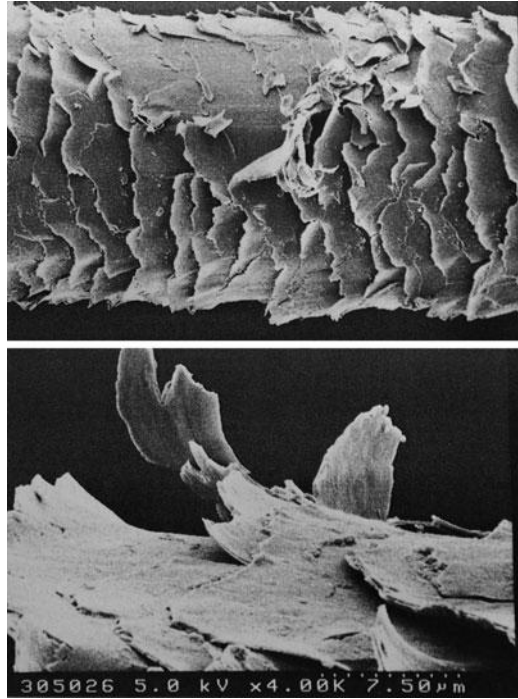


Fig. 9.33 Fiber fatigued to 100,000 cycles with a 30 g load in 31 h and then extended. Note the severe fracture effects causing the separation of cortical cells indicating weakening of the cell membrane complex. (a) Low magnification. (b) High magnification. SEMs kindly provided by Sigrid Ruetsch

Fig. 9.34 Fiber fatigued to 100,000 cycles with a 30 g load in 31 h and then extended to break (near the fracture site). Note the severe cuticle cracking and lifting in addition to the separation and lifting of cortical cells. SEM kindly provided by Sigrid Ruetsch

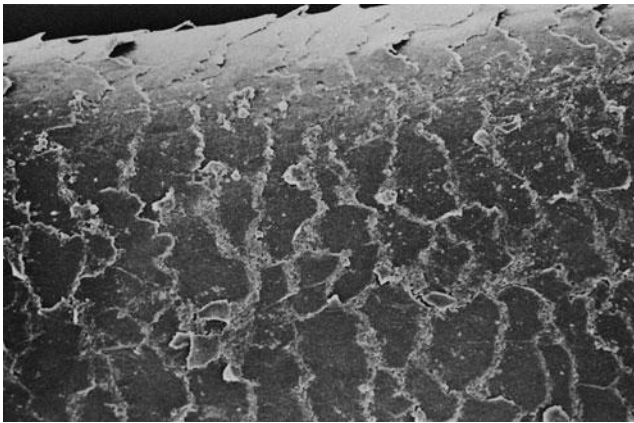
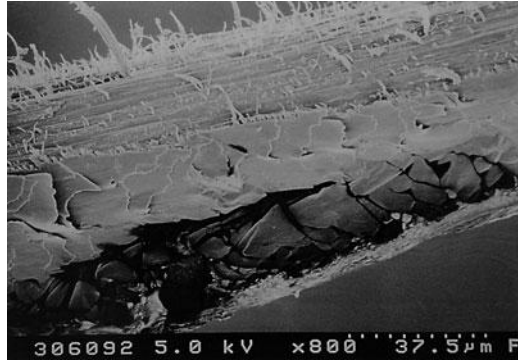


Fig. 9.35 Hair fiber chemically bleached with alkaline peroxide and then fatigued. Note the severe chipping and crumbling of the cuticle scale edges. Contrast this effect to that of Fig. 9.5 (top) involving no chemical bleaching. SEM kindly provided by Sigrid Ruetsch

The process of cuticle loss or fragmentation was described in detail in Chap. 6. A mechanism was also presented to explain this phenomenon. Chemical or physical attack to the cell membrane complex and the endocuticle weakens these vital regions producing increased swelling and even cracks that accelerate the processes of fragmentation and in some cases catastrophic failure. Penetrating chemicals can enter damaged areas more rapidly. Certain chemicals either strengthen the fiber (not often) or more likely produce scale lifting and/or distortion and in this manner either inhibit or accelerate the process of cuticle degradation and scale removal. The next section of this manuscript describes the effects of penetrating ingredients on the cell membrane complex and the endocuticle and the consequences of these actions using the techniques of mechanical fatiguing and extension cycling coupled with microscopy.

If cuticle cracks are formed by stretching or fatiguing and the fibers are treated with water and dried, the scales sometimes return to their “normal” appearance at a microscopic level. However, subsequent treatments (other than water) to cracked or damaged scales can either inhibit further damage or accelerate cuticle fragmentation. Even pre-treatments can affect fragmentation.

Gamez-Garcia [16] determined that pre-treatment of hair fibers with hydrogen bonding plasticizers such as glycerine or propylene glycol (without rinsing) inhibits scale lifting from extension cycling. These effects may be similar to the effects of pre-shampoo treatments with oils such as coconut oil which has been shown by Ruetsch et al. [197] to reduce cuticle fragmentation.

Hilterhaus-Bong and Zahn [198] demonstrated that intercellular lipids can be extracted from hair by multiple detergent washings. Gould and Sneath [199] examined root and tip sections of scalp hair by transmission electron microscopy (TEM) and observed holes or vacancies in the thin cross-sections. These holes (cracks) were attributed to breakdown and removal of intercellular components by shampoos. Removal of parts of the cell membrane complex by shampoos will weaken this domain making the hair more susceptible to cuticle fragmentation. This effect is consistent with the finding in our laboratories that cuticle fragmentation and protein loss (see Chap. 6) is greater in the tip ends of hair fibers treated only with shampoos and no other cosmetic treatment.

Polymer JR-400 when applied to fatigued or stretched hair inhibits cuticle scale lifting. This effect is illustrated by comparing Fig. 9.35 (bleached, fatigued control fiber) to Fig. 9.36 (bleached, JR treated, fatigued). Note the breakage and crumbling of the scales at the cuticle edges in the control versus the fewer broken scale edges of the treated fiber of Fig. 9.36. This effect is illustrated further by comparing Figs. 9.37 (bleached, fatigued and extended control) and 9.38 (bleached, JR treated,

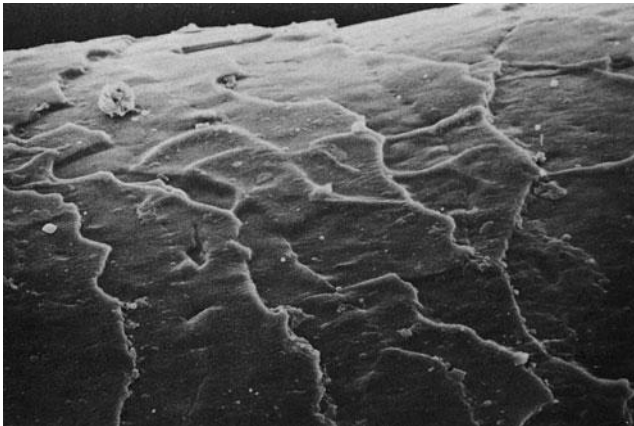


Fig. 9.36 Hair fiber chemically bleached with alkaline peroxide then treated with Polymer JR-400 solution and then fatigued 100,000 times with a 30 g load. Note virtually no scale lifting or crumbling of the cuticle scale edges compared to that of Figs. 9.35 and 9.37. SEM kindly provided by Sigrid Ruetsch

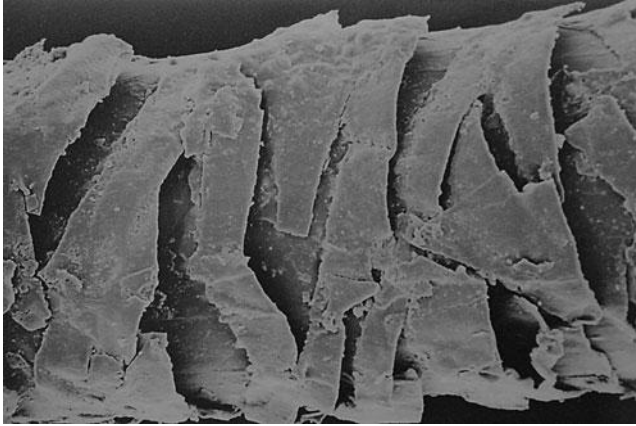


Fig. 9.37 Hair fiber chemically bleached with alkaline peroxide then fatigued 100,000 times with a 30 g load and then extended. Note the extensive scale lifting and fracturing underneath the scales at the weakened cell membrane complex. SEM kindly provided by Sigrid Ruetsch

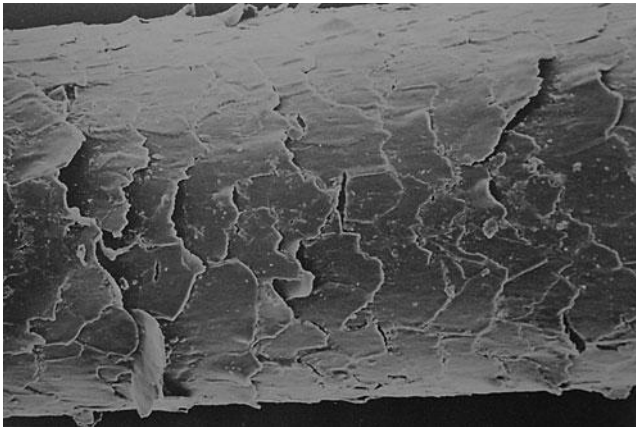


Fig. 9.38 Hair fiber chemically bleached and treated with Polymer JR-400, then fatigued and extended. Note the minimal scale lifting compared to the micrograph of Fig. 9.37. SEM kindly provided by Sigrid Ruetsch

fatigued and extended). Note the large difference in the cuticle scale lifting of Fig. 9.37 versus that of the JR treated hairs in Fig. 9.38.

Post treatment of extension cycled hair with 3% aqueous solutions of polymers such as a hydrolyzed wheat-polysiloxane copolymer or a protein-silicone copolymer inhibits scale lifting that can be induced by additional bending after extension cycling (Fig. 9.39) [16]. On the other hand, polymers such as polyethylene-imine (3%) fail to prevent scale lifting from additional fiber extension. But, blow drying of polyethylene-imine treated hair produces cuticle lifting and distortion (Fig. 9.40) [16].

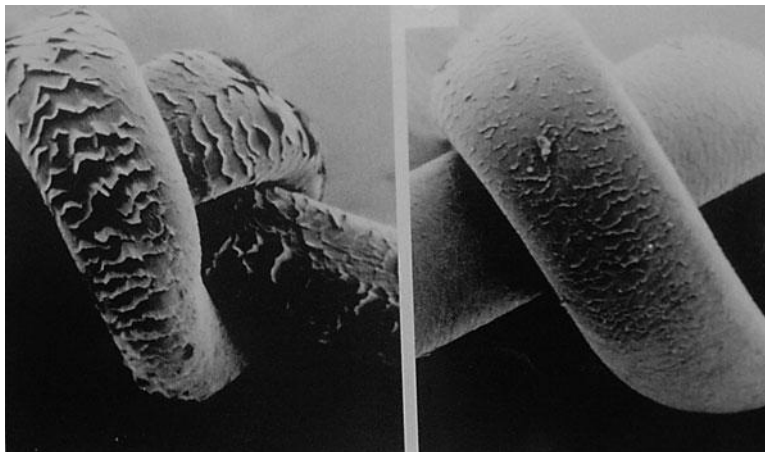


Fig. 9.39 Both hair fibers extension cycled 200 times to 20% extension at 10% RH and put into water and knotted by Gamez-Garcia [16]. *Right:* Fiber treated with 3% cystine polysiloxane prior to knotting. *Left:* Control fiber. Note the lack of scale lifting from the polysiloxane treated fiber (reprinted with permission of the Journal of Cosmetic Science)

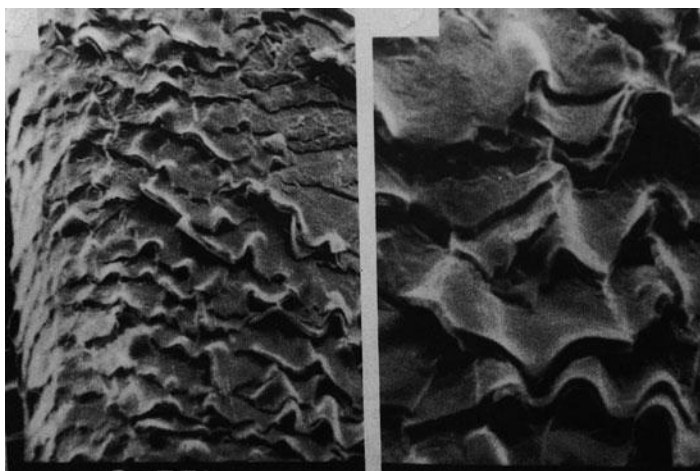


Fig. 9.40 Hair fiber extension cycled to provide scale lifting then treated with 3% polyethylene imine and then three cycles of wetting and blow drying by Gamez-Garcia [16]. Note the severe scale lifting and folding caused by this polymer treatment (Reprinted with permission of the Journal of Cosmetic Science)

Inhibition or promotion of scale lifting and hair fragmentation by isolated polymers or ingredients can be informative in terms of helping to explain the mechanism of fiber degradation from stretching, bending, torsion and abrasive actions. However, such treatments are often of limited use in product formulation

studies, because the addition of other ingredients to make a finished and aesthetic formulation often changes the nature and effects of the active ingredient on cuticle fragmentation or protein loss. For example, hair fibers with a weakened cell membrane complex from permanent waving and stretching when treated alternately with triethanol ammonium lauryl sulfate and stearylalkonium chloride produced pronounced scale lifting and distortion. On the other hand, the addition of cetyl alcohol (a common additive in cr me rinses) to the stearylalkonium chloride produces noticeably less scale lifting and distortion.

Certain shampoo formulations with cationic guar produce scale lifting. However, other formulations with only small formula changes produce no detectable lifting or less protein loss. Thus the combination of ingredients in a formulation can either retard penetration and/or deposition into the cuticle or alter the interactions of an active ingredient with functional groups that are a part of the structure of hair and change the effects on cuticle/hair damage.

Hair fibers with a weakened cell membrane complex/endocuticle are exceedingly sensitive to penetrating ingredients. Ingredients that penetrate into these regions can either remove or breakdown non-keratin components or can deposit and promote cuticle lifting and scale distortion. On the other hand, those penetrating ingredients that diffuse into the cell membrane complex-endocuticle and interact by bonding so as to either plasticize or provide adhesive bridges to the weakened layers can strengthen the cuticle and make it more resistant to fragmentation and protein loss. Furthermore, scale lifting methodology (extension cycling or fatiguing evaluated by microscopy and/or light scattering) is more effective for distinguishing between these types of damage and repair than tensile or load-elongation methods which have not been shown to be capable of detecting changes in the cuticle.

References

1. Robbins CR, Scott GV (1978) Prediction of hair assembly characteristics from single fiber properties. *J Soc Cosmet Chem* 29:783–792
2. Hough PS, Huey JE, Tolgyesi WS (1976) Hair body. *J Soc Cosmet Chem* 27:571–578
3. Robbins CR, Reich C (1986) Prediction of hair assembly characteristics from single fiber properties. Part II: The relationship of fiber curvature, friction, stiffness and diameter to combing behavior. *J Soc Cosmet Chem* 37:141–158
4. International dictionary of physics and electronics. Van Nostrand Reinhold, New York (1956)
5. Feughelman M (1982) The physical properties of alpha-keratin fibers. *J Soc Cosmet Sci* 33:385–406
6. Wolfram LJ, Lindemann M (1971) Some observations on the hair cuticle. *J Soc Cosmet Chem* 22:839–850
7. Robbins CR, Crawford R (1991) Cuticle damage and the tensile properties of human hair. *J Soc Cosmet Chem* 42:59–67
8. Persaud D, Kamath YK (2004) Torsional method for evaluating hair damage and performance of hair care ingredients. *J Cosmet Sci(Suppl)* 55:S65–S77

9. Weigmann HD (1991) Analysis and quantification of hair damage. Progress Report No. 2, TRI Princeton, Princeton, Nov 1991
10. Simpson WS (1965) A comparison of methods of measurement of Young's modulus for keratin fibers. *J Text Inst* 51:T675
11. Huck P, Baddiel C (1971) The mechanical properties of virgin and treated human hair fibers; a study by means of the oscillating beam method. *J Soc Cosmet Chem* 22:401–410
12. Hamburger W, Morgan HM, Platt MM (1950) Some aspects of the mechanical behavior of hair. *Proc Sci Sect T.G.A.* (14):10–16
13. Berthiaume MD, Riccio DA, Merrifield JH (1994) Silicone based products for damaged hair in various ethnic groups. *Drug Cosmet Ind* 155(6):24–32
14. Robbins CR (2006) Hair breakage during combing. II: Impact loading and hair breakage. *J Cosmet Sci* 54:245–257
15. Kamath YK, Hornby S, Weigmann H-D (1985) Effect of chemical and humectants treatments on the mechanical and fractographic behavior of negroid hair. *J Soc Cosmet Chem* 36:39–52
16. Gamez-Garcia M (1998) Cuticle decementation and cuticle buckling produced by Poisson contraction on the cuticular envelope of human hair. *J Cosmet Sci* 49:213–222
17. Henderson GH et al (1978) Fractography of human hair. *J Soc Cosmet Chem* 29:449–467
18. Kamath Y, Weigmann H-D (1982) Fractography of human hair. *J Appl Polym Sci* 27:3809–3833
19. Kamath Y, Hornby S, Weigmann H-D (1984) Mechanical and fractographic behavior of negroid hair. *J Soc Cosmet Chem* 35:21–43
20. Robbins C et al (2004) Failure of intercellular adhesion in hair fibers with regard to hair condition and strain conditions. *J Cosmet Sci* 55:351–371
21. Feughelman M, Willis BK (2001) Mechanical extension of human hair and the movement of the cuticle. *J Cosmet Sci* 52:185–193
22. Negri A et al (1996) A transmission electron microscope study of covalently bound fatty acids in the cell membranes of wool fibers. *Textile Res J* 66:491–495
23. Ruetsch SB, Kamath YK, Weigmann H-D (2003) The role of cationic conditioning compounds in reinforcement of the cuticle. *J Cosmet Sci* 54:63–83
24. Deem D, Rieger M (1968) Mechanical hysteresis of chemically modified hair. *J Soc Cosmet Chem* 19:395–410
25. Harris M et al (1942) Elasticity of wool as related to its chemical structure. *J Res Natl Bur Stand* 29:73–86
26. Sikorski J, Woods H (1950) The effect of rate of extension on the Young's modulus of keratin fibers. *Proc Leeds Philos Lit Soc (Sci Sect)* 5:313
27. Rebenfeld L, Weigmann H-D, Dansizer C (1963) Forces and kinetics of supercontraction of keratin fibers in 9 M LiCl. *Textile Res J* 33:779–784
28. Speakman JB (1947) Mechano-chemical methods for use with animal fibers. *J Text Inst* 37:T102–T126
29. Sookne AM, Harris M (1937) Stress strain characteristics of wool as related to its chemical structure. *J Res Natl Bur Stand* 19:535–549
30. Wolfram LJ, Lennhoff M (1966) The effect of chemical treatment on the tensile properties of keratin fibers. *J Text Inst* 57:T591–T592
31. Beyak R et al (1969) Elasticity and tensile properties of human hair. I: Single fiber test method. *J Soc Cosmet Chem* 20:615–626
32. Feughelman M, Robinson M (1967) The relationship between some mechanical properties of single wool fibers and relative humidity. *Textile Res J* 37:441–446
33. Speakman JB (1928) The plasticity of wool. *Proc Roy Soc* 103(Series B):377–396
34. Menkart J, Wolfram LJ, Mao I (1966) Caucasian hair, negro hair and wool: similarities and differences. *J Soc Cosmet Chem* 17:769–788
35. Breuer M (1972) The binding of small molecules to hair. I: The hydration of hair and the effect of water on the mechanical properties of hair. *J Soc Cosmet Chem* 23:447–469

36. Chamberlain N, Speakman JB (1931) Uber hysteresiserscheinungen in der wasseraufnahme des menschenhaares. *Z Electrochem* 37:374–375
37. Speakman JB (1929) The rigidity of wool and its changes with adsorption of water vapor. *Trans Faraday Soc* 25:92–103
38. Robbins CR, Scott GV (1970) Prediction of dry extension properties of keratin fibers from wet extension data. *J Soc Cosmet Chem* 21:639–641
39. Rebenfeld L, Weigmann H-D, Dansizer C (1966) Temperature dependence of the mechanical properties of human hair in relation to structure. *J Soc Cosmet Chem* 17:525–538
40. Astbury WT, Street A (1931) X-ray studies of the structures of hair, wool and related fibers. I: General. *Philos Trans Proc R Soc Series A* 230:75–101
41. McMillen R, Jachowicz J (1998) Thermal degradation of hair. I: Effect of curling irons. *J Cosmet Sci* 49:223–244
42. Humphries W et al (1972) The thermomechanical analysis of natural and chemically modified human hair. *J Soc Cosmet Chem* 23:359–370
43. Dankovich TA, Kamath YK, Ruetsch SB (2004) Tensile properties of twisted hair fibers. *J Cosmet Sci* 55:S79–S90
44. Syed S et al (1995) African-American hair: its physical properties and differences relative to Caucasian hair. *Cosmet Toiletries* 110:39–48
45. Wolfram LJ (2003) Human hair: a unique physicochemical composite. *J Am Acad Dermatol* 48(Suppl):106–114
46. Duvel L et al (2005) Analysis of hair lipids and tensile properties as a function of distance from scalp. *Int J Cosmet Sci* 27:193–197
47. Porter C et al (2009) The behavior of hair from different countries. *J Cosmet Sci* 60:97–109
48. Hardy D (1973) Quantitative hair form variation in seven populations. *Am J Phys Anthropol* 39:7–18
49. Scott GV, Robbins CR (1978) Stiffness of human hair fibers. *J Soc Cosmet Chem* 29:469–485
50. Khayatt RM, Chamberlain NH (1948) The bending modulus of animal fibers. *J Text Inst* 39: T185
51. Chaikin M, Chamberlain NH (1955) The propagation of longitudinal stress pulses in textile fibers. *J Text Inst* 46:T44
52. Alexander P et al (1951) The reaction of oxidizing agents with wool. 5: The oxidation products of the disulfide bond and the formation of a sulfonamide in the peptide chain. *Biochem J* 49:129–138
53. Alexander P et al (1963) *Wool, its chemistry and physics*, 1963rd edn. Franklin Publishing Co, NJ, pp 61–65
54. Harris M, Brown A (1946) *Symposium on fibrous proteins*. Publ. Soc. Dyers Col, Bradford, p 203
55. Garson JC et al (1980) The transverse vibrational properties of keratin fibers in the presence of water and other materials. *Int J Cosmet Sci* 2:231–241
56. Robbins CR, Kelly C (1969) Amino acid analysis of cosmetically altered hair. *J Soc Cosmet Chem* 20:555–564
57. Edman W, Marti M (1961) Properties of peroxide bleached hair. *J Soc Cosmet Chem* 12:133–145
58. Robbins CR (1971) Chemical aspects of bleaching human hair. *J Soc Cosmet Chem* 22:339–348
59. Harris M, Sookne AM (1937) Stress strain characteristics of wool related to its chemical composition. *Proc Am Assoc Tex Chem & Col*, 19:535–549
60. Tate J et al (1993) Quantification and prevention of hair damage. *J Soc Cosmet Chem* 44:347–371
61. Hermann KW (1963) Hair keratin reaction, penetration and swelling in mercaptan solutions. *Trans Faraday Soc* 59:1663–1671
62. Freytag H (1964) Untersuchungen uber das phanomen der daververformung menschlichen haares. *J Soc Cosmet Chem* 15:667–690

63. Hamburger WJ, Morgan H (1952) Some effects of waving lotion on the mechanical properties of hair. *Proc Sci Sect T.G.A* 18:44–48
64. Kubu E, Montgomery D (1952) II. Kinetics of the reduction of wool keratin by cysteine. *Textile Res J* 22:778–782
65. Wortmann F-J, Souren J (1987) Extensional properties of human hair and permanent waving. *J Soc Cosmet Chem* 38:125–140
66. Heilengotter R, Komarony R (1958) *Am Perfumer & Aromatics* 71:31–32
67. Whitman R (1952) Some effects of waving lotions on the mechanical properties of hair. *Proc Sci Sect T.G.A* (18):27
68. Brown J (1967) The chemistry of synthetic dyes used in cosmetics. *J Soc Cosmet Chem* 18:225–244
69. Brown KC et al (1985) Oxidative dyeing of keratin fibers. *J Soc Cosmet Chem* 36:31–37
70. Wall FE (1957) In: Sagarin E (ed) *Cosmetics, science and technology*, Ch. 21. Interscience, NY
71. Pande CM, Albrecht L, Yang B (2001) Hair photoprotection by dyes. *J Cosmet Sci* 52:377–390
72. Zahn H et al (1968) Der einfluss von tensiden aur eigenschaften von keratinfasern. *Fette Seifen Anstrichmittel* 70(10):757–760
73. Speakman JB, Stott E (1934) From measurements of the swelling of wool fibers. *Trans Faraday Soc* 30:539–548
74. Valko E, Barnett G (1952) A study of the swelling of hair in mixed aqueous solvents. *J Soc Cosmet Chem* 3:108–117
75. Breuer M, Prichard D (1967) *The behavior of hair at low pH values*. *J Soc Cosmet Chem* 18:643–650
76. Beyak R et al (1971) Elasticity and tensile properties of human hair. II: light radiation effects. *J Soc Cosmet Chem* 22:667–678
77. Robbins CR, Kelly C (1970) Amino acid composition of human hair. *Textile Res J* 40:891–896
78. Harris M, Smith A (1938) Photochemical reactions of wool. *J Res Natl Bur Stand* 20:563–569
79. Dubief C (1992) Experiments with hair photodegradation. *Cosmetics and Toiletries* 107:95–102
80. Korner H et al. (1995) Changes in the content of 18-methyleicosanoic acid in wool after UV-irradiation and corona treatment. In: 9th inter-national wool textile research conferences, Biella 2, pp 414–419
81. Korastoff E (1970) Normalized stress strain relationship in human hair perturbation by hypothyroidism. *Br J Dermatol* 83:27–36
82. Swanbeck G et al (1970) Mechanical properties of hairs from patients with different types of hair diseases. *J Invest Dermatol* 54:248–251
83. Wilson JT (1985) International symposium on forensic hair comparisons, *Quantic*
84. Anzuino G, Robbins CR (1971) Reactions of metal salts with human hair containing synthetic polymers. *J Soc Cosmet Chem* 22:179–186
85. Hirsh F (1960) Structure and synchronized stretch-rotation of hair keratin fibers. *J Soc Cosmet Chem* 11:26–37
86. Robinson MS, Rigby BJ (1985) Thiol differences along keratin fibers: stress strain and stress relaxation behavior as a function of temperature and extension. *Textile Res J* 55:597–600
87. Brown AE, Pendergrass JH, Harris M (1950) Prevention of supercontraction in modified wool fibers. *Textile Res J* 20:51–52
88. Kawabata S et al. (2000) Micro-mechanics of wool single fiber, www.mat.usp.ac.jp/polymer-composite/10thwool.pdf
89. Scott GV, Robbins CR (1969) A convenient method for measuring fiber stiffness. *Textile Res J* 39:975–976
90. Baltenneck F et al (2001) A new approach to the bending properties of hair fibers. *J Cosmet Sci* 52:355–368

91. Guthrie JC et al (1954) An investigation into bending and torsional rigidities of some fibers. *J Text Inst* 59:T912–T929
92. Morton W, Hearle JWS (1962) Physical properties of textile fibers, Ch. 17. Butterworths, London
93. Nagase S et al (2008) Characterization of curved hair of Japanese women with reference to internal structures and amino acid composition. *J Cosmet Sci* 59:317–332
94. Thibaut S et al (2005) Human hair keratin network and curvature. *Int J Dermatol* 46(suppl 1): 7–10
95. Bryson W et al (2009) Cortical cell types and intermediate filament arrangements correlate with fiber curvature in Japanese human hair. *J Struct Biol* 166:46–58
96. Kawabata S et al (2004) Apparent elastic modulus of scale estimated from bending property of single wool fiber. *J Text Eng* 50:21–24
97. Masaaki Y (2002) Physical properties of human hair. 2: evaluation of human hair torsional stress and a mechanism of bending and torsional stress. *Journal of SCCJ* 36(4):262–272
98. Swift JA (2000) Letter: *The cuticle controls bending stiffness of hair*. *J Cosmet Sci* 51:37–38
99. Atsushi S, Masaaki Y, Arika N (2007) Physical properties of human hair. I: evaluation of bending stiffness by measuring the major and minor axis of human hair. *J Soc Cosmet Chem Japan* 36:207–216
100. Hadjur C et al. (2003) Morphology of the cuticle of African hair. In: 2nd international symposium on ethnic hair & skin, New Directions in Research, Chicago
101. Hearle JWS, Peters R (1960) Moisture in textiles. Butterworths, London, p 173
102. Meredith R (1954) The torsional rigidity of textile fibers. *J Text Inst* 45:T489–T503
103. Goodings A (1968) Double pendulum a method for the measurement of the rigidity of fibers immersed in liquid: the torsion double pendulum. *Textile Res J* 38:123–129
104. Morton WE, Permanyer F (1949) The measurement of torsional relaxation in textile fibers. *J Text Inst* 40:T371–T380
105. Mitchell T, Feughelman M (1960) The torsional properties of single wool fibers. Part I: torque-twist relationship and torsional relaxation in wet and dry fibers. *Textile Res J* 30:662–667
106. Bogaty H (1967) Torsional properties of hair in relation to permanent waving and setting. *J Soc Cosmet Chem* 18:575–590
107. Wolfram LJ, Albrecht L (1985) Torsional behavior of human hair. *J Soc Cosmet Chem* 36:87–99
108. Meredith R, Hearle JWS (1959) Physical methods of investigating textiles, Ch. 8.3. Interscience, NY
109. Abbott N, Goodings AC (1949) Moisture absorption, density and swelling properties of nylon filaments. *J Text Inst* 40:T232–T246
110. King AT (1926) The specific gravity of wool and its relation to swelling and sorption in water and other liquids. *J Text Inst* 17:T53–T67
111. Hearle JWS, Peters R (1960) Moisture in textiles. Butterworths, London, p 144
112. Yin N et al (1977) The effect of fiber diameter on the cosmetic aspects of hair. *J Soc Cosmet Chem* 28:139–150
113. Li C-T, Tietz JV (1990) Improved accuracy of the laser diffraction technique for diameter measurement of small fibers. *Journal Materials Sci* 25:4694–4698
114. Barnard W, White H (1954) The swelling of hair and a viscose rayon monofil in aqueous solution. *Textile Res J* 24:695–704
115. White H, Stam P (1949) An experimental and theoretical study of the adsorption and swelling isotherms of human hair in water vapor. *Textile Res J* 19:136–151
116. Eckstrom M (1951) Swelling studies of single human hair fibers. *J Soc Cosmet Chem* 2:244–249
117. Montgomery D, Milloway W (1952) The vibroscopic method for determination of fiber cross-sectional area. *Textile Res J* 22:729–735
118. Dart S, Peterson L (1949) A strain gauge system for fiber testing. *Textile Res J* 19:89–93

119. Busch P (1984) In: 3rd international hair science symposium, Syburg, W. Germany
120. Brancik J, Daytner A (1977) The measurement of swelling of wool fibers in solvents by laser beam diffraction. *Textile Res J* 47:662–665
121. Barnett G (1952) The swelling of hair in aqueous solutions and mixed solvents. M.S. Thesis, Polytechnic Institute of Brooklyn, NY
122. Stam R et al (1952) The swelling of human hair in water and water vapor. *Textile Res J* 22:448–465
123. Watt I (2008) OFDA laser scanning: the basics, *Alpacas Magazine*, pp 168–170, Spring www.elitealpacobreedingsystems.com/library/SPR08_OFDA.pdf
124. Courtois M et al (1995) Aging and hair cycles. *Br J Derm* 132:86–93
125. World book encyclopedia. Field Enterprises Educational Corp., Chicago (1969)
126. Randebrock R (1964) Neue erkenntnisse uber den morphologischen aufbau des menschlichen haares. *J Soc Cosmet Chem* 15:691–700
127. Kaswell ER (1953) *Textile fibres & fabrics*. Reinhold, New York, p 52
128. Elert G (ed) (1999) Width of a human hair. In: *The physics factbook*. hypertextbook.com/facts/1999/BrianLey.shtml
129. Steggarda M, Seibert H (1941) Size and shape of head hair from six racial groups. *J Heredity* 32:315–318
130. Wolfram LJ (2003) Human hair: a unique physicochemical composite. *J Am Acad Derm* 48(6):S106–S114
131. Trotter M (1930) The form and color of head hair in American whites. *Am J Phys Anthropol* 14:433–445
132. Franbourg A et al (2003) Current research on ethnic hair. *J Am Acad Derm* 48(6):S115–S119
133. Trotter M, Dawson HL (1934) The hair of French Canadians. *Am J Phys Anthropol* 18:443–456
134. Otsuka H, Nemoto T (1988) Study on Japanese hair. *Koshokaishi (J Cosmet Assoc Japan)* 12:192–197
135. Tajima M et al (2007) Characteristic features of Japanese women's hair with aging and with progressing hair loss. *J Dermatol Sci* 45:93–103
136. Galliano A (2010) et al, *Resistance of human hair cuticle after shaking process in wet conditions: comparison between Chinese and Caucasian hair*. *Int J Cosmet Sci* 49:1–13
137. Vernall DG (1961) A study of the size and shape of cross-sections of hair from four races of men. *Am J Phys Anthropol* 19:345–350
138. Seibert H, Steggarda M (1942) The size and shape of human head hair: along its shaft. *J Heredity* 33:302–304
139. Hutchinson PE, Thompson JR (1997) The cross-sectional size and shape of human terminal scalp hair. *Br J Dermatol* 136:159–165
140. Nissimov J, Elchalal U (2003) Scalp hair diameter increases during pregnancy. *Clinical & Exptl Dermatol* 28:525–530
141. Mamada A, Nakamura K (2007) A study of volume and bounce in hair with aging using bending elastic measurements. *J Cosmet Sci* 58:485–494
142. Orwin DFG (1989) Variations in wool follicle morphology. In: Rogers GE, Reis PJ, Ward KA, Marshall RC (eds) *Biology of wool & hair*. Chapman & Hall, London, New York, p 229
143. Trotter M, Duggins OH (1930) Age changes in head hair from birth to maturity: index and size of hair of children. *Am J Phys Anthropol* 6:489–506
144. Nagase S et al (2009) Changes in structure and geometric properties of human hair by aging. *J Cosmet Sci* 60:637–648
145. Bogaty H (1969) Differences between adult and children's hair. *J Soc Cosmet Chem* 20:159–171
146. Pecoraro V et al (1964) Cycle of the scalp hair of the new born child. *J Invest Dermatol* 43:145–147
147. Furdon SA, Clark DA (2003) Scalp hair characteristics in the newborn infant. *Adv Neonatal Care* 3(6):286–296

148. Robbins CR, Dawson TL et al. What women want—a new more perception relevant model of scalp hair, hair amount. Variation in scalp hair diameter and density with age in caucasian women, *Br. J. Derm.*, in press
149. Mirmirani P, Dawson TL Jr et al (2010) Hair growth parameters in pre- and post-menopausal women. In: Treub R, Tobin D (eds) *Hair aging*. Springer-Verlag, Heidelberg
150. Lindelof B et al (1988) Morphology revealed by light and scanning electron microscopy and computer aided three dimensional reconstruction. *Arch Dermatol* 124:1359–1363
151. Saitoh M et al (1970) Human hair cycle. *J Invest Dermatol* 54:65–81
152. Tolgyesi E (1983) A comparative study of beard and scalp hair. *J Soc Cosmet Chem* 34:361–382
153. DeBerker DAR et al (2004) Disorders of Hair, In: Burns T et al (eds) *Rook's textbook of dermatology*, 4th edn. Blackwell, Malden, London
154. Schwan-Jonczyk A (1999) *Hair Structure*, 1st edn. Wella AG publisher, Darmstadt, pp 39–49
155. Fitzpatrick TB et al (1958) In: Montagna W, Ellis RA (eds) *The biology of hair growth*. Academic, New York, p 287
156. Hollfelder B et al (1995) Chemical and physical properties of pigmented and non-pigmented (grey hair). *Int J Cosmet Sci* 17:87–89
157. Gao T, Bedell A (2001) Ultraviolet damage on natural gray hair and its photoprotection. *J Cosmet Sci* 52:103–118
158. De La Mettrie R et al (2006) Shape variability and classification of human hair: a worldwide approach. *Hum Biol* 79(3):265–281
159. Loussouarn G et al (2007) Worldwide diversity of hair curliness: a new method of assessment. *Int J Dermatol* 46(suppl 1):2–6
160. Hausman LH (1924) Further studies of the relationships of the structural characters of mammalian hair. *Am Nat* 58:544–557
161. Wynkoop EM (1929) A study of the age correlations of the cuticular scales, medullas and shaft diameters of human head hair. *Am J Phys Anthropol* XIII(2):177–188
162. Takahashi T et al (2006) Morphology and properties of Asian and Caucasian hair. *J Cosmet Sci* 57:327–338
163. Trotter M (1938) A review of the classification of hair. *Am J Phys Anthropol* 24:105–126
164. Deniker J (1900) *The races of man: an outline of anthropology and ethnography*. W. Scott, London, C. Scribner's Sons, New York
165. Martin R (1928) *Lehrbuch der Anthropologie*, 2nd edn. Jena Publ., Germany
166. Kajiura Y et al (2006) Structural analysis of human hair single fibers by scanning microbeam SAXS. *J Struct Biol* 155:438–5444
167. Robbins C, Crawford RJ (1984) A method to evaluate hair body. *J Soc Cosmet Chem* 35:369–377
168. Porter CE et al (2005) The influence of African American hair's curl pattern on its mechanical properties. *Int J Dermatol* 44(suppl 1):4–5
169. www.aaanet.org/stmts/racepp.htm
170. Swift JA (1992) In: 8th international hair science symposium of the DWI, Kiel
171. Spei M, Zahn H (1979) Small angle X-ray examination of swollen keratin fibers. *Melliand Textilber* 60(7):523–527
172. Steinhardt J, Harris M (1940) Combination of wool protein with acid and base: hydrochloric acid and potassium hydroxide. *J Res Natl Bur Stand* 24:335–367
173. Shansky A (1963) The osmotic behavior of hair during the permanent waving process as explained by swelling. *J Soc Cosmet Chem* 14:427–432
174. Powers D, Barnett G (1953) A study of the swelling of hair in thioglycolate solutions and its re-swelling. *J Soc Cosmet Chem* 4:92–100
175. Reed R et al (1948) Permanent waving of human hair: the cold process. *J Soc Cosmet Chem* 1:109–122
176. Keil F (1960) Die quellung des hares in kaltwellmitteln untersuchungen in polarisiertem lichte. *J Soc Cosmet Chem* 11:543–554

177. Wickett R (1983) Kinetic studies of hair reduction using a single fiber technique. *J Soc Cosmet Chem* 34:301–316
178. Klemm E et al (1965) The swelling behavior of hair fibers in lithium bromide. *Proc Sci Sect TGA* 43:7–13
179. Mercer EH (1949) Some experiments on the orientation and hardening of keratin in the hair follicle. *Biochem Biophys Acta* 3:161–169
180. Howell H et al (1959) Friction in textiles. Butterworths, London
181. Robbins CR (1984) 3rd International Hair Science Symposium of DWI, Syburg, Germany and described in detail at TRI/Princeton, Continuing professional education in lectures and in the course book from 1997 to 2006
182. Schwartz A, Knowles D (1963) Frictional effects in human hair. *J Soc Cosmet Chem* 14:455–463
183. Scott GV, Robbins CR (1980) Effects of surfactant solutions on hair fiber friction. *J Soc Cosmet Chem* 31:179–200
184. Howell HG, Mazur J (1952) Amonton's law and fiber friction. *J Text Inst* 43:T59–T69
185. Meredith R, Hearle JWS (1959) Physical methods of investigating textiles, Ch. 11. Interscience, NY
186. King G (1950) Some frictional properties of wool and nylon fibers. *J Text Inst* 41:T135–T144
187. Wool Research (1955) Physical properties of wool fibers and fabrics, Ch. 8, vol 2. Wool Industries Research Assoc, Leeds
188. Fishman D, Smith AL, Harris M (1948) Measurement of the frictional properties of wool fibers. *Textile Res J* 18:475–480
189. Martin A, Mittleman R (1946) Some measurements of the friction of wool and mohair. *J Text Inst* 37:T269
190. Swift J, Bews B (1976) The chemistry of human hair cuticle. III: the isolation and amino acid analysis of sub-fractions of the cuticle obtained by pronase and trypsin digestion. *J Soc Cosmet Chem* 27:289–300
191. Alexander P et al (1963) Wool, its chemistry and physics, 2nd edn. Franklin, NJ, pp 25–46
192. Hambidge A, Wolfram LJ (1984) In: 3rd international hair science symposium, Syburg, W. Germany
193. Kamath YK et al (1985) Effect of chemical and humectants treatments on the mechanical and fractographic behavior of Negroid hair. *J Soc Cosmet Chem* 36:39–52
194. Kamath YK, Weigmann HD (1986) Measurement of combing forces. *J Soc Cosmet Chem* 37:111–124
195. Robbins C (2006) Hair breakage during combing. I: pathways of breakage. *J Cosmet Sci* 57:233–243
196. Evans TA, Park K (2010) A statistical analysis of hair breakage. II. Repeated grooming experiments. *J Cosmet Sci* 61:439–456
197. Ruetsch SB, Kamath YK, Rele AS, Mohile R (2001) Secondary ion mass spectrometric investigation of penetration of coconut and mineral oils into human hair fibers: relevance to hair damage. *J Cosmet Sci* 52:169–184
198. Hilterhaus-Bong S, Zahn H (1989) Contribution to the chemistry of human hair. II. Lipid chemical aspects of permanently waved hair. *Inter J Cosmet Sci* 11:167–174
199. Gould JS, Sneath R (1985) Electron microscopy image analysis: quantification of ultrastructural changes in hair fiber cross-sections as a result of cosmetic treatment. *J Soc Cosmet Chem* 36:53–59